BRNO UNIVERSITY OF TECHNOLOGY
VYSOKÉ UČENÍ TECHNICKÉ V BRNĚ

FACULTY OF CHEMISTRY
FAKULTA CHEMICKÁ

INSTITUTE OF MATERIALS SCIENCE
ÚSTAV CHEMIE MATERIÁLŮ

MODIFICATION OF POLYMER BLENDS BASED ON POLYHYDROXYBUTYRATE AND THEIR PROPERTIES
MODIFIKACE POLYMERNÍCH SMĚSÍ NA BÁZI POLYHYDROXYBUTYRÁTU A JEJICH VLASTNOSTI

MASTER'S THESIS
DIPLOMOVÁ PRÁCE

AUTHOR
AUTOR PRÁCE

Bc. Veronika Melčová

SUPERVISOR
VEDOUCÍ PRÁCE

Mgr. Radek Přikryl, Ph.D.

BRNO 2017

VYSOKÉ UČENÍ TECHNICKÉ V BRNĚ
FAKULTA CHEMICKÁ

Zadání diplomové práce

Číslo práce:	FCH-DIP1094/2016
Ústav:	Ústav chemie materiálů
Studentka:	**Bc. Veronika Melčová**
Studijní program:	Chemie, technologie a vlastnosti materiálů
Studijní obor:	Chemie, technologie a vlastnosti materiálů
Vedoucí práce:	**Mgr. Radek Přikryl, Ph.D.**
Akademický rok:	2016/17

Název diplomové práce:

Modifikace polymerních směsí na bázi polyhydroxybutyrátu a jejich vlastnosti

Zadání diplomové práce:

Studium vlivu struktury polymerní směsi na bázi P3HB na krystalinitu, reologické a mechanické vlastnosti. Sruktura polymeru bude ovlivňována reaktivními kompaundacemi P3HB a dalších biopolymerů s reakčními činidly.

Termín odevzdání diplomové práce: 5.5.2017

Diplomová práce se odevzdává v děkanem stanoveném počtu exemplářů na sekretariát ústavu. Toto zadání je součástí diplomové práce.

Bc. Veronika Melčová student(ka)	Mgr. Radek Přikryl, Ph.D. vedoucí práce	prof. RNDr. Josef Jančář, CSc. vedoucí ústavu

V Brně dne 31.1.2017

prof. Ing. Martin Weiter, Ph.D.
děkan

ABSTRACT

Theoretical part of this work describes properties and modification possibilities of poly(3-hydroxy butyrate) (PHB) and amorphous poly(lactic acid) (PLA) and their blends. In experimental part, reactivity of Joncryl, Raschig, and phosphite reagents triphenyl phosphite, tris(nonylphenyl) phosphite, and diphenyl isodecyl phosphite with neat PLA and PHB are studied. Raschig, an oligomeric polycarbodiimide based additive, was proven to enhance melt viscosity of both polymers in amount 2%wt., therefore was used for preparation of blends in five PHB/(PHB+PLA) ratios. Samples with Raschig and corresponding non-reactive samples were studied using rheology, gel permeation chromatography and modulated differential scanning calorimetry. Results showed possible reaction of Raschig and PHB/PLA blends leading to branched structures. However, the rate of reaction is not sufficient to completely compensate decrease in viscosity due to processing degradation. Thus, non-reacted amount of Raschig remains in matrix. On the basis of these findings, it is concluded that Raschig behaves rather as a relatively effective stabilizer of rheological properties than as a reagent for the intentional modification of PHB/PLA blends' structure. In order to study mechanical properties of these blends, samples plasticized with acetyltributylcitrate were prepared using twin screw extruder.

ABSTRAKT

Teoretická část této diplomové práce popisuje vlastnosti a možnosti modifikace poly(3-hydroxybutyrátu) (PHB) a amorfní poly(mléčné kyseliny) (PLA) a jejich směsí. V experimentální části je studována reaktivita Joncrylu, Raschigu a fosfitových činidel trifenylfosfitu, tris(nonylfenyl) fosfitu a difenylisodecylfosfitu s čistým PLA a PHB. Raschig, oligomerní aditivum na bázi polykarbodiimidu, prokázal v množství 2hm. % zvýšení viskozity taveniny obou polymerů, a proto byl použit k přípravě směsí o pěti hmotnostních poměrech PHB/(PHB+PLA). Vzorky s Raschigem a odpovídajícími nereaktivními vzorky byly studovány pomocí reologie, gelové permeační chromatografie a modulované diferenční kompenzační kalorimetrie. Výsledky naznačily reakce Raschigu v PHB/PLA směsích vedoucí k rozvětveným strukturám. Rychlost reakce však není nedostatečná ke kompenzaci poklesu viskozity v důsledku degradace při zpracování. Následně zůstává nezreagované množství Raschigu v matrici. Na základě těchto zjištění se dospělo k závěru, že Raschig se chová spíše jako relativně účinný stabilizátor reologických vlastností, než jako činidlo pro záměrnou modifikaci struktury směsí PHB/PLA. Za účelem studia mechanických vlastností těchto směsí byly ve dvoušnekovém extrudéru připraveny vzorky plastifikovány acetyltributylcitrátem..

KEYWORDS

Poly(3-hydroxy butyrate), poly(lactic acid), polymer blending, compatibilization, reactive extrusion, polycarbodiimide, branching

KLÍČOVÁ SLOVA

Poly(3-hydroxy butyrate), poly(mléčná kyselina), polymerní směsi, kompatibilizace, reaktivní extruze, polykarbodiimid, větvění

MELČOVÁ, V. Modification of polymer blends based on polyhydroxybutyrate and their properties. Brno: Brno University of Technology, Faculty of Chemistry, 2017. 75 s. Supervisor of Diploma thesis Mgr. Radek Přikryl, Ph.D.

DECLARATION

I declare that my diploma thesis was worked out independently and that the used references are quoted correctly and fully. The content of the above mentioned thesis is considered a property of BUT Faculty of Chemistry and can be used for commercial purpose s only with the supervisor‘s and dean‘s consents.

.....

Student signature

PROHLÁŠENÍ

Prohlašuji, že jsem diplomovou práci vypracovala samostatně a že všechny použité literární zdroje jsem správně a úplně citovala. Diplomová práce je z hlediska obsahu majetkem Fakulty chemické VUT v Brně a může být využita ke komerčním účelům jen se souhlasem vedoucího diplomové práce a děkana FCH VUT.

.....

Podpis studenta

ACKNOWLEDGEMENT

Most of all, I would like to thank my supervisor Mgr. Radek Přikryl, Ph.D. for his time, attitude, precious advice and his belief in me. Further, I would like to express my thanks to prof. Ing. Pavel Alexy, PhD. and Ing. Petr Lepcio for valuable professional advice and time, they have spent and Lujza Štulrajterová for their willingness and help. And finally, my family and my loved ones deserve my deepest gratitude for preservation of sanity during writing this thesis.

CONTENT

INTRODUCTION

Recently, use and research concerning bioplastic materials have gained a great attention, as they are linked to many benefits compared to the fossil-based plastics, such as reduction of fossil fuel usage, reduction of carbon footprint, or reduction of global warming potential. The term bioplastics may easily be misunderstood as it involves both biodegradable and biobased polymers, which is commonly not distinguished although one polymer might not exhibit both of these properties. A bioplastic that is biobased may not necessarily be biodegradable, and a biodegradable bioplastic may not be biobased.

Biobased material has some or all of its carbon produced from a renewable plant or animal source, or produced in yeast, bacteria, or algae grown and cultivated with biobased feedstocks such as sugar or lipids. Todays, most biobased bioplastics are sourced from plant-based raw materials coming from traditional crops like corn and sugar cane. However, efforts have been made to move to second and third generation feedstocks including agricultural, forest, and municipal waste, as well as algae and other non-food biobased feedstocks. Biobased plastics have an equal performance as corresponding polymers produced from a fossil source. For example, common commodity plastics poly(ethylene) (PE), poly(ethylene terephthalate) (PET), and several types of polyamides exist in a fully biobased equivalents with the same properties and processing characteristics. Biobased plastics that are not biodegradable are ideal for applications such as durable goods and items that are highly recycled.

Biodegradable plastics are able to completely degrade through biological process into carbon dioxide, methane, and water in a defined environment and in a defined timescale. Environments include composting, anaerobic digestion, and marine and soil environments. Biodegradable plastic can be recycled during its lifetime and after deterioration of its properties beyond usability be submitted for biodegradation. Biodegradable polymers derived from petroleum resources include poly(glycolide), poly(lactic acid), poly(caprolactone), poly(butylene succinate) and many others; the group of biodegradable polymers derived from renewable resources include proteins, polysaccharides like chitin, starch and cellulose, microbial polyesters, such as polyhydroxyalkanoates (PHA) or poly(lactic acid).

This work is focused on the blends of two polymers, both biobased and biodegradable, poly(3-hydroxy butyrate) and poly(lactic acid). Unfortunately both exhibit drawbacks limiting their utilization, for poly(lactic acid) it is low heat distortion temperature and poor processing window whereas for poly(hydroxy butyrate) it is its brittleness, low melt viscosity, and thermal instability.

1. THEORY

1.1. Poly(3-hydroxybutyrate)

Poly(3-hydroxybutyrate) (PHB) is a natural polyester of 3-hydroxybutanoic acid belonging to the group of short chain length poly(hydroxy alkanoates) (scl-PHA) firstly described by Maurice Lemione in 1926 [1].

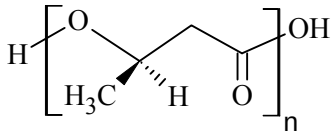

Figure 1 Poly(3-hydroxybutyrate) structure unit

The polymer can be produced by bacteria from various renewable and waste carbon resources, although the cost of the production is still too high to compete with oil-based plastic [1].

PHB is completely biodegradable, highly hydrophobic thermoplastic polyester material with melting point (T_m) lying between 170–180 °C, crystallinity ranging from 55 to 80 % and the glass transition temperature (T_g) around 6 °C. It is highly stereoregular with all of monomer units in *R* configuration. The summary of the mechanical properties with the comparison with the poly(lactic acid) and commercial polymers lies in the Table 1 [2].

Table 1 Properties of PHB, PLA and selected commercial polymers [2]

	Young's moulus ***E* (GPa)**	**Tensile strenght** ***σ* (MPa)**	**Elongation at break** ***ε* (%)**
PHB	3.5	40	5
PDLLA	–	44	100–180
PP	1.7	34.5	400
PET	2.2	56	300
PS	3.1	50	–
LDPE	0.2	10	620

One of the main drawbacks of commercially using PHB is its brittleness. It is caused by its high crystallinity and crystallites morphology. PHB forms lamellar structure when crystallized from the solution and spherulitic structure when crystallized from the melt. In the latter case, neat PHB exhibits low nucleation density leading to the existence of large spherulites with inter-spherulitic cracks [3]. Moreover, at a room temperature secondary crystallization occurs in PHB upon storage making the material stiff and brittle. PHB similarly to most semicrystalline polymers have a three-phase structure made of one crystal phase and two amorphous fractions. Mobile amorphous fraction (MAF) is made of the polymer chains that mobilize at T_g and nanosized rigid amorphous fraction (RAF) exists at the interface of crystal and amorphous phase as a result of the immobilization of a polymer chain due to the existence of the crystal. During the storage at 25 °C, crystallization of PHB

occurs firstly by crystal growth at the expenses of the MAF and after 240 min, a mechanism changes to local rearrangements of the RAF phase. The ratio between the amount of amorphous and crystalline phase measured soon after crystallization from the melt cooled at 20 °C/min is 1.4 and drops down to 0.06 after 1 year at room temperature [4].

Other serious problem is PHB low thermal stability and narrow processing window. Thermal degradation of polyesters can be carried out by two molecular reaction pathways, intramolecular ester exchange (transesterification) and *cis*-elimination (depicted for PHB in Figure 2). Beside these, radical reactions can also proceed at high temperatures (> 300 °C). Due to c*is*-elimination reaction polymer chains are cleaved randomly which leads to lowering the molar mass and decreasing the melt viscosity. The reaction proceeds rapidly consequently giving rise to the formation of crotonic acid and its oligomers [5].

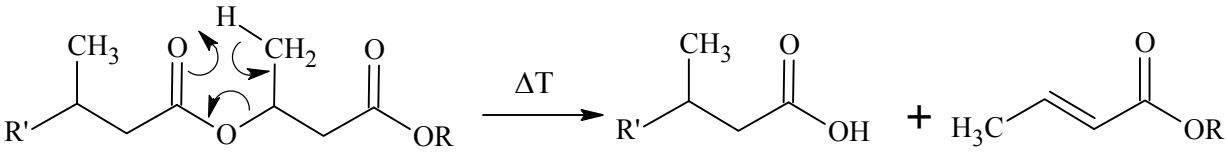

Figure 2 PHB decomposition by cis-elimination [5]

1.1.1. Additives for PHB

Many efforts have been made to overcome the problems mentioned in previous chapter including stabilization, plasticization and nucleation.

The effect of already mentioned chain scission of PHB during its processing can be hindered by addition of antioxidants, which react with formed free radicals disabling their further propagation. This way it should stabilize the melt during the whole processing time and prevent the polymer from degradation. As melt stabilizers, various phenol-based compounds are used, namely antioxidant 1010 [6] and tannic acid [7]. Furthermore, usage of pomace extract [8], carboxyl-terminated butadiene acrylonitrile rubber (CTBN) and polyvinylpyrrolidone (PVP) [8] was proven to enhance PHB thermal stability.

To ensure sufficiently high crystallization rate and temperature and homogeneity, nucleating agents are added to PHB usually in amounts less than 1% (w/w). Their presence causes formation of smaller and more homogenous spherulites, which considerably improves mechanical properties of the material. The nucleating agents include boron nitride [10] (one of the most commonly used), cyanuric acid [11], saccharin [12] or orotic acid [13].

Plasticizing the polymer causes reduced stiffness and a drop of glass transition (T_g) and as well as flow temperatures which allows us to lower the processing temperature. For semi-crystalline polymers, the crystallization process can also be affected. Recently, mainly citrate-based plasticizers gained great attention as they are non-toxic derivates of citric acid, for example acetyl tributyl citrate (ATBC) [14], [15] which leads to the decrease in T_g. Other plasticizers include acetyl triethyl citrate, glycerol or triacetin [12], dioctyl (o-phthalate), dioctyl sebacate [15], soybean oil, epoxidized soybean oil, dibutyl phthalate and triethyl citrate [16].

1.1.2. Chemical treatment of PHB

To improve the physical and mechanical properties of PHB, its morphology and crystalline structure needs to be changed first and therefore various chemical method were developed aiming to do this.

Chemical modification of PHB can be done for example via chlorination [17], maleic anhydride grafting [18] or copolymerization. Block copolymers can be prepared by catalysed transesterification reaction with isosorbide succinate or (*S*)-lactic acid mers [19], butyleneadipate [20] or poly(ethylene glycol) (PEG) [21] and [22]. Graft copolymers of PHB are prepared by radiation grafting in nitrogen atmosphere via radical mechanism with isoprene [23], sodium p-styrene sulfonate, acrylic acid, styrene and methyl acrylate [24] or methyl methacrylate [25].

Apart from this, attempts to disrupt crystalline structure of PHB through reactive modification in the melt state have been made. It was reported, that using dicumyl peroxide (DCP) for reactive extrusion of PHB led to generation of long-branched structure and therefore decrease in average crystallite size. DCP concentration 0.1%wt. resulted in distinct increase of melt viscosity during rheology measurements, while further addition of DCP had an opposite effect due to chain scissions. Increasing concentrations of DCP influenced the crystallization temperature which reached maximum for the sample with 0.3%wt. The authors concluded, that during reactive extrusion microgels are formed having a high nucleating effect [26].

Homogenous blend of PHB and 50% epoxidized natural rubber (ENR-50), which are immiscible under normal conditions, was prepared by melt reaction. In the structure of ENR-50 half of the double bonds of the isoprene units have been epoxidized as shown in Figure 3. These epoxide groups react with carboxyl group formed at the end of PHB macromolecules during its degradation.

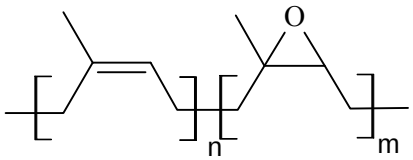

Figure 3 50% epoxidized natural rubber

The blend annealing was performed for the temperatures between 184–199 °C and resulted in single glass transition temperature materials [27].

To enhance PHB melt strength chain extender triallyl trimesate (TAM) together with DCP was studied. During the melt processing of PHB with DCP free radicals are generated by abstraction of tertiary hydrogen. The radicals are subsequently able to react with chain extender to form branched and cross-linked structures as indicated on the scheme in Figure 4.

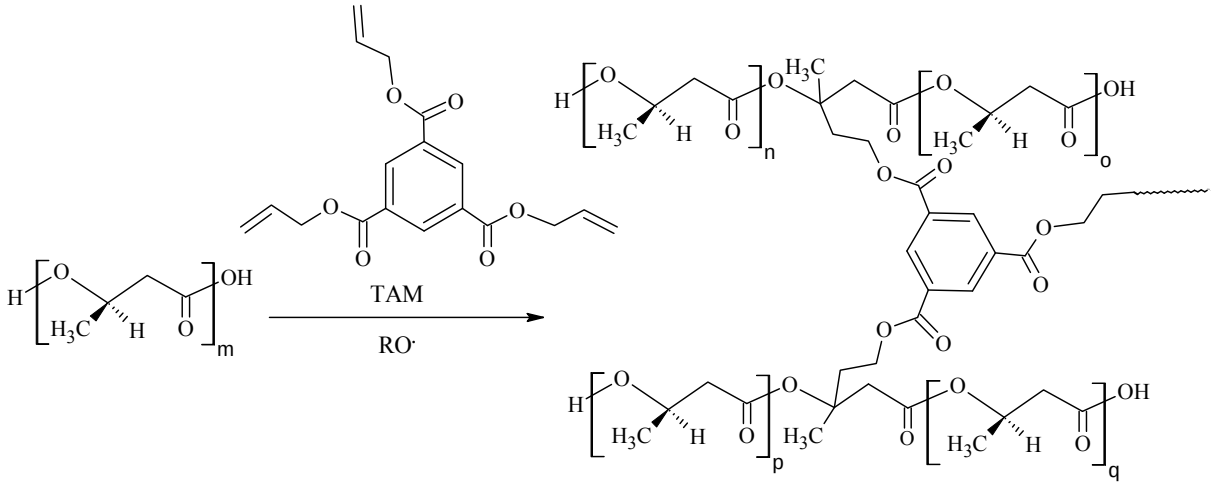

Figure 4 Reaction of PHB with TAM in the presence of free radicals

The changes in the structure of PHB were proven by rheological measurements where samples with 0.2%wt. DCP and addition of TAM resulted in increased melt viscosity compared to neat PHB. The existence of cross-linked regions was examined by measuring the gel content which reached the value 30%wt. for the sample containing 0.3%wt. DCP and 0.4%wt. TAM. For this sample the crystallization temperature was increased up to 118 °C compared to 96 °C for neat PHB. It was also shown, that this treatment led to the improvement in thermal stability of PHB [28].

1.2. Poly(lactic acid)

Poly(lactic acid) (PLA) is biodegradable thermoplastic polymer chemically belonging to the group of polyesters. High molecular weight PLA was first synthesized by Lowe in 1954 according to the procedure suggested by Carothers et al. in 1932 [29].

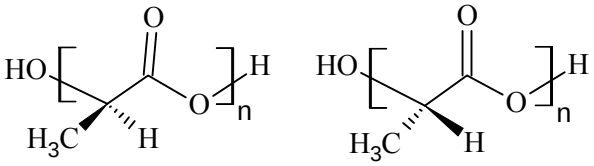

Figure 5 Poly(lactic acid) in(S), L (left) and (R), D (right) configuration

As can be seen from Figure 5, the presence of a chiral carbon atom in PLA monomer unit, lactic acid, makes the structure optically active. Therefore two stereoisomers of PLA exist – *D*-poly(lactic acid) (PDLA) and *L*-poly(lactic acid) (PLLA) [29].

PLLA is a semi-crystalline polymer with crystallinity around 37%, melting temperature between 170–180 °C and a glass transition temperature in the region of 60–67 °C, which contributes to the brittleness of the material at ambient temperature. Melting enthalpy of 100% crystalline polymer is 135 g/mol. PDLLA is an amorphous polymer which has a glass transition temperature between 50–60 °C [29].

In the blends of PLLA and PDLA stereocomplexation occurs between equimolar amounts of D- and L-lactyl units if either of enantiomers has the molecular weight (MW) below

10^4 g/mol. These stereocomplexes are created exclusively when the sequence length of L- or D-lactyl units is at least 14. The stereocomplexation is responsible for increasing mechanical performance, thermal and hydrolytic degradation resistance and gas barrier properties. Melting temperature of stereocomplexes is 50°C higher than PLLA homocrystals and they also exhibit higher crystallization rate than homocrystals because of self-nucleating effect. It is necessary to say, that stereocomplexes do not change T_g though leaving the material still brittle. In chloroform solution these stereocomplexes can act as cross-linking areas causing formation of gel. In case of non-racemic mixture, stereocomplexes are created and the excess of one stereoisomer crystallizes in the form of homocrystals. The crystallinity reaches values up to 63% making the polymer stiff and brittle with low values of deformation at break [29], [30].

PLA can be synthesized by bacterial fermentation of carbohydrates like starch or by chemical synthesis. The former is preferred by two main producers of PLA, NatureWorks LLC and Corbion®. Chemical synthesis can be performed by polycondensation of lactic acid (2-hydroxy propionic acid) or by ring opening polymerization (ROP) of lactide (3,6-dimethyl-1,4-dioxane-2,5-dione). However, its restricted production capacity and high manufacturing costs together with the fact that this method is suitable only for producing *L* isomer limits its using [30].

1.2.1. Additives for PLA

Additivation of PLA aims to improve its mechanical properties enough to be suitable for use as commodity plastics. From the methods trying to overcome PLA brittleness, plasticization has gained the most attention. Plasticizing effect leads to decrease in elasticity modulus and maximum tensile strength, while values of elongation at break are increased. Moreover, glass transition temperature and crystallinity should be affected. For example, using PEG, glucosemonoester and partial fatty acid esters as plasticizing agents have been reported. Addition of 10%wt. of PEG has shown not only influence on mechanical properties and drop in T_g by 30 °C, but also enhancement of the impact stress of PLA [31].

Citrate plasticizers, namely triethyl citrate and acetyl triethyl citrate, are nontoxic derivates of citric acid which have been studied as plasticizers for PLA. Both were miscible with PLA at all compositions and possessed improved toughness and elongation at break values [32].

Other plasticizers include adipates [33], lactic acid oligomer, *L*-lactide and epoxidized soybean oil (USE) [34] or poly(propylene glycol) [35].

To obtain a material with induced crystallization various nucleating agents have been tested with PLA. Talc, which is chemically neutrally charged silicate, was proven to have a nucleating effect on PLA. It reduces crystallization half-time and time to full crystallization and also increases heat distortion temperature (HDT), which is low for neat PLA [36]. Other nucleating agents include phthalimide [37], cyclodextrin, calcium carbonate ($CaCO_3$) [38] or star-structured *L*-poly(lactides) [39].

1.2.2. Chemical treatment of PLA

The reasons, why so many attempts have been made to chemically graft PLA, are to tailor its biodegradation behaviour, susceptibility to hydrolysis and last but not least mechanical properties. Similarly to PHB, PLA can be maleated using commercial peroxide Luperox L101 (2,5-bis(tert-butylperoxy)-2,5-dimethyl hexane), which structure is shown in Figure 6 [40].

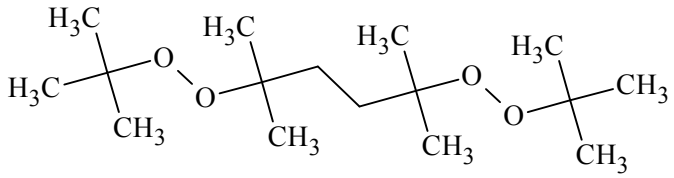

Figure 6 The structure of Luperox L101 peroxide 65[40]

PLA exhibits processability drawbacks in the means of poor melt strength and lack of strain hardening. Branching and chain extension are generally considered to be a way how to solve this.

It has been proven, that using peroxide, namely Lupersol 101 (the same chemical structure as Luperox L101), during processing leads to change in PLA structure due to coupling, chain-scission, branching and cross-linking reactions. Using peroxide concentration and temperature ranges 0.1–0.25%wt. and 170–180 °C, respectively, resulted in increased MW and melt viscosity [41].

Recently, systems of peroxy-initiated melt reactions with chain extenders have attracted a great attention. Triallyl trimesate (TAM) [42], triallyl isocyanurate (TAIC) [43] and pentaerithritol triacrylate (PETA) [44] were used together with dicumyl peroxide (DCP) bis((1-methyl-1-phenylethyl)) peroxide. Chemical structures of these reagents lie in Figure 7. TAM is reported to significantly enhance crystallinity and crystallization rates and melt properties of PLA, using TAIC resulted in improved thermal stability, while poor mechanical properties of the material remained. PETA showed nucleating effect on PLA by increasing its nucleation density and crystallization rate.

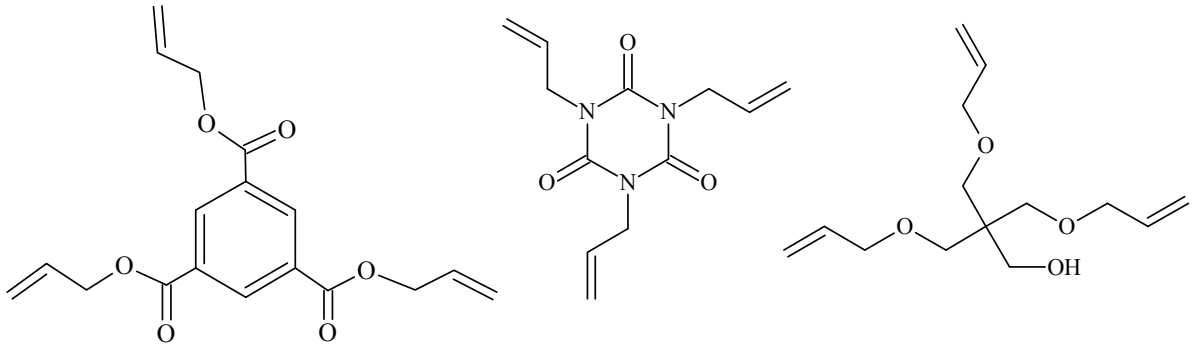

Figure 7 The structure of TAM (left), TAIC (middle) and PETA (right) [42], [43], [44]

Moreover, to increase MW and promote branching in PLA a multi-functional epoxide styrene-acrylic oligomeric chain extenders (shown in Figure 8) with commercial names Joncryl® ADR-4368 [42], [45], [46], [47], and Joncryl® ADR-4370 [48] from the company BASF and CESA-Extend OMAN698493 from Clariant [45], [49] are used. Epoxide groups of Joncryl and CESA react predominantly with carboxyl end groups on polyesters and the excess

epoxide groups are able to react with terminal hydroxyl groups and with the newly formed hydroxyl groups from the reaction between epoxide and carboxyl groups. The outcome is long chain branched (LCB) structure of PLA with increased MW, wider molecular weight distribution (MWD), and enhanced melt properties. The LCB structure hinder the folding of chains into growing crystalline lamellae, which causes reduced overall crystallization rate and increase the cold-crystallization temperature.

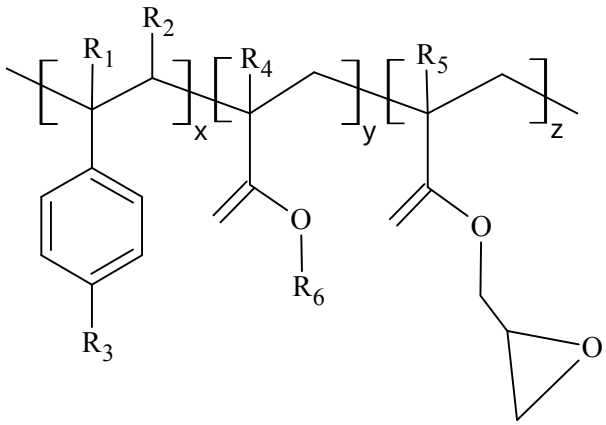

Figure 8 The structure of multi-functional epoxide styrene-acrylic oligomeric chain extender, Joncryl® ADR, where x, y, and z are all between 1 and 20 [46]

It was found, that LCB structure can be achieved also by two-step reaction of PLA with pyromellitic dianhydride (PMDA) and triglycidyl isocyanurate (TGIC) (Figure 9) through reactive processing. This way a topological structure consisting of linear, star-like chains with three arms and tree-like chains can be achieved [50]

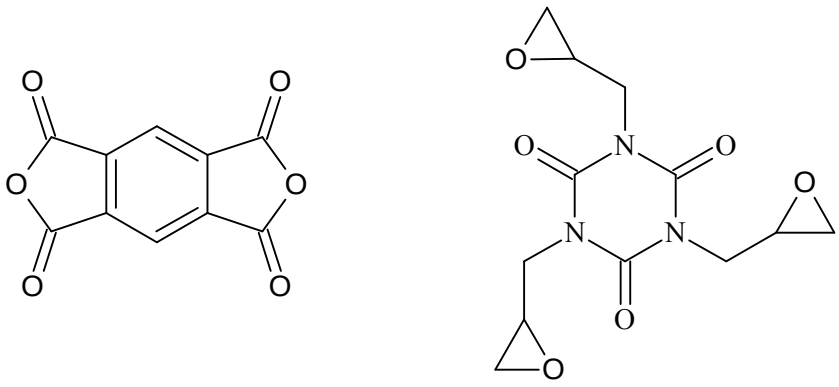

Figure 9 The structure of PDMA (left) and TGIC (right) [50]

Poly(carbodiimide) (PCDI, poly-(1,3,5-triisopropylphenylene-2,4-carbodiimide) and tris(nonyl phenyl) phosphite (TNPP) (Figure 10) were also studied as chain-extenders for PLA in order to uplift its thermal stability. Opposite to Joncryl, PCDI and TNPP stabilize the polymer by producing longer linear chains of PLA. Addition of 2%wt. of PCDI or 0.35%wt. of TNPP ensured an acceptable stability of the complex viscosity of PLA at 160–200 °C over 30 min. In addition, TNPP was proven to intensify the crystallization process and as a result the degree of crystallinity, crystal growth rate, and spherulite size increased [46], [47].

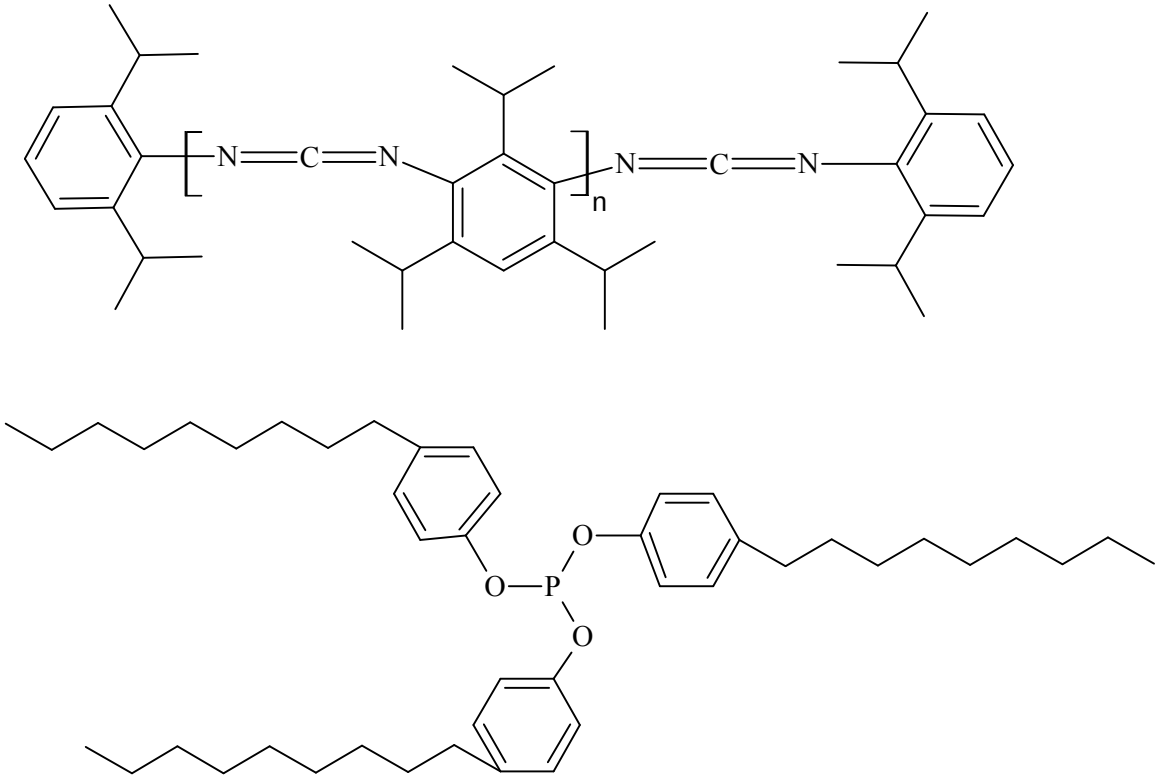

Figure 10 The structure of PCDI (up) and TNPP (down) [46]

Last but not least, chain-extended PLLA was prepared through reactions with triphenyl phosphite (TPP, showed in Figure 11). With the optimal amount of 2%wt., molecular weight of PLLA increased from 62,100 to 126,000 g/mol. TPP is considered to work as an esterification promoter [51].

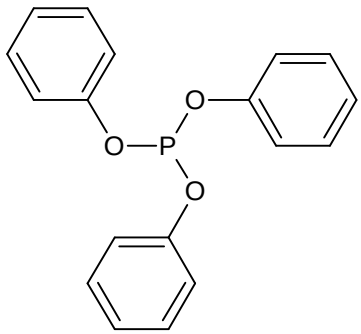

Figure 11 The structure of TPP

1.3. Blends of PHB and PLA

Chemically, PLA and PHB are both polyesters and their structures differ only in a single -CH_2- group suggesting no special interaction apart from hydrogen bonding. Both polymers crystalline forms have orthorhombic structures.

However, their miscibility is a rather complicated phenomena. When precipitated from chloroform, they are immiscible in the whole concentration range [52]. In the melt, transesterification occurs enhancing the miscibility. Studies have shown that in the melt PHB is miscible with low-molecular-weight PLLA (MW < 18000) over the whole composition

range, whereas the PHB blends with high-molecular-weight PLLA (Mw > 18000) exhibit biphasic separation. This is usually explained by means of the Flory-Huggins solution theory neglecting mutual interactions between the polymers. In parallel, PLLA is miscible with low-molecular-weight PHB (Mw < 9400) in the melt up to 50%wt. and immiscible with high-molecular-weight PHB [53].

From miscible blends of PHB and low-molecular-weight PLLA, both polymers can crystallize simultaneously. Two types of spherulites are formed during cooling from the melt, dendritic PLLA spherulites and PHB spherulites. Crystallization rate of PLA is much slower, even though PLLA starts to crystallize earlier [53].

1.3.1. Melt blended

In the blends where there is a majority of PLA (90%), PHB exists in the form of well-dispersed droplets improving the properties of resulting polymer alloy. The heat deflection temperature, tensile strength and foam nucleation density are enhanced relatively to neat PLA. Moreover, the toughness of PLLA is substantially increased without reduction in optical clarity of the blend. This is due to the finely dispersed PHB crystals acting as filler and a nucleating agent in PLA [54]. Phase separation for the blend PLLA/PHB 75/25 can be suppressed by addition of 7%wt. of polyester plasticizer Lapol 108 as shown by SEM. Plasticizing effect was also confirmed by the reduction of T_g [55]. The use of a lactic acid oligomer (OLA) as a plasticizer for PLLA/PHB blend with the majority of PLLA was also studied. Glass transition temperature shifted to lower temperatures and the main degradation peak for the blend decreased when compared to neat PLA as well [56].

When blended in the ratio 1:1, PLLA changes the crystallization mechanism of PHB and lowers its T_c. In miscible blends of PHB and low Mw PLLA, at 110 °C 8 hours is needed to finish the co-crystallization. In immiscible blends, PLLA showed depressed crystallization rate caused by the dilution effect of PHB melt, while T_g remained unchanged [53].

Adding PLLA to the PHB matrix leads to increase of T_g and T_c and drop of T_m together with broadening the melting peaks, which may be explained by recrystallization and/or lamella thickening. In addition, crystallinity and the number of large spherulites are reduced and crystallization rate for PHB is decreased. In case of amorphous PDLLA, the spherulites of PHB are volume-filling with PDLLA incorporated in the inter-spherulitic regions [57].

1.3.2. Partially cross-linked blend

In order to further improve the performance of PHB/PDLLA blends, the blends were partially cross-linked using different concentrations of DCP as a free radical initiator (0.1; 0.5 and 1%wt.), while the ratio PHB/PDLLA was kept 70/30.

DCP causes hydrogen absorption from PDLLA and PHB chains and consequently combination of free radicals at the interphases. Complex products can be obtained, including branched/cross-linked PHB, branched/cross-linked PDLLA, PHB-g-PDLLA copolymers and PHB-cross-linked-PDLLA network. Moreover, competitive reaction of chains scission occurs because of the thermal instability of PHB and the free radicals.

The process of compounding was monitored by measuring the torque of the Haake mixer. As can be seen from the typical curve of torque plotted against time shown in Figure 12, the values increased at the beginning because of feeding and began to drop as the polymer started to degrade thermally. After addition of DCP, the torque values raised rapidly, suggesting a formation of crosslinking/branching structures. Then the curve reached its maximum and the degradation reaction started to prevail reducing the melt strength and consequently the torque values.

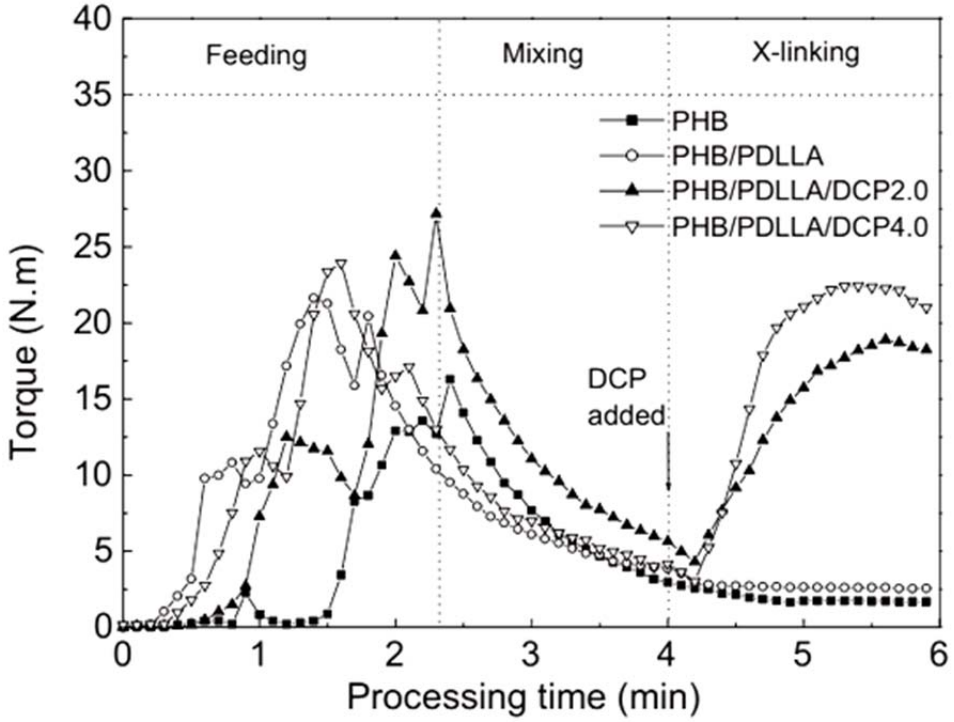

Figure 12 Torque values of the Haake mixer during processing of PHB/PDLLA reactive blends [58]

Improved compatibilization of these two polymers was confirmed by SEM observation of compounded blend compared with blend without DCP addition. The phase boundaries became unclear indicating an enhanced interfacial adhesion and compatibility.

Using these amounts of DCP, up to 20% of gel content was formed in the resulting material containing 10% more PDLLA fraction than the overall blend.

PHB exhibited deterioration of crystallization ability caused by reactive compounding. Thermal behaviour of PHB PDLLA blends showed reduced peak crystallization temperature and crystallinity with addition of DCP. On the contrary, cold crystallization temperature and enthalpy were increased. The existence of two melting peaks is attributed to recrystallization process upon heating. Both T_{m1} and T_{m2} values are decreased by addition of DCP indicating the presence of imperfections and small-sized lamellar crystals formed as a consequence of the partial crosslinking and branching.

Moreover, the mechanical properties namely tensile and flexural strength and impact toughness of the blends were enhanced after the partially crosslinking as well as

the rheological properties of the melt, the storage modulus (G_0) and the complex viscosity (h^*) were increased [58].

1.4. Blending and compatibilization of polymers

Polymer blend is a mixture of at least two polymers or copolymers, comprising more than 2%wt. of each component. Miscibility of polymer blends is explained in the means of extended Flory-Huggins theory with binary polymer-polymer interaction parameter as the key element, which is a complex function of all variables: polymer structure, MW and distribution, blend composition, pressure, temperature, stress field, etc.

Miscible blend is associated with a negative value for the free energy of mixing and a positive value of the second derivative of concentration. Its domain size is comparable to the dimension of the macromolecular statistical segment as it is homogeneous down to the molecular level.

In immiscible polymer blends we consider three cases:

1) crystalline matrix/amorphous dispersed phase – nucleation behaviour and the spherulite growth rate may be affected by the second phase,
2) amorphous matrix/crystalline dispersed – a fractionated crystallization occurs which may lead to a drastic reduction in the degree of crystallinity,
3) crystalline matrix and dispersed phase – in this case, both phases may affect each other, rarely simultaneous crystallization is present.

Since glass transition temperature is relatively simple to measure, that's why detection of a single T_g in a blend has been used as a test for miscibility. However, T_g is rather sensitive to the degree of dispersion, thus a single value can be detected in immiscible blends with small enough domain size ($\leq$ 30 nm) [59].

Blending of two immiscible polymers necessarily leads to phase-separated material. Its morphology and interfaces have to be well controlled which is done by compatibilization. This process leads to the reduction of the interfacial tension coefficient, stabilisation of the desired morphology against the processing stresses and improving interaction between phases in the solid state. Chemical compatibilization is divided into two categories: compatibilization by addition of a compatibilizer, and reactive compatibilization. In the former case, one of the strategies is addition of a small amount (0.5–2%wt.) of a tailored copolymer. However, the added copolymer has a tendency to form micelles, which do not participate in the process and it has the disadvantage that it has to diffuse to the interfacial region. Therefore, a compatibilizing copolymer is nowadays formed simultaneously with generation of interphase morphology during extrusion processing, which is the principle of reactive compatibilization [59],[60].

1.4.1. Reactive compatibilization

During the last three decades, polymer blending has become important part of the commercialization of polymers. Reactive compounding has been used mainly for modification of engineering resins such as PP, PA, thermoplastic polyesters, PC or POM. Copolymer formation in situ is a heterogeneous reaction taking place across a melt-phase

boundary. A compatibilizer must therefore be located at the interfaces in order to play its roles [59],[60].

Reactions taking place during reactive compounding can be classified as follows [59]:

1) redistribution or trans-reaction – block and random copolymers formation
   a) reactive end-groups of polymer-1 (P1) attack main chain of polymer-2 (P2)
   b) chain cleavage/recombination involving all polymers
2) graft copolymer formation
   a) direct reaction of end-group of P1 with pendent groups of P2
   b) reaction of end group of P1 with pendent group of P2 in the presence of a condensing or a coupling agent
   c) reaction of pendent group of P1 with main chain of P2 in a degradative process
3) block polymer formation
   a) direct reaction of end-group of P1 with end group of P2
   b) reaction of end-group of P1 with end-group of P2 in the presence of a condensing or a coupling agent
   c) reaction of end-group of P1 with main chain of P2 in a degradative process
4) cross-linked copolymer formation
   a) direct reaction of pendent functionality of P1 with pendent functionality of P2
   b) reaction between pendent functionalities of P1 and P2 in the presence of a condensing or a coupling agent
   c) main chain of P1 reacts with main chain of P2 in the presence of a radical initiator
5) Ionic bond formation – block, graft or cross-linked structures
   a) ion-ion association mediated by metal cations as linking agents
   b) ion-neutral donor group association mediated by metal cations
   c) inter-chain protonation of a basic polymer by an acidic polymer

The type 1 reactions (trans-reactions) have mainly been used to compatibilize polyester blends. As the trans-reaction proceeds, the amount of crystallinity decreases which results in improved toughness, but reduced solvent and chemical resistance. For many applications only limited transesterification can be allowed. Addition of organo-phosphites (e.g. triphenylphosphite), supposing their conversion to di-phosphonates, is used to stop the exchange reaction. Block polymer formation (type-3 reaction) usually involves a coupling or condensing agent, e.g. epoxide, anhydride, phosphite or tri-phosgene. Compatibilization by formation of a compatibilizing copolymer with low level of crosslinking (type-4) usually involves reaction of multiple pendent groups.

Efficient reactive compatibilization should lead to high molecular weight copolymers. This together with crowding of the copolymer at the interface causes thick and rigid interphases, enhanced stability of morphology, increased melt viscosity and superior stress transfer in the solid state. The effect of compatibilization on crystallinity is more ambiguous. Since it increases the interfacial area the overall nucleation rate is increased. By contrast, diffusion of the nuclei to the crystallisable phase is slowed down. Furthermore, at high degree of

compatibilization, when the crystallisable polymer forms a dispersed phase and the drop/domain size is reduced below a critical limit for trapping nucleating particles, the crystallisation rate may be drastically reduced. Crystallisation within the small domains may only proceed by the homogeneous crystallisation mechanism [59].

1.4.2. Mechanism of reaction compatibilization

During reactive compatibilization using peroxides reaction proceeds by radical mechanism.

In initiation step thermally induced homolytic scission of O–O bond of the peroxides leads to the creation of primary radicals containing unpaired electrons. Subsequently, these highly reactive species form active centre in two different ways, abstraction of hydrogen atom from polymer chain or addition of monomer (in this case compatibilizer). Preference for the reaction is given mainly by the nature of radical species (initiator), more efficient in abstraction reactions are stable, heteroatom centred radicals. Susceptibility of polymer towards abstraction is also important and is controlled by the strength of bond between hydrogen and polymer.

Subsequent step until termination is referred as propagation. This step determines the kinetics of the overall compatibilizing reaction and is controlled by the diffusion of compatibilizer towards the reactive radicals. Large number of reactions occurs during propagation, including desired reaction between macro-radicals and compatibilizer. Apart from this, polymerization of a compatibilizer, chain transfer to a polymer or other additives or chain scission by β-scission mechanism can take place.

Termination is rapid combination of two radicals forming non-radical species with no energetic barrier. Growing macro-radical may react with oligomeric radical or other macro-radical. The latter case leads to a generation of cross-linked structures. Termination is diffusion controlled, therefore it is more likely for the polymer radical to be combined with smaller radical than other macro-radical. In the mixture of two polymers, compatibilizer and initiator, expected products include graft and block copolymers, cross-linked structure containing both polymers, branched and cross-linked homopolymers, polymerized compatibilizer and products of scission [61].

1.4.3. Processing technology

When two immiscible polymers are mixed in the form of solid pellets, morphology development starts with melting the pellets, then the polymer is stretched/deformed to slender threads which subsequently break-up to small particles. Possible coalescence of small particles to larger ones can be avoided by ensuring much greater rate of dispersion than rate of melting/plastification.

This can be done by any type of mixer capable of melting and mixing polymer system. Two basic types of mixers are distinguished: batch and continuous mixers. The former is mainly used for preliminary and laboratory-scale studies, while the latter is used for both laboratory studies and industrial production, depending on the size of the machine. For reactive compounding in continuous mixers screw extruders are mainly used. They are classified into single and twin-screw extruders. Even today, choosing adequate mixer (type, size, etc.) remains empirical because of lack of fundamental understanding and quantitative

evaluation of the common features and differences among these different types of mixers. Co-rotating self-wiping twin-screw extruders are used most frequently for polymer blending and alloying.

In a screw extruder, the morphology development is a function of screw length, while in an internal mixer it is a function of time. In the resulting blend, the minor component forms drops or filaments dispersed in a continuous matrix of the second polymer. Elementary steps in the mixing process are deformation of dispersed phase in the flow field in order to increase the interfacial area between the two components and decrease of local dimensions perpendicular to the flow direction (striation thickness).

The presence of a copolymer as a macromolecular compatibilizer has essential effect on the development of blend morphology:

1) it accelerates the melting/plastification rate through enhanced heat conductivity at the interphase between two polymers,
2) it modifies the sheet/thread formation and break-up via interfacial tension modification,
3) it reduces or prevents from coalescence.

1.4.4. Controlling factors of reactive compatibilizing

Generally speaking, the faster the copolymer formation kinetics the faster the morphology development and the finer the ultimate morphology. The complexity of compatibilizing process indicates that it can be affected by both nature of the used compounds and technological parameters. Variables include the nature of the polymers, compatibilizer, initiator, and eventually other additives, temperature, mixing time and intensity etc.

1.4.4.1. Effect of temperature and mixing time

It is straightforward, that processing temperature affects the half lifetime of the free radical initiator, $t_{1/2}$. Increased temperature causes rise of thermal decomposition rate of initiator and the initiator efficiency in producing free radicals on polymer, which results in increased polymer macro-radicals concentration and therefore the reactivity of the system [61]. The activation energy of the decomposition of the initiator is usually very high and thus it´s $t_{1/2}$ is decreased with increasing temperature. Temperature should be chosen so that the following inequalities are satisfied:

$$5t_{\text{mixing}} < t_{1/2} < 0.2\ t_{\text{process}}.$$

That means that if we want the initiator to be consumed at the end of the process, the overall processing time (t_{process}) should be at least 5 times $t_{1/2}$ of the initiator. Moreover, initiator should be well mixed in the polymer before a significant amount is decomposed, therefore time necessary for mixing up the grafting system, t_{mixing}, should be 5 times shorter than $t_{1/2}$ of the initiator [60].

Other effect of temperature is on the kinetics of co/polymerization occurring in the system. In case of radical grafting, grafting yield increases with increasing temperature, until some limit is reached. One factor in this can be enhanced diffusion of reactive species [61].

1.4.4.2. Polymer

As compounding of two polymers involves covalent attachment between them, the nature of polymer backbones defines grafting process due to its structure and chemical composition. The presence of reactive groups on the backbone chains is the major requirement for the reactive blending. Strong interactions (covalent bonds, ionic bonds) between two polymers in the melt are limited to a few percent of the polymers chains. The miscibility between two components is improved by the introduction of intermolecular H-bonds. For example in case of PHB, the carbonyl groups form an inter-H-bond with the hydroxyl groups of hydrogen bonding additives, competing with the self-H bonding formed by the hydroxyl groups themselves. The crystallinity and melting temperature obviously decrease for PHB H-bonded miscible blends [63].

As already mentioned, the polymer backbone influences the generation of active centres responsible for further reactions. It is straightforward, that the reactivity of so formed reactive centres and its precedence towards the reaction with reactive agents and other components of the mixture are affected as well. During the compounding reactivity slightly changes due to the β-scission [61].

1.4.4.3. Compatibilizer

A number of factors relating the additives need to be considered in designing experiments. These include: its concentration, solubility in the polymer melt, volatility, the method of introducing into the mixture, reactivity towards initiator and substrate derived radicals, and susceptibility to homopolymerisation.

As far as the homopolymerisation is concerned, in case of reactive blending it is an undesired reaction. The susceptibility to homopolymerisation depends both on its propagation rate constant and the propagation/depropagation equilibrium constant and is suppressed above the ceiling temperature. One way to avoid it is to use oligo- or polymeric compounds, which exhibit lesser tendency to undergo homopolymerisation due to steric factors. It is important to note, that their non-volatility makes them difficult to remove them from reaction product afterwards [64].

The effect of increasing the reactive agent concentration on the reaction yield is favourable up to a certain limit and is reversed further on. If the compatibilizer concentration becomes too high, phase separation can occur resulting in reduced grafting yields and an increased likelihood for homopolymerisation. To a certain extent it can affect degradation rate of a polymer, as it traps radicals that would otherwise undergo chain scission or crosslinking [61].

Equally important is chemical reactivity of the agent towards the polymers. For example, an epoxy moiety at the end of the macromolecule is highly reactive with COOH and OH end groups of PHB and PLA, although the reaction with COOH occurs primarily. Moreover, a temperature raise shifts the epoxy/COOH reaction to the product side. Pre-introduction of polymers with glycidyl methacrylate (GMA), containing an epoxy moiety at one end, could also be an effective way to achieve reactive PHB-based blends [64].

1.4.4.4. Initiator

A selection of an appropriate initiator should be emphasized on the concentration and residence time of transient radical species generated during the reaction, which is mainly given by the half-life of the initiator. Ideally, it should be short compared with the residence time in the extruder. A shorter half-life initiator will initially give a higher transient radical concentration for the same concentration of initiator, which may increase the likelihood of crosslinking by radical–radical combination. In opposite case, residual initiator may have a negative effect on product stability [64].

Initiator concentration follows similar trend as reactive agent, once a certain concentration is reached, higher levels of initiator do not increase the conversion of grafted monomer, as formed radicals participate in the termination of the growing polymer and other termination reactions [61].

A variety of other factors relating initiator have to be considered for an experiment:

1) the solubility of the initiator in the polymer melt and its partition coefficient between the various phases in case of multiphase melts,
2) volatility of the initiator - this is a concern both in choosing the method of introduction and for safety,
3) physical form of the initiator,
4) the method of introducing the initiator - the initiator may be:
    a) introduced with the feedstock,
    b) added with the monomer,
    c) added as a separate feed,
    d) added directly or adsorbed onto the polymer,
    e) added as a solution in the monomer or a solvent,
    f) added all at once or by multipoint addition,
5) the extent of cage reaction and the formation of initiator derived by-products – it depends on the nature of the initiator and on other reactants presented in the reaction system such as polymer substrate, monomer, additives, etc,
6) susceptibility of the initiator to induce decomposition and other side reactions - diacyl peroxides and hydroperoxides are particularly prone to induced decomposition [64].

1.4.4.5. Additives

Grafting yield or the extent of graft co-polymerization depends also on the reactivity of possible additives in the mixture. The reaction between the desired reactant and the polymers must compete with undesirable reactions pathways, such as chain-transfers or radical trapping. Nevertheless, various coagents have been studied and proved to enhance the agent/backbone reaction and to improve the grafting efficiency, and/or to reduce side reactions during melt phase processing [64].

2. EXPERIMENTAL

2.1. Materials

2.1.1. PHB

PHB with a production name Hydal 8-10/3V and 2V were kindly provided by Nafigate, which is an Exclusive Licensee of the initial patent developed by the team of Professor Ivana Márová at Brno University of Technology. Hydal biotechnology is a technological process of converting third generation feedstock, waste cooking oil, into PHB by means of fermentation and subsequent polymer isolation. Polymer isolation process consists of separation of microbes, their disruption and polymer extraction, polymer precipitation, solvent removal and solvent recovery steps.

Polymer, in the form of flakes was firstly dried in an oven at 60 °C for two hours and processed using HAAKE™ Rheomex OS single screw extruder with the HAAKE™ PolyLab™ OS driving unit. Setting of temperature zones from hopper to dye was as follows: 180 °C - 180 °C -170 °C - 160 °C, rotational speed was set to 200 RPM. Extruded profile was guided through water bath with a temperature 60 °C in order to finish the crystallization process, air dried and fed into the pelletizing machine.

2.1.2. PLA

PLA Ingeo™ 4060D (amorphous PDLLA, referred to as PLA), suitable for thermoformed, coating, injection molded, blow molded, and fiber applications, was provided by NatureWorks LLC in the form of pellets and used as recieved. This grade may be used in food packaging materials and, as such, is a permitted component of such materials pursuant to section 201(s) of the Federal, Drug, and Cosmetic Act, and Parts 182, 184, and 186 of the Food Additive Regulations. Glass transition temperature is 55–60 ºC.

2.1.3. Reactive agents

Following reactive agents were purchased from Kingyorker and used as received:

- triphenyl phosphite (TPP): molecular formula $C_{18}H_{15}O_3P$ (shown in Figure 11), MW 310.28 g/mol, boiling point 360 °C,
- tris nonylphenyl phosphite (TNPP): molecular formula $C_{45}H_{69}O_3P$ (as shown in Figure *10*), MW 689.00 g/mol, boiling point 180 °C at 4 hPa,
- diphenyl isodecyl phosphite (DPDP): molecular formula $C_{22}H_{31}O_3P$ (as shown in Figure *13*), MW 374.45 g/mol, melting point 54.75 °C, boiling point 435.74 °C.

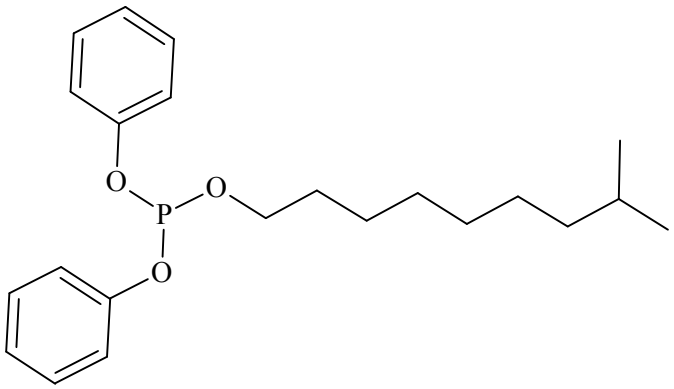

Figure 13 The structure of DPDP

Joncryl ADR-4368 (referred to as Joncryl, shown in Figure 8), with MW 6800 g/mol and T_g 54 °C was purchased from BASF SE and used as recieved. It reacts to increase melt viscosity and intrinsic viscosity in polyesters, while being proven for specific food applications.

Raschig 9000 (referred to as Raschig, shown in Figure 10), a high-molecular-weight ($2–3·10^4$ g/mol) polycarbodiimide was purchased from RASCHIG GmbH and used as recieved. It should work as a chain extender for polyesters and therefore cause a significant increase of intrinsic viscosity and additionally enhanced hydrolytic stability.

Citroflex A-4, chemically acetyltributylcitrate (referred to as ATBC, shown in Figure 14), with MW 402.50 g/mol and boiling point 327 °C was purchased from Vertellus Holdings LLC and used as recieved. It is widely used in children's toys and food contact applications and also as a plasticizer for bioplastics such as a PLA, cellulose acetate and poly(hydroxyalkanoic acids).

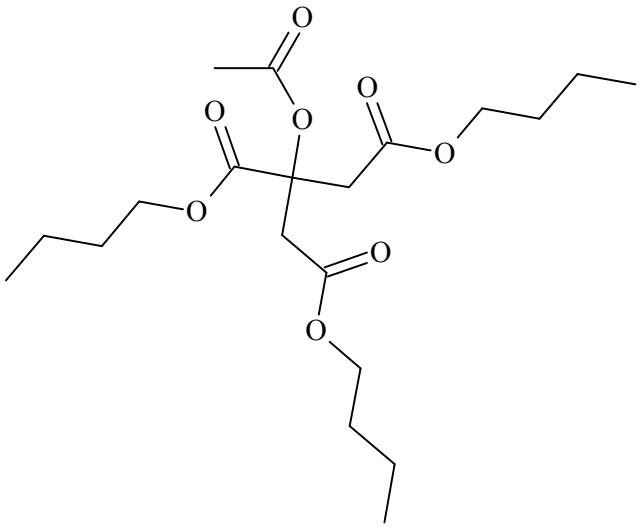

Figure 14 The structure of acetyltributylcitrate

2.2. Characterization methods

2.2.1. Gas chromatography – flame ionization detector

Gas-liquid chromatography (GC; often called just gas chromatography) is analytical separation technique used to separate complex mixtures for both quality and quantity measurements. The mobile phase is a inert gas such as helium and the stationary phase is a high boiling point liquid (for example polydimethylsiloxane) adsorbed onto a solid support in a very thin layer. A flexible tube containing stationary phase is often coiled inside a thermostatically-controlled oven to keep it at a constant temperature. Volatile samples, or samples volatilized by heating, are introduced into the gas phase and flow through the column. Substances with a greater affinity for the mobile phase reach the detector at the end of the column more quickly than those with a greater affinity for the stationary phase.

A flame ionization detector typically uses a hydrogen/air flame, into which the sample is passed to oxidise organic molecules and produces electrically charged particles (ions). The ions are collected to produce an electrical signal which is then measured. The FID is also extremely sensitive to hydrocarbon impurities, which can cause increased baseline noise and reduce the detector sensitivity. This detector is used to quantify residuals and determine the purity profile of the material. This analysis is important mainly for purity determination of PHB. Considering its production process, it may contain traces of residual solvent and biomass or impurities from used equipment, which could influence its behaviour and stability.

Analysis was performed on Hydal 8-10/3V and 2V. Polymer was firstly dried at 105 °C for 12 hours and 9–11 μg of sample was methanolysed at elevated temperatures with 15%wt. solution of sulphuric acid in methanol afterwards. GC-2010Plus machine with ZB-WAX plus 30 m × 0.32 mm column with internal diameter 0.50 μm was used. Temperature programme was set as follows: 5 min at 40°C, then 15°C/min to 260°C and isothermal for 7 min. Dispenser and detector temperatures were set to 250 and 300 °C, respectively. Helium as the eluent at a flow rate of 2.6 ml/min was used. Detection was performed by method of internal standard (99.6 % PHB) with FID detector.

2.2.2. Gel permeation chromatography

Gel permeation chromatography (GPC; also known as size exclusion chromatography, SEC) is a type of high performance liquid chromatography, which can be performed in a wide range of solvents, from non-polar organics to aqueous. It uses columns packed with small, round, porous particles made from polymers that have been cross-linked in order to be insoluble, or inorganic materials, such as spherical silica. Molecules contained in the solvent passing through the particles are separated on the basis of their size. Small polymer creating small coils can enter many pores in the beads and it takes a long time for them to pass through the column. Conversely, large polymer coils that cannot enter the pores take less time to leave the column and they are eluted first. Comparing measured data to a calibration that shows the elution behaviour of a series of polymers for which the MW is known we can determine the MWD of a sample.

This measurement is important for characterization of a raw material to help building a picture of its likely behaviour. The MW values of a polymer are important as they influence

properties such as brittleness, toughness, and elasticity. Analysis was performed on Hydal 8-10/3V. Six samples were taken and subjected to 0–6 heating cycles using conventional DSC (more in chapter 2.2.4.1) and the change in MW and MWD were analyzed.

In case of polymer blends GPC doesn't tell us if the sample contains different compounds. It gives information regardless chemistry of the sample. Analysis was performed on kneaded samples as the ratios in the mixtures are not influenced by an error that may arise in case of extrusion.

The samples were firstly dissolved in chloroform and diluted to a concentration 3–6 μg/ml. Measurements were performed on Agilent Technologies 1100 Series instrument equipped with isocratic pump, fraction collector and autosampler. PLgel 10 μm mixed B column thermostated to 30 °C with chloroform as the eluent at a flow rate of 0.1 ml/min against linear polystyrene standards with narrow distribution were used (10 points in calibration). Instrument is equipped with refractive index detector (RID), which measures the refractive index of an analyte relative to the solvent.

2.2.3. Rheology

Rheology is a science dealing with deformation and flow of matter. Relationships between stresses and deformations are fundamental concepts of continuum mechanics. These relations can be formulated in a standard form as:

$$\sigma = G \cdot \gamma ,$$

$$\sigma = \eta \cdot \dot{\gamma} ,$$

where σ is the shear stress, γ is shear strain (deformation) and $\dot{\gamma}$ is the shear rate. Proportionality constant in the relationship between shear stress and strain is called shear modulus (G). The constant coefficient of proportionality in the relationship between shear stress and rate, η, is called viscosity (or shear viscosity). If the shear stress is not proportional to the shear rate, such liquid is called non-Newtonian and the ratio $\sigma/\dot{\gamma}$ is called apparent viscosity, which is not necessarily constant. Polymer melts or the most polymer solutions are among the Non-Newtonian fluids. Measurements of rheological properties are strongly linked with their molecular structure and conditions. Polymers are viscoelastic fluids, which behave viscous or elastic, depending on how fast they flow or are deformed in the process.

Samples for rheology measurements were prepared by pressing approximately 5 g of the sample from reactive kneading between two metal plates using hydraulic laboratory press machine to prepare films with the thickness of 500 μm. The plates were shaped by pressing into rounded specimens with a diameter 25 mm.

Rotational (Shear) Stress Control (combined motor and transducer, CMT) TA Rheometer AR-G2 with the radiation oven was used for the measurements. Torque range of the instrument is 0.003–200 μN·m, frequency range is $1 \cdot 10^{-7}$–$1 \cdot 10^{2}$ Hz, displacement resolution is 0.025 μRad and normal force range is 0.005–50 N. Environmental Test Chamber (ETC) system was used and parallel plate geometry with diameter 25 mm was chosen for all the measurements, gap was adjusted to appropriate value according to the sample from 0.5–2 mm.

2.2.3.1. Time sweep

Time sweep (TS) of the material is used to determine if properties are changing over the time of testing. Important is stability against thermal degradation. The material response is monitored at a constant frequency, amplitude and temperature.

The TS procedure, which was used for the measurements, is shown in Table 2. To ensure comparable condition for all samples, the first three steps were added to all further experiments. These contained firstly condition step 1, which aimed in pre-heating the sample, while the normal force control was active and set for 1 N with a tolerance of changing the gap limit ± 800 μm. Next step was time sweep 1, where the sample started heating up to the temperature of measurement, while withstanding oscillation with amplitude of deformation 0.1 %strain in order to settle down the sample before measurement. In the third step, condition step 2, active normal force control was turned off ensuring the gap would not be changed during the measurement.

The measurement itself (time sweep 2) was performed for 10 min at 190 °C, frequency used was 0.833 Hz and amplitude of deformation was chosen 300 % in order to simulate conditions during processing.

Time sweep 3 was used for structure recovery in order to distinguish between effect of thermal degradation and structure distortion by the influence of shear. It was performed for 5 min at 190 °C with unchanged frequency however, the strain used was 1 %.

From obtained data, a total drop (from the beginning of the time sweep 1 to the highest point of recovery) and a recovery ability of storage and loss shear modules and complex viscosity are evaluated.

Table 2 Procedure of TS measurements

	1	**2**	**3**	**4**	**5**
	Condition step1	Time sweep 1	Condition step 2	Time sweep 2	Time sweep 3
Temperature (°C)	170	190	190	190	190
Wait for temperature	yes	no	no	yes	no
Control normal force	active	active	non-active	non-active	non-active
Duration (min)	5	2	–	10	5
Frequency (Hz)	–	0.833	–	0.833	0.833
Strain (%)	–	1	–	300	1

2.2.3.2. Frequency sweep

During frequency sweep (FS), the material response to increasing frequency (rate of deformation) is monitored at a constant amplitude and temperature. At high frequencies, the elastic properties dominate. At low frequencies, the viscous properties dominate. The test

assumes stability of the sample. Strain used should be in linear viscoelastic region (LVR), which is a region of small or slowly applied deformations, where the magnitudes of stress and strain are related linearly, and the behaviour for any liquid is completely described by a single function of time. The length of LVR is highly dependent on frequency, higher frequency means shorter LVR.

The FS procedure, which was used for the measurements, is shown in Table 2. The first three steps are the same as in case of TS. Frequency step was performed for frequencies from 0.1 to 20 Hz in order to achieve the widest possible range of frequencies and maintain the experiment length as small as possible and therefore avoid the degradation of the material at the same time.

After that, strain sweep 1 step was added to minimize the number of used samples. Strain sweep with the amplitudes of deformation 0.5–300 %strain and frequency 0.833 Hz was performed. Strain sweep is used to determine LVR for polymers.

Table 3 Procedure of TS measurements

	1	**2**	**3**	**4**	**5**
	Condition step1	Time sweep 1	Condition step 2	Frequency sweep 1	Strain sweep 1
Temperature (°C)	170	190	190	190	190
Wait for temperature	yes	no	no	yes	no
Control normal force	active	active	non-active	non-active	non-active
Duration (min)	5	2	–	–	–
Frequency (Hz)	–	0.833	–	0.1–20	0.833
Strain (%)	–	1	–	1	0.5–300

2.2.4. Thermal characterization

2.2.4.1. Conventional DSC

Differential Scanning Calorimetry, or DSC, is a thermal analysis technique that looks at how a material's heat capacity (C_p) is changed by temperature. A sample of known mass is heated or cooled and the changes in its heat capacity are tracked as changes in the heat flow. This allows the detection of transitions such as melts, glass transitions, phase changes, and curing.

Two types of DSC instruments are widely used: the heat flux DSC and the power compensated DSC. In a heat flux DSC system the sample and reference are heated at the same rate from a single heating. The temperature difference between the pans is recorded and converted to a difference in heat flow. In the second one the sample and reference are heated separately. Thermocouples attached to the disk platforms measure the differential heat flow. The heat flow to each pan is adjusted to keep their temperature difference close to zero, while the furnace temperature is increased linearly.

TA Instruments model DSC 2920 was used for the measurements. Hydal 8-10/3V underwent following heat programme:

- equilibrate as 40 °C,
- temperature ramp to 190 °C at a heating rate 10 °C/min under nitrogen atmosphere,
- cooling to 40 °C,
- repeating cycle for 0–5 times (1–6 heating cycles).

2.2.4.2. Modulated differential scanning calorimetry

Thermal properties of prepared samples were determined using modulated differential scanning calorimetry (MDSC). The interpretation of non-modulated DSC results is difficult due to various transformations occurring simultaneously during heating. MDSC has an ability to distinguish apparent thermodynamic (reversing signal) and kinetic (non-reversing signal) events under the prevailing DSC modulation conditions. Three types of curves can be derived from the experiments: total heat flow or heat capacity curve (C_p^{total}, the same as a conventional DSC curve), the in-phase curve (reversing or storage C_p) and out-of-phase curve (loss C_p). In addition, a non-reversing heat capacity (kinetic) curve can be obtained from the difference between the total C_p and reversing C_p. Glass transition temperature T_g, melting temperature T_m and cold crystallization temperature T_c were determined from MDSC curves. Crystallinity X_c was calculated from measured data using the following equation:

$$X_c = \frac{\Delta H_m}{\Delta H_m^0} \cdot 100\ \%,$$

where ΔH_m, and ΔH_m^0 (J/g) are enthalpies of melting and enthalpy of melting 100% crystalline polymer (93.1 and 146 J/g for PLLA and PHB, respectively).

Measurements were performed on TA Instruments model Q200 DSC with refrigerated cooling. All samples were firstly heated to 190 °C (10 °C/min) to remove thermal history followed by a cooling scan (5 °C/min) to −50 °C. Then MDSC measurements were obtained for heating scans from −50 °C to 190 °C, at an average heating rate of 3 °C/min with a period of 20 s and modulation amplitudes of 0.8 °C.

All measurements were carried under nitrogen atmosphere. Polymer sample masses varied from 5 to 10 mg. Aluminium pans with samples were sealed before measurement. The top part of the pan was pressed down to improve thermal contact with the sample, taking care that the flatness of the bottom face contacting the temperature sensor in the chamber was maintained.

2.2.4.3. Thermogravimetry

Thermogravimetry (TG) is used to measure the mass or change in mass of a sample as a function of temperature or time or both. Measurements are used primarily to determine the composition of materials and to predict their thermal stability at temperatures up to 1000 °C. Nevertheless, changes in mass occur during sublimation, evaporation, decomposition, and chemical reaction, magnetic or electrical transformations. From the TG curve of a loss of mass step, T_o (onset of change) and T_{mp} (midpoint) are evaluated.

Crucial factors are the choice of purge gas and the conditions present in the specimen chamber. The purge gases consist of inert or oxidizing gases, such as nitrogen, helium, argon and oxygen, or air.

Measurements were performed using Q500/ Q50 TGA thermogravimetric analyzer with a responsive low-mass furnace; sensitive thermobalance, and efficient horizontal purge gas system (with mass flow control). Used heat programme was as follows:

- equilibrate as 40 °C,
- temperature ramp to 550 °C at a heating rate 10 °C/min under nitrogen atmosphere,
- change to oxidative air atmosphere,
- temperature ramp to 600 °C at a heating rate 10 °C/min.

2.2.5. Mechanical and thermo-mechanical testing

2.2.5.1. Dynamic mechanical analysis

Dynamic mechanical analysis (DMA) is a basic tool used to measure the viscoelastic properties of materials (particularly polymers). DMA instrument applies an oscillating force of a defined amplitude and frequency to a sample of known geometry and measures its response. The mechanical modulus of the material can be expressed as an in-phase component, the storage modulus (G'), and an out of phase component, the loss modulus (G''). The storage modulus is the measure of the sample's elastic behaviour. The ratio of the loss to the storage is the tan delta and is often called damping. It is a measure of the energy dissipation of a material.

Modulus values change with temperature and during transitions in materials. For example the glass transition, can be seen as changes in the G' or tan delta curves.

DMA measurements were obtained with DMA 2980 device from TA Instruments. Single cantilever geometry was used with a deformation frequency 1 Hz and amplitude of deformation 25 μm. Testing specimens with typical dimensions 30×12×2 mm were prepared from extruded flat tapes. Used rating programme was as follows:

- equilibrate at 40 °C,
- heating to 150 °C (130 °C for PLA samples) with a rating rate 5 °C/min.

2.2.5.2. Tensile testing

Tensile test is a standard engineering procedure to characterize properties related to mechanical behaviour of materials. The properties describe the response of the material during the actual loading conditions. The variation in geometry of the specimen has to be considered. Tensile tests are simple, relatively inexpensive, and fully standardized. Under pulling type of loading it can be quickly determined how the material will react to the type of forces being applied in tension. Tensile test allows to determine tensile (Young's) modulus of elasticity E and other material's mechanical characteristics like yield stress σ_y or strain at yield point ε_y, where first macroscopic plastic deformation occurs, strength of material σ and strain at break ε. These mechanical characteristics further determine the usage of material for specific application.

Testing specimens with typical dimensions 75×12×2 mm were prepared from extruded flat tapes. Zwick-Roel Z010 device was used for tensile testing. Load indicator with maximum 10 kN and grips with 10 kN maximum workable force were used for the measurements. Testing speed was set to 10 mm/min. The device is not equipped with extensometer for Young's elastic modulus determination.

2.2.6. Scanning electron microscope

The scanning electron microscope (SEM) uses a focused beam of electrons to generate a signal at the surface of specimens. Electrons are accelerated and carry significant amounts of kinetic energy. As they decelerate in the solid specimen, their energy is dissipated and a variety of interactions occur between electrons and sample. These signals include secondary electrons (that produce SEM images), backscattered electrons (BSE), X-rays, diffracted backscattered electrons (EBSD that are used to determine crystal structures and orientations of minerals), photons, visible light, and heat. Secondary electrons and backscattered electrons are commonly used for imaging samples: secondary electrons are most valuable for showing morphology and topography on samples and backscattered electrons are most valuable for illustrating contrasts in composition in multiphase samples. Emitted X-ray spectrum is used to obtain a localized chemical analysis by identification of the lines in the spectrum by Energy Dispersive X-ray Spectrometry (EDS or EDX). All elements from atomic number 4 to 92 can be detected in principle. Only one, but important disadvantage of SEM is requirement of conductivity of sample. That does not mean, that nonconductive samples cannot be imaged (or measured), but surface of the sample must be coated with a conductive layer.

In most applications, data are collected over a selected area of the surface of the sample, and a 2-dimensional image is generated that displays spatial variations in these properties. Areas ranging from approximately 1 cm to 5 microns in width can be imaged in a scanning mode using conventional SEM techniques

Samples were freeze fractured under liquid Nitrogen and attached to aluminium disc. Afterwards, fractured areas were coated with Pt/Pd layer under Argon atmosphere using BALZERS sputtering device. JEOL 7500F microscope with resolution up to 1 nm was used for observations of samples' morphology. Microscope is equipped with a system of several detectors that make secondary electron images and in addition with RIBE and LABE detectors for backscattered electrons. Used accelerating voltages in kV, working distances in mm (WD) and magnification are in the bottom part of the pictures.

2.3. Reactive kneading

Samples of both polymers with reactive agents were prepared using a 50 ml internal chamber Brabender laboratory kneader operating at 200 °C (oil temperature) and 45 RPM. Total sample weight was kept 30 g. Polymer was fed into the chamber within two minutes and was homogenized continuously for 1 min. At the time of three minutes reactive agent was added to the mixture. The time evolution of the torque (N·m) was recorded during the whole processing experiment. Polymer granules were dried in an oven at 60 °C for 2 h before processing.

Firstly neat polymers were mixed with reactive agents and time evolution of the reaction was studied *in situ* by torque measurements for 5 minutes after feeding, which is sufficient for the reaction to proceed. From these measurements, one reactive agent was chosen for series of reactive and nonreactive blends preparation.

2.4. Sample preparation

A day before processing itself, series of reactive and non-reactive blends were firstly weighed and mixed. Due to the lack of material, 300 g of each mixture was prepared. Afterwards they were dried in polymer dryer at 80 °C for four hours and sealed together with silica gel in order to remain dry.

In the first step, so prepared samples were reactively extruded using Brabender® co-rotating meshing twin screw extruder TSE 20/40 with Brabender® Plasti-Corder Lab-Station driving unit (see Figure 15). The temperature profile was set from hopper to die as 138 °C - 158 °C - 165 °C - 165 °C - 165 °C in the five different extrusion areas, rotational speed was kept 150 RPM to ensure the same mixing time for all samples. Brabender® DDW-MD0-MT-0.5 gravimetric feeder was used to dose the mixtures in a rate from 0.2–0.7 kg/h. The feeding was held under nitrogen atmosphere. Extruded profiles were put into water bath with a temperature 60 °C in order to finish the crystallization process, air dried and fed into the pelletizing machine.

In the second step, granules of extruded blends were processed under the same conditions with addition of plasticizer. In this case extruder was equipped with extrusion die for flat tape profile processing. However, because of dysfunction of diaphragm pump for dosing, the plasticizer couldn´t be fed directly into the extruder. Instead, it was mixed with granules and the mixtures were fed manually. This caused insufficient mixing of the plasticizer in the blends as the majority of it remained in the feed throat enabling further feeding.

Figure 15 Brabender® twin screw extruder system, Central European Institute of Technology Brno

3. RESULTS AND DISCUSSION

3.1. Raw material characterization

3.1.1. PHB Hydal

Since the polymer that has been used has not been purchased commercially, but comes from the Nafigate pilot plant, it was necessary to perform the initial characterization of the material for each batch.

GC-FID analysis determined 98.2 %wt. of pure PHB in dry matter of Hydal 8-10/2V and 99.5 %wt. for the sample of 8-10/3V.

As described in the theoretical part of this work, PHB is highly sensitive to thermal degradation, which occurs during every heat treatment including processing and sample preparation. Changes in polymer properties with heating cycles were studied by means of DSC measurements combined with GPC analysis. Crystallization exotherms of cycled samples are shown in Figure 16. As can be seen from the figure, crystallization mechanism of PHB was affected. Broadening of peaks can be observed and the crystallization temperature (T_c) decreased from 110.2 °C (1 cycle) to 91.5 °C (6 cycles). Melting point dropped from 176.6 °C (1 cycle) to 172.5 °C (6 cycles).

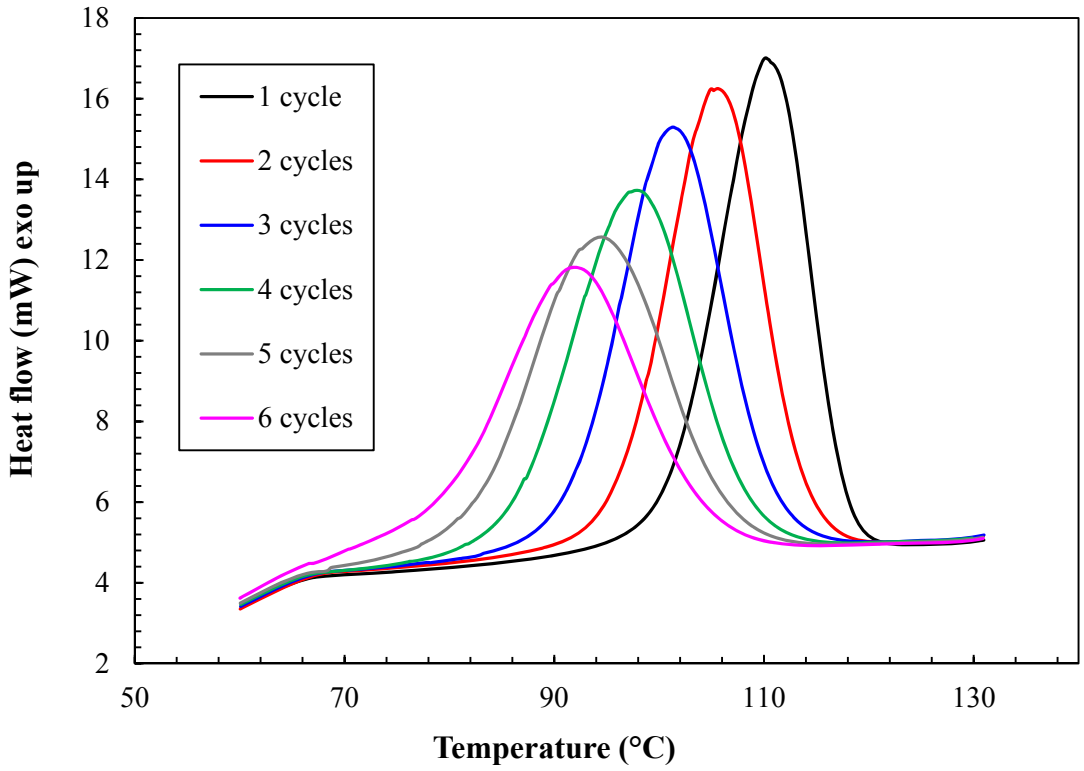

Figure 16 Crystallization exotherms of Hydal 8-10/3V for 1–6 heating cycles

GPC measurement confirmed expected drop in MW (number average was decreased to 21 % of initial value) and narrowing of MWD caused by random cleavage of PHB chains. Figure 17 shows MWD change for all samples including raw polymer (marked 0 cycles). MW averages and polydispersity index (PDI) obtained by GPC analysis are listed in Table 4.

Table 4 GPC analysis of cycled samples of Hydal 8-10/3V

Cycles	0	1	2	3	4	5	6
M_n (g/mol)	177,900	106,700	72,760	75,750	56,920	37,480	37,590
M_w (g/mol)	526,100	275,700	183,700	158,000	123,800	97,540	87,660
M_z (g/mol)	1,177,000	542,500	357,200	276,700	220,500	186,200	153,600
PDI	2.96	2.58	2.53	2.09	2.18	2.60	2.33

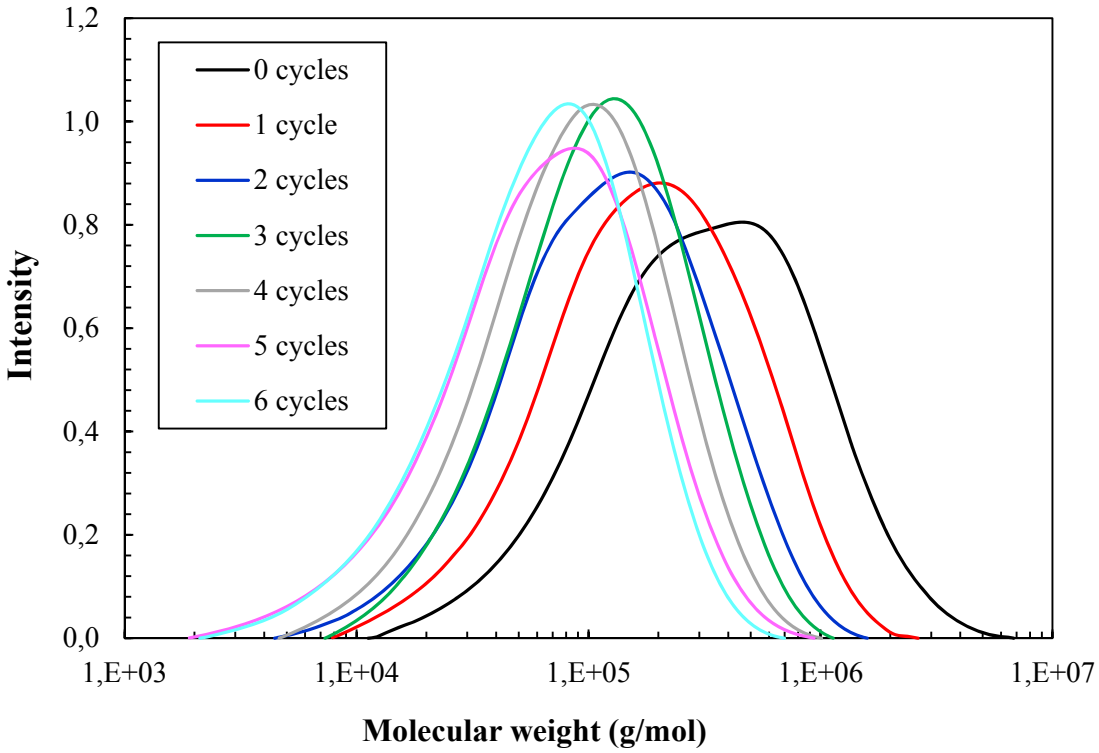

Figure 17 MWD of Hydal 8-10/3V after 0–6 heating cycles

From rheology TS measurements, thermal stability of the polymer under mechanical stress was determined. The values of the drop of $|\eta|$, G' and G'' and the overall recovery capacity are given in Table 5. Complex viscosity and loss modulus dropped by 89 % and their recovery ability is 3 %. Total decrease of storage modulus was 98 % and recovery ability 1 %. This suggests thermal degradation of sample during the measurement.

Table 5 Results of TS of Hydal 8-10/3V

	Total drop by (-)			Recovery ability (-)		
Sample	$\lvert\eta^*\rvert$	G'	G''	$\lvert\eta^*\rvert$	G'	G''
1	0.89	0.98	0.88	0.02	0.00	0.02
2	0.90	0.98	0.90	0.03	0.01	0.03
3	0.88	0.97	0.88	0.03	0.01	0.03
average	0.89	0.98	0.89	0.03	0.01	0.03

3.1.2. PLA

In case of PLA, MW analysis was performed using GPC. Results are listed in Table 6.

Table 6 MW of PLA analyzed by GPC

M_n (g/mol)	80,200
M_w (g/mol)	179,400
M_z (g/mol)	320,200
PDI	2,24

3.2. *In situ* reactions with reactive agents

Firstly, mixtures of both neat polymers with selected reactive agents were prepared. Three phosphite reagents were studied, namely TPP, DPDP and TNPP, from which the reaction of TPP and TNPP with PLA has already been described in literature (see chapter 1.2.2). Moreover, Joncryl and Raschig are both proven to react with PLA. In order to find suitable compatibilizing agent for PHB/PLA blends, it is necessary to choose a reagent reactive with both polymers. The amount of reagent 2%wt. was chosen according to literature and reaction time 5 minutes was chosen on the basis of previous experiments so that time for the reaction is sufficient. The list of prepared samples is shown in Table 7. In sample name, K stands for kneaded samples, following number denotes PHB/(PHB+PLA) weight ratio and at the end there is reactive agent abbreviation.

Table 7 The list of samples of PHB and PLA with different additives

Sample name	**Amount (%wt.)**							**Reaction time (min)**
	PHB	**PDLLA**	**TPP**	**DPDP**	**TNPP**	**Joncryl**	**Raschig**	
K100	100							5
K100TPP	98		2					5
K100DPDP	98			2				5
K100TNPP	98				2			5
K100J	98					2		5
K100R	98						2	5
K0		100						5
K0TPP		98	2					5
K0DPDP		98		2				5
K0TNPP		98			2			5
K0J		98				2		5
K0R		98					2	5

Melt torque of samples during the compounding was recorded and showed expected decrease in time due to thermal degradation. Parts of the curves after feeding were normalized by subtracting the values of neat polymer in order to evaluate the difference between individual additives. The graphs for PHB and PLA with additives are shown in Figure 18 and Figure 19, respectively.

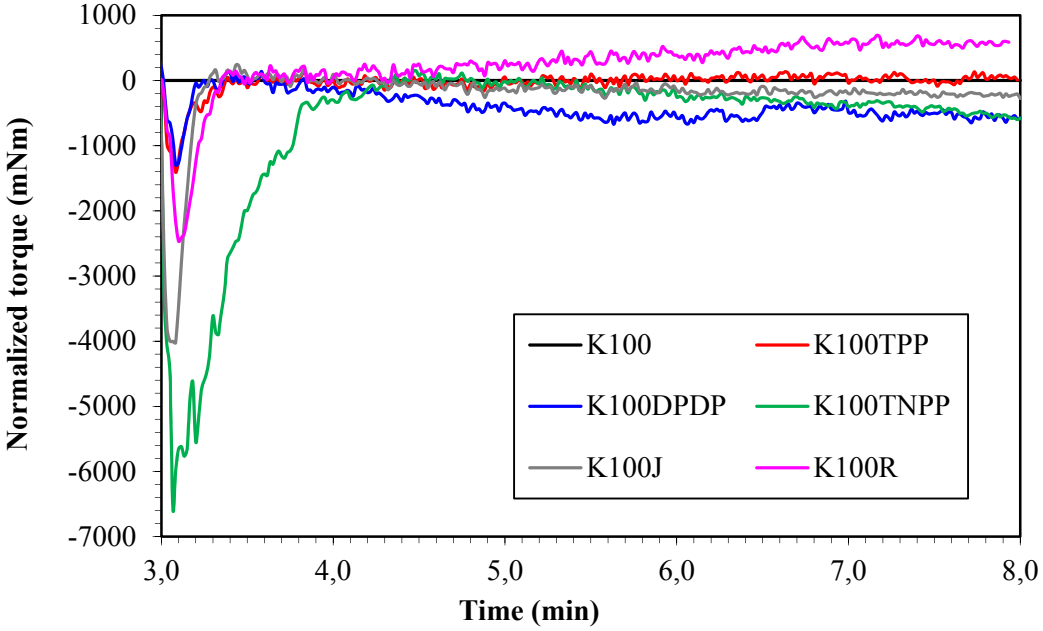

Figure 18 Differential curves of time evolution of torque during processing of reactive PHB samples

As can be seen from Figure 18, only Raschig showed enhanced melt viscosity compared to neat PHB indicating their reaction. As for DPDP, TNPP and Joncryl, melt torque showed more rapid decrease than in case of neat PHB. This may be explained by pro-degrading or lubricating effect of the agents. TPP did not influence torque values.

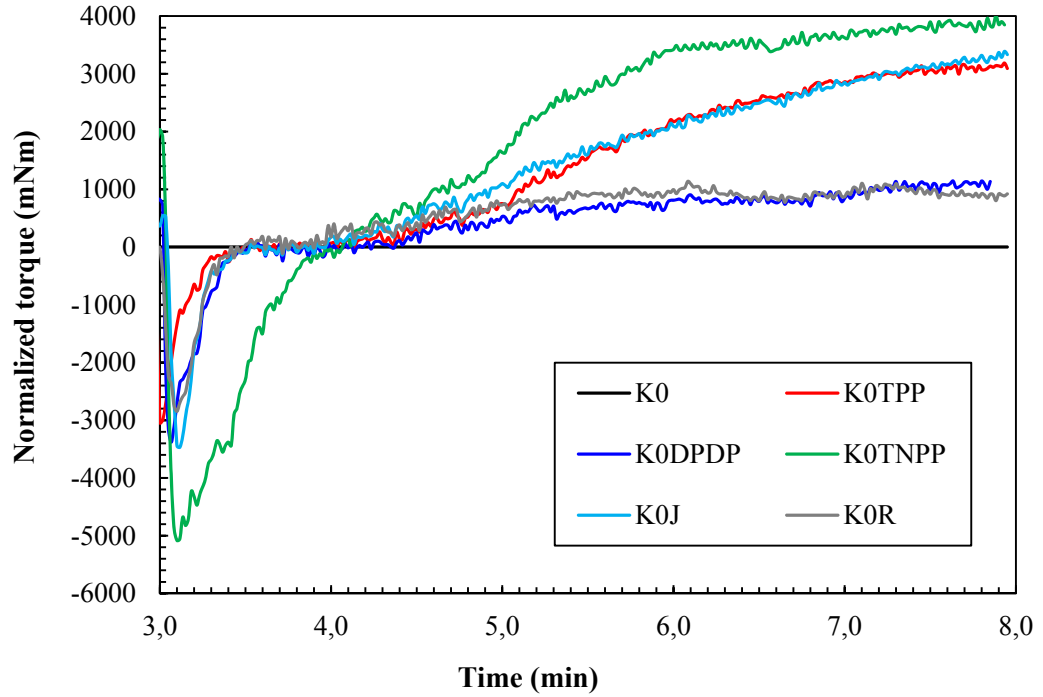

Figure 19 Differential curves of time evolution of torque during processing of reactive PLA samples

PLA showed increased melt viscosity as measured by torque with all studied additives. With TNPP added, the curve showed rapid increase which mitigated three minutes after feeding and then continued mildly. For samples with TPP and Joncryl, melt torque began to rise one minute after feeding and continued with steady increase. In case of TPP, the curve settled in the end of the experiment. Time evolution of torque for samples of PLA with DPDP and Raschig showed increase in period of approximately 1–2 minutes after feeding and then remained steady.

3.3. PHB/PLA kneaded blends

For purpose of studying PHB/PLA blends, mixtures with three different weight ratios of polymers were prepared. On the basis of previous experiments, for preparation of reactive blends Raschig was selected as it is supposed to react with both PHB and PLA. Amount of reagent 2%wt. and reaction time 5 minutes was left untouched. Samples of prepared blends with corresponding PHB/(PHB+PLA) weight ratios and weight composition of samples are listed in Table 8. Time evolution of torque for all blends is shown in Figure 20.

Table 8 The list neat and reactive PHB/PLA blends

Sample name	PHB/(PHB+PLA) ratio	Amount (%wt.)			Reaction time
		PHB	PDLLA	Raschig	
K70	70/100	70	30		5
K50	50/100	50	50		5
K30	30/100	30	70		5
K70R	70/100	68.6	29.4	2	5
K50R	50/100	49.0	49.0	2	5
K30R	30/100	29.4	68.6	2	5

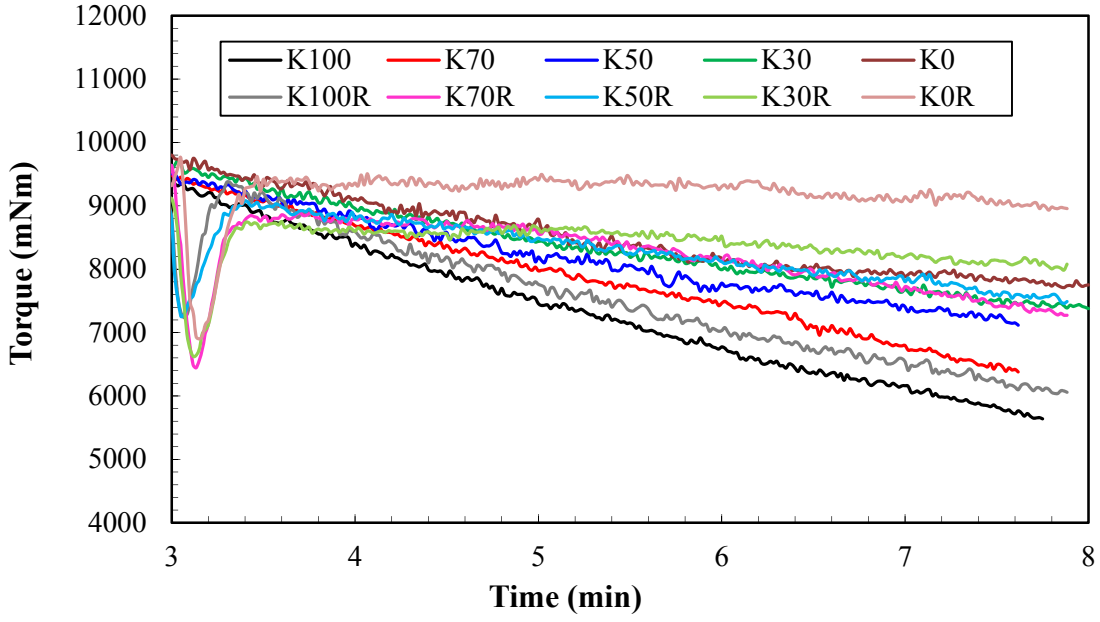

Figure 20 Torque values of mixer during processing of PHB/PLA blends

As can be seen from the picture, decrease in torque values attributed to decrease in viscosity is the most significant in case of neat PHB and became slower proportionally with addition of PLA, which is less sensitive to thermal degradation than PHB. With addition of Raschig melt viscosity was enhanced for all blends. However, except of K0R containing PLA with Raschig, degradation reaction still competes with extending reaction.

3.4. Characterization of kneaded samples

3.4.1. Rheology time test

As already mentioned and depicted, both polymers and mainly PHB are susceptible to thermal degradation. This was evaluated by calculating a total drop and recovery ability for storage and loss shear modules and complex viscosity from obtained data. Table 9 shows results of the measurements.

As for nonreactive series of samples, an overall decrease of complex viscosity and loss modulus is lower with increasing amount of PLA. Furthermore, recovery ability of this parameter is higher with increasing amount of PLA. This supports the idea that PLA is more thermally stable and its viscosity and loss modulus drop during time sweep was rather caused by entanglement and molecule orientation than thermal degradation. Similar trend is observed for storage modulus, except for K100 (kneaded PHB), where total drop was 79 %, which is 19 % less than for raw PHB. Also recovery ability of G′ is 19 % whereas 0 % for raw material and therefore a measurement error is expected.

Reactive series of samples demonstrate similar trends. Decrease in characteristic rheological parameters is lower with increasing PLA amount apart from complex viscosity and loss modulus of K0R sample (PLA with Raschig). The ability of structure recovery is increasing with increasing PLA weight percentage for all samples but storage modulus of K100R.

Due to probable error of K100 measurement, K100R was compared with raw PHB. Addition of Raschig led to smaller relative drop of observed parameters and higher recovery ability of elastic component and therefore enhanced rheological stability. Similarly, in case of PHB/PLA blends in all ratios, Raschig caused less sensitivity to thermal degradation against neat blends. As for K0 (kneaded PLA), complex viscosity and loss modulus drop was higher for reactive sample. However, their recovery ability remained comparable. Storage modulus total decrease was 13 % in case of K0, while 0 % for K0R meaning it was fully recovered. This indicates improved thermal stability and melts strength of PLA with Raschig.

Table 9 Results of TS of kneaded samples

Sample name	PHB/(PHB+PLA) ratio	Total drop by (-)			Recovery ability (-)		
		$\lvert\eta^*\rvert$	G'	G''	$\lvert\eta^*\rvert$	G'	G''
K100	100/100	0.89	0.79	0.89	0.00	0.19	0.00
K70	70/100	0.83	0.94	0.83	0.00	0.02	0.00
K50	50/100	0.76	0.89	0.76	0.01	0.03	0.01
K30	30/100	0.62	0.77	0.62	0.00	0.06	0.00
K0	0/100	0.18	0.13	0.18	0.49	0.69	0.49
K100R	100/100	0.79	0.82	0.79	0.01	0.13	0.01
K70R	70/100	0.76	0.86	0.76	0.00	0.04	0.00
K50R	50/100	0.70	0.73	0.70	0.13	0.16	0.13
K30R	30/100	0.36	0.05	0.36	0.37	0.71	0.36
K0R	0/100	0.42	0.00	0.43	0.48	0.89	0.47

Typical record for time sweep measurement is shown in Figure 21 for samples K50 and K50R. The rest of the graphs is enclosed in appendix 1-4. Absolute values of rheological parameters are higher with Raschig for all samples except K100 and K100R. K100R sample showed lower initial complex viscosity and loss modulus comparing to K100. Nevertheless, the slope of decrease was lower for K100R suggesting Raschig's thermal stabilizing function. It is interesting to note, that samples with PHB/(PHB+PLA) ratio 50/50, K50 and K50R, obtain higher values of viscosity and storage modulus than PLA samples, K0 and K0R.

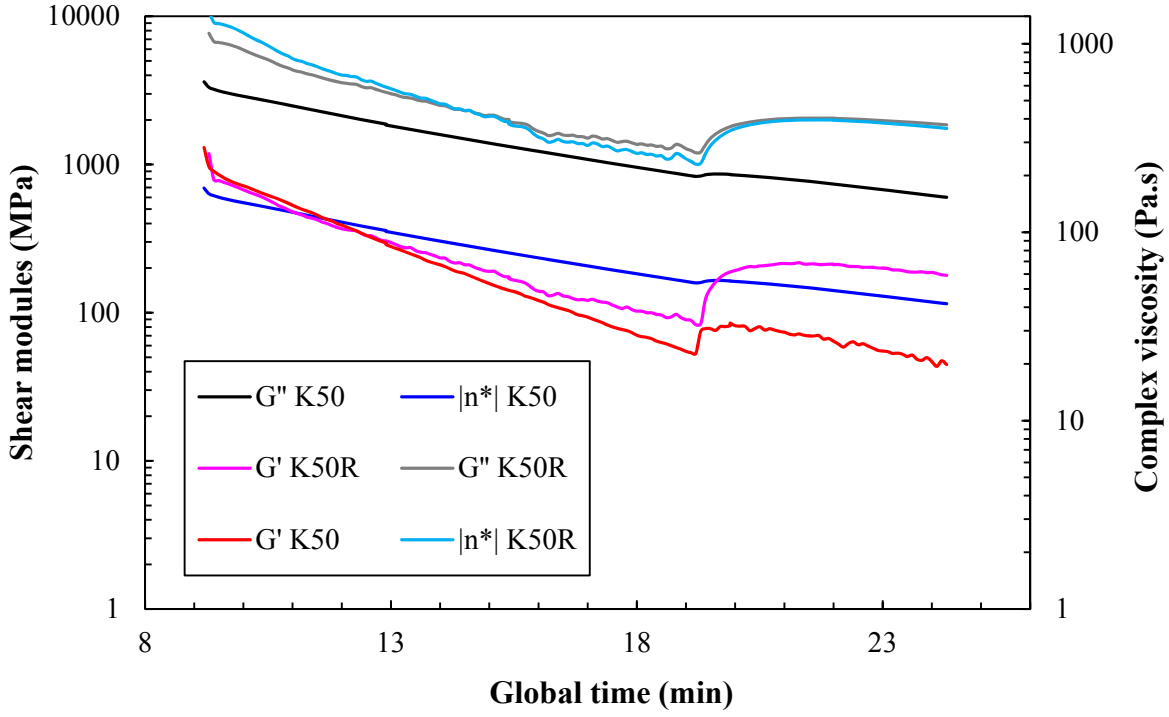

Figure 21 Time sweep measurement for samples K50 and K50R

3.4.2. Frequency sweep

Data obtained from frequency sweep of prepared blends were evaluated by means of G′ and G″ crossover point. The crossover frequency is indirectly proportional to the MW and the crossover modulus is indirectly proportional to the width of the MWD. It is not possible to determine absolute values of MW without calibration, however, blends with matching PHB/(PHB+PLA) ratio can be compared. In Table 10, there are coefficients of linear regressions for relations between dynamic modules and angular frequency $\log(G') = f(\log(\omega))$ and $\log(G'') = f(\log(\omega))$ as well as calculated values of intersection angular frequency and modulus. These results indicate higher MW for reactive samples as their crossover angular frequency is lower in comparison with non-reactive samples. In addition, for all reactive samples except K70R crossover modulus was shifted to lower values suggesting broader MWD than non-reactive samples.

Table 10 Measured and calculated data for frequency sweep analysis

Sample name	PHB/(PHB+PLA) ratio	G'		G''		Crossover point	
		y-intercept	slope	*y*-intercept	slope	Angular frequency (rad/s)	Modulus (Pa)
K100	100/100	1.63	0.83	−0.58	1.34	$2.05 \cdot 10^4$	$1.56 \cdot 10^5$
K70	70/100	0.68	1.31	2.36	0.83	$3.44 \cdot 10^3$	$2.03 \cdot 10^5$
K50	50/100	1.74	1.31	3.01	0.83	$4.81 \cdot 10^2$	$1.73 \cdot 10^5$
K30	30/100	0.61	1.30	2.27	0.87	$7.63 \cdot 10^3$	$4.60 \cdot 10^5$
K0	0/100	0.87	1.39	2.46	0.91	$2.16 \cdot 10^3$	$3.13 \cdot 10^5$
K100R	100/100	0.17	1.36	2.03	0.84	$4.12 \cdot 10^3$	$1.19 \cdot 10^5$
K70R	70/100	1.74	1.19	2.93	0.79	$1.02 \cdot 10^3$	$2.04 \cdot 10^5$
K50R	50/100	2.33	1.17	3.33	0.76	$2.68 \cdot 10^2$	$1.48 \cdot 10^5$
K30R	30/100	2.11	1.16	3.12	0.82	$9.73 \cdot 10^2$	$3.75 \cdot 10^5$
K0R	0/100	2.16	1.25	3.25	0.82	$3.18 \cdot 10^2$	$1.97 \cdot 10^5$

Assuming the validity of Cox-Merz rule, measured results were transformed into relations of viscosity on flow rate, flow curves. They are depicted in Figure 22 and Figure 23 for non-reactive and reactive blends, respectively. No distinct shear thinning was observed. Low shear viscosities are descending with PHB/(PHB+PLA) ration in the following order: 50/50, 0/100, 70/100, 30/100, 100/100 for non-reactive samples and 50/50, 0/100, 30/100, 70/100, 100/100 for reactive series. At the same time, samples with Raschig exhibit higher viscosity for compositions.

However, it is assumed that competing reactions of chain cleavage due to thermal degradation and reaction between Raschig and both components take place during measurement.

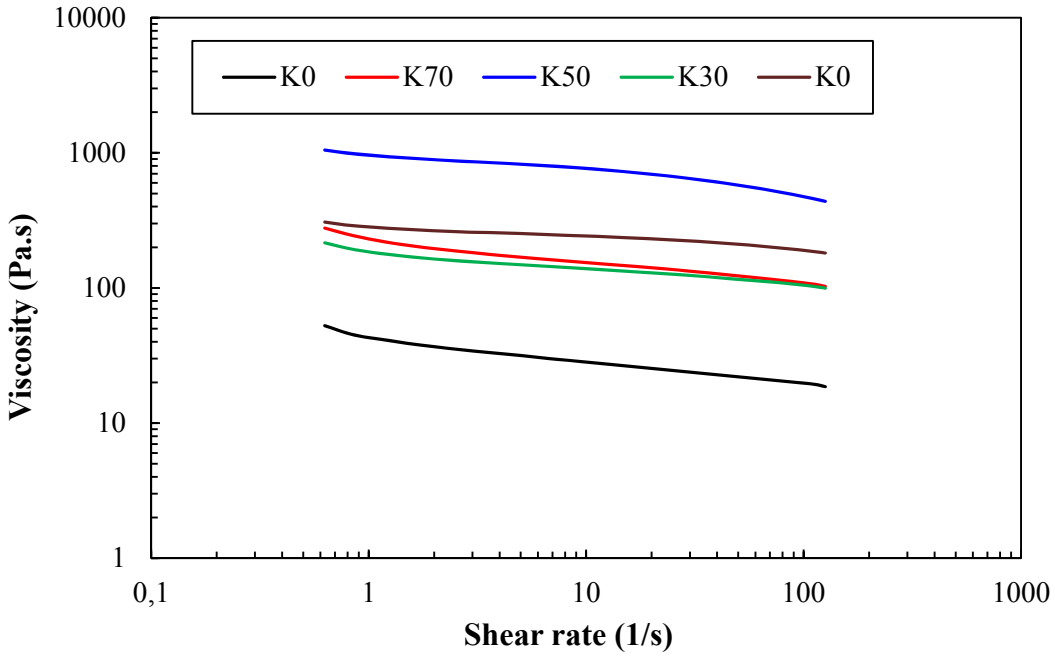

Figure 22 Cox-Merz curves for non-reactive series

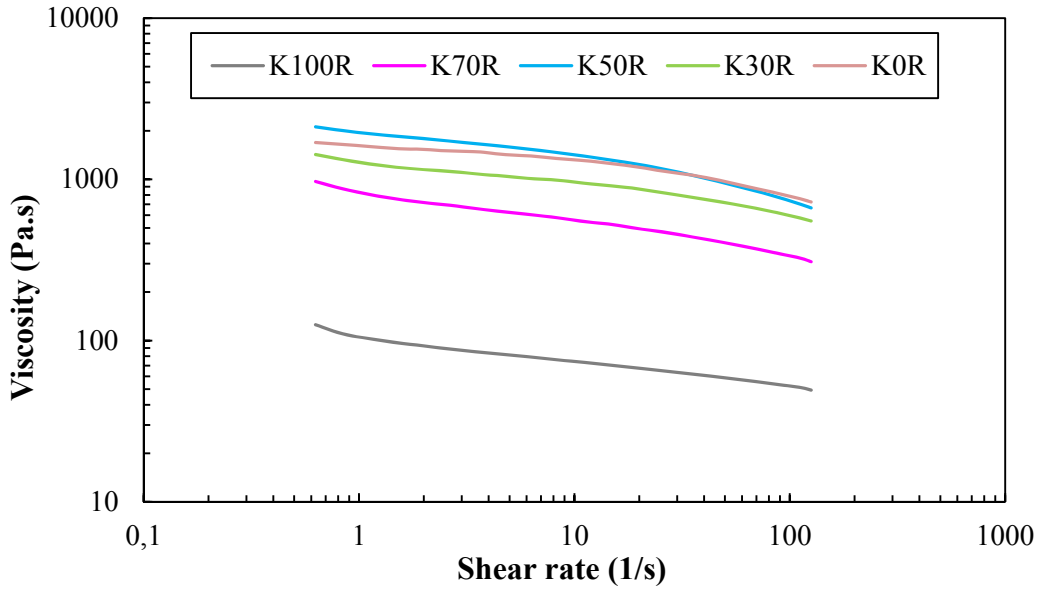

Figure 23 Cox-Merz curves for reactive series

3.4.3. Molecular weight determination

In an effort to identify changes in molecular structure of reactive samples which resulted in change of the rheology, molecular weight determination was performed. Measurement results for all samples are shown in Figure 24 and obtained MW averages and polydispersity indexes (PDI) are listed in Table 11. As for nonreactive series, MW averages decrease with increasing PLA amount according to the mixing rule. MWD is distinctly broader for all samples containing PHB, than for K0 (kneaded PLA). With addition of Raschig, MW averages are shifted to lower values. Moreover PDI values are increased with addition of Raschig meaning a broader distribution.

Table 11 Results of GPC analysis of kneaded samples

Sample name	PHB/(PLA+PHB) ratio	M_n (g/mol)	M_w (g/mol)	M_z (g/mol)	PDI
K100	100/100	121,800	315,100	621,200	2.59
K70	70/100	108,800	284,900	565,300	2.62
K50	50/100	100,700	263,500	536,700	2.62
K30	30/100	91,390	228,400	458,000	2.50
K0	0/100	95,370	193,500	328,200	2.03
K100R	100/100	77,300	296,800	601,200	3.84
K70R	70/100	71,280	270,000	559,600	3.79
K50R	50/100	68,320	253,100	524,200	3.71
K30R	30/100	66,950	229,700	471,800	3.43
K0R	0/100	61,350	190,000	338,400	3.10
Raschig	–	15,350	41,350	104,300	2.69

As can be seen from the figure, for reactive samples occurrence of molecules with lower MW than in case of the nonreactive samples is observed. Moreover, low-molecular fraction is present in larger quantities causing broader MWD. As reported in Raschig data sheet, its M_n is $2–3 \cdot 10^4$ g/mol, which was confirmed by GPC measurement (see Table 11). Therefore, low-molecular fraction present in reactive samples is attributed to existence of the separate peak of non-reacted Raschig. This caused distinct decrease in number average MW observed for reactive samples as this attribute is sensitive to the presence of low-molecular weight fraction. The decrease in M_w and M_z is less significant and is smaller with increasing amount of PLA. This leads to the conclusion that no rapid change in MW occurred with Raschig addition.

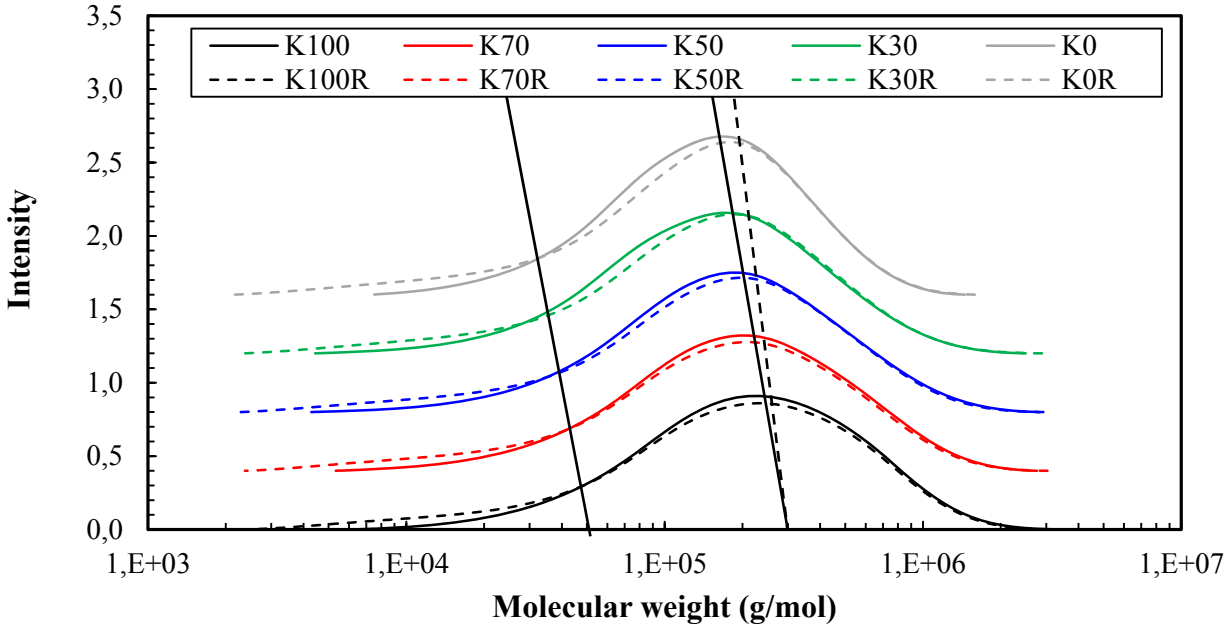

Figure 24 GPC measurements of kneaded samples

3.4.4. MDSC measurement

The study of change of thermal properties was performed by MDSC measurements with results in Table 12. Amount of PHB crystalline phase was calculated using the formula referred in chapter 2.2.4.2.

For nonreactive series, crystallization temperature is decreased with addition of PLA indicating slightly influenced crystallization kinetics of PHB in presence of the amorphous PLA phase. Crystallization heat is decreased proportionally to addition of PLA. Glass transition temperatures were obtained from reversing MDSC curves being difficult to detect for PHB due to its low amount of mobile amorphous phase. T_g values for both polymers did not show any distinct trend. Melting temperature corresponding to PHB remained unchanged around 170 °C and melting enthalpy decreased proportionally to increasing amount of PLA meaning the overall crystallinity of PHB was not changed. With addition of Raschig, there was no significant change in thermal properties of neat polymers and their blends.

Table 12 Results of MDSC analysis of kneaded samples

Sample name	PHB/(PLA+PHB) ratio	T_c (°C)	H_c (J/g)	T_g PHB (°C)	T_g PLA (°C)	T_m (°C)	H_m (J/g)	X_c (%)
K100	100/100	113	81	10		171	103	70
K70	70/100	108	58	12	58	170	76	75
K50	50/100	110	41	13	58	170	52	71
K30	30/100	107	20	10	57	170	31	71
K0	0/100				58			
K100R	100/100	112	80	13		170	103	70
K70R	70/100	111	57	14	57	170	74	72
K50R	50/100	110	39	10	57	170	51	70
K30R	30/100	106	24	7	57	169	33	75
K0R	0/100				58			

Typical curve obtained from MDSC measurement is shown in Figure 25 for samples K50 and K50R, while the rest is enclosed in appendix 5-8. Glass transitions for both polymers are visible on a total heat curve, one in range between 0 and 25 °C (for PHB) and the second between 50 and 60 °C (for PLA). PHB exhibits characteristic double melting peak in both cases. This is caused by recrystallization from the melt, which is supported by presence of the exothermic crystallization peak in the melting region.

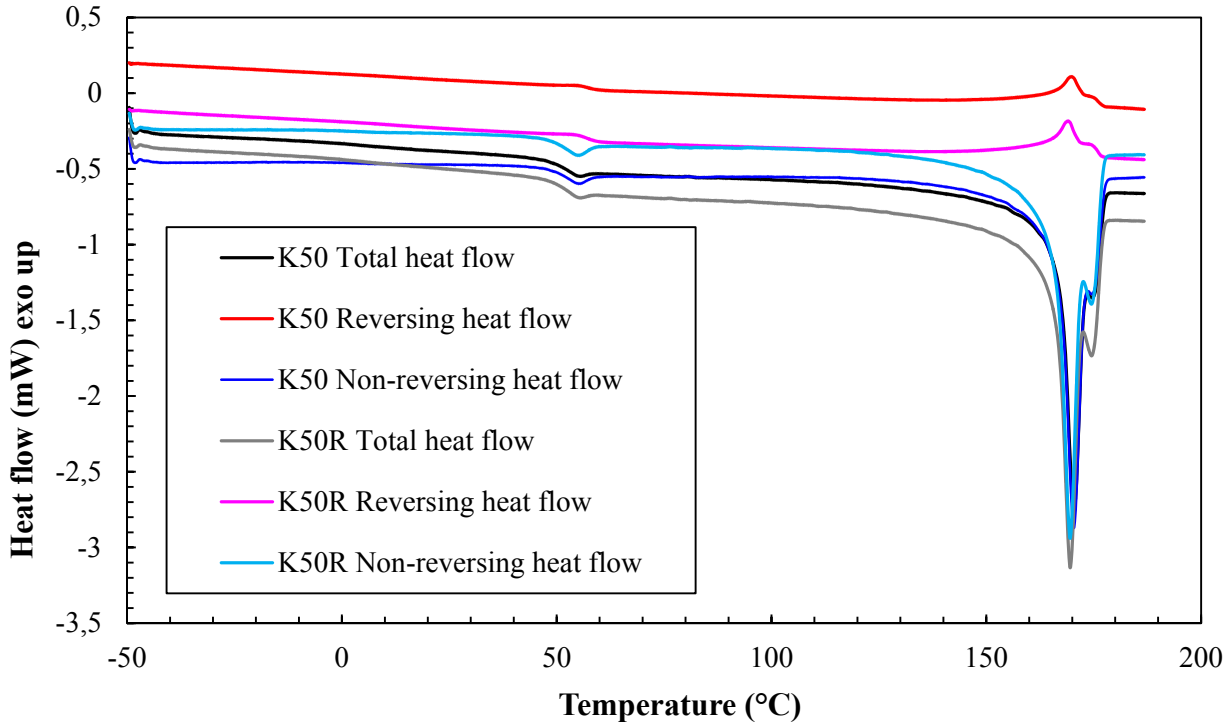

Figure 25 Typical MDSC curve for K50 and K50R sample

3.5. Samples prepared by twin-screw extrusion

In order to study the behaviour of tested materials during conventionally used processing technique for polymers and to determine their mechanical properties, series of extruded samples were prepared. As visible from Table 13, firstly prepared granules are marked with a letter G and flat tapes processed from granules mixed with plasticizer in second cycle are marked T.

Table 13 The list of samples prepared during twin-screw extrusion

PHB/(PLA+PHB) ratio	Sample name	Amount (%wt.)			Sample name	Amount (%wt.)	
		PHB	PDLLA	Raschig		G sample	Citrate A4
100/100	G100	85.0			T100	85	15
70/100	G70	59.5	25.5		T70	85	15
50/100	G50	42.5	42.5		T50	85	15
30/100	G30	25.5	59.5		T30	85	15
0/100	G0		85.0		T0	85	15
100/100	G100R	83.0		2	T100R	85	15
70/100	G70R	58.1	24.9	2	T70R	85	15
50/100	G50R	42.5	42.5	2	T50R	85	15
30/100	G30R	24.9	58.1	2	T30R	85	15
0/100	G0R		83.0	2	T0R	85	15

3.6. Characterization of granulates

3.6.1. MDSC measurements

MDSC measurement of granules was performed to characterize and compare thermal properties with kneaded samples. Results are listed in Table 13.

Results follow same trends observed in case of kneaded samples. Crystallization temperature and crystallization enthalpy are decreased with addition of PLA. Values of T_g for both polymers and as well as melting temperature of PHB did not show any trend. Melting enthalpy decreased with increasing amount of PLA. Raschig did not lead to any significant changes.

However, in case of G30, calculated crystallinity was 122 %. This was probably caused during sample preparation. Because of lack of the material, delay between sampling was not sufficient and therefore an error in mixing ratio of PHB/(PLA+PHB) was caused. Supposing PHB crystallinity is not changed by addition of PLA and/or Raschig being in range of 70–75 % as determined from MDSC measurement of kneaded samples, deviation from the initial weight composition could occur for all samples.

Table 14 Results of MDSC analysis of granules

Sample name	PHB/(PLA+PHB) ratio	T_c (°C)	H_c (J/g)	T_g PHB (°C)	T_g PLA (°C)	T_m (°C)	H_m (J/g)	X_c (%)
G100	100/100	95	74	8		175	101	69
G70	70/100	95	52	11	60	175	72	71
G50	50/100	87	33	7	59	176	46	63
G30	30/100	82	38	11	59	174	53	122
G0	0/100				61			
G100R	100/100	96	74	6		174	99	68
G70R	70/100	91	53	13	59	174	79	77
G50R	50/100	84	31	5	60	174	43	59
G30R	30/100			5	59	173	5	11
G0R	0/100				60			

3.6.2. Weight composition of blends

Weight composition of granules was quantified by TGA measurement. As you can see from Figure 26, although the peak temperatures of Raschig's decomposition are 372.4 °C and 406.3 °C, there is no visible peak corresponding to Raschig in case of G100R and G0R samples. This may be caused by changed decomposition kinetic of Raschig in polymer matrix or its chemical attachment to polymer molecules. Nevertheless, in subsequent discussion its amount 2%wt. is neglected.

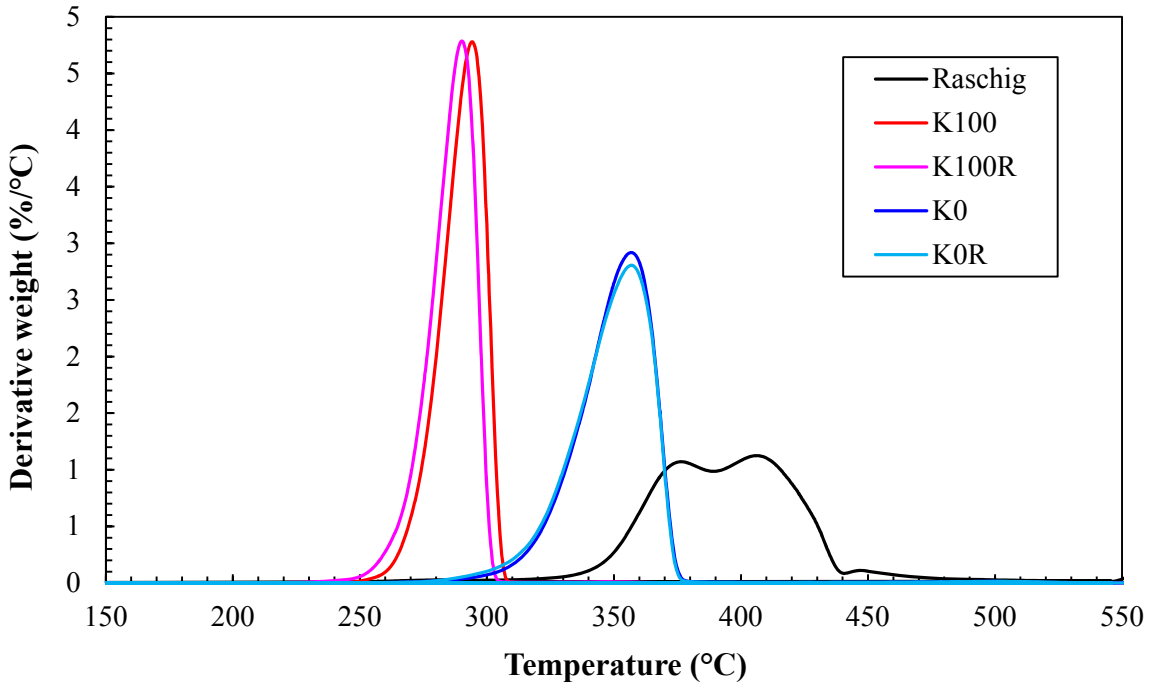

Figure 26 TG curve for G100, G0, G100R, G0R samples and Raschig

TG curves for polymer blends with analysed amounts of PLA in the samples are shown in Figure 27. Samples G70, G30 and G30R are enriched with PLA phase, while samples G50, G50R and G70R contain lower amounts of PLA than considered.

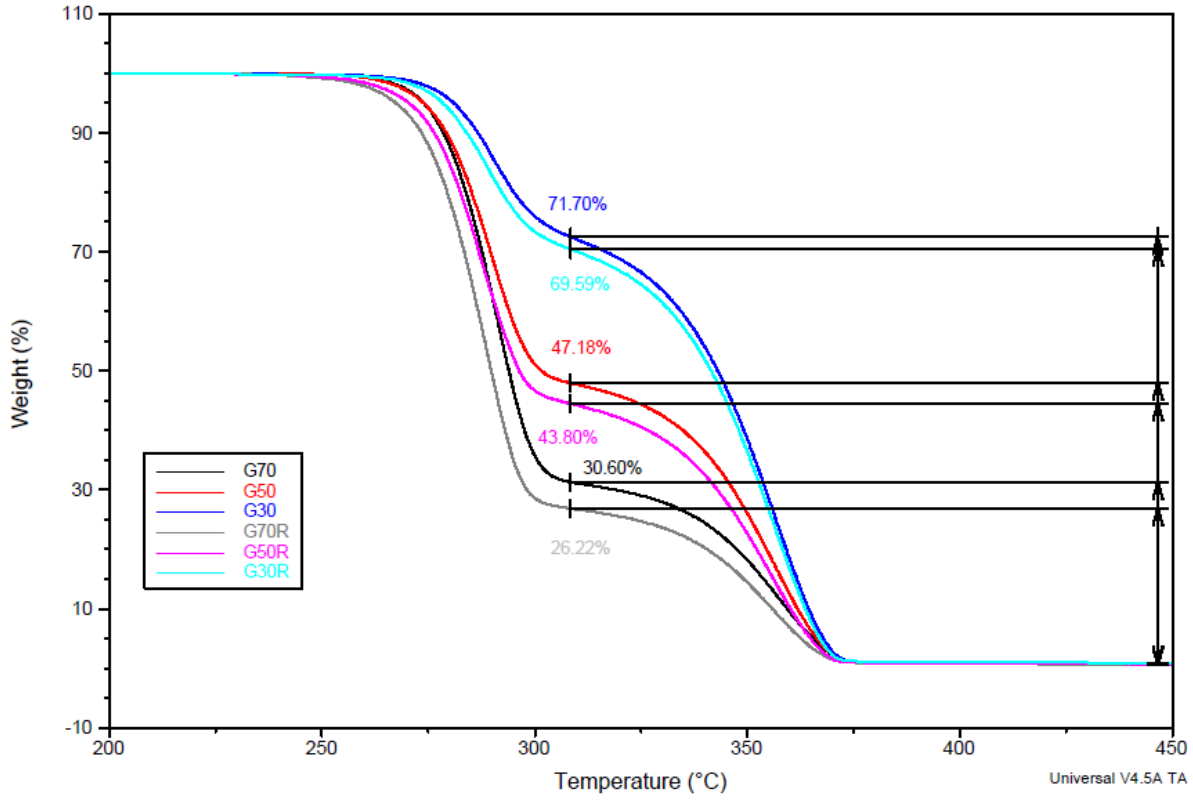

Figure 27 TGA of granulated blends

3.6.3. Morphology study via SEM

In case of reactive blends, homogeneity obtained by processing is a key parameter for the reaction to be carried out uniformly throughout volume. Twin-screw extrusion method is commonly used for these purposes due to high shear stress of polymer melt. Resulting morphology of melt processed mixtures is driven by rheology of the blends. For PHB/PLA blends, there is a big difference between viscosities of both components. In case of reactive series, low viscosity component Raschig is added.

In Figure 28, there are SEM images of G100 and G100R samples. In both images there are holes with approximately 1 μm diameter most probably caused by air presence. As the system was not vacuum degassed, gas stayed in the melt during processing and led to the formation of pores in cooled extruded profiles. Otherwise, G100 is homogeneous material as expected from neat PHB. On the contrary, there are well-wetted formations with size from 1 to 2 μm on the fracture surface of G100R. In order to exclude the possibility, that Raschig is not miscible with PHB and forms drops in polymer matrix reacting exclusively on the surface of these drops, EDX map of this sample was measured (shown in Figure 29). This proves Raschig is well dispersed in PHB matrix and does not form Raschig enriched clusters with PHB.

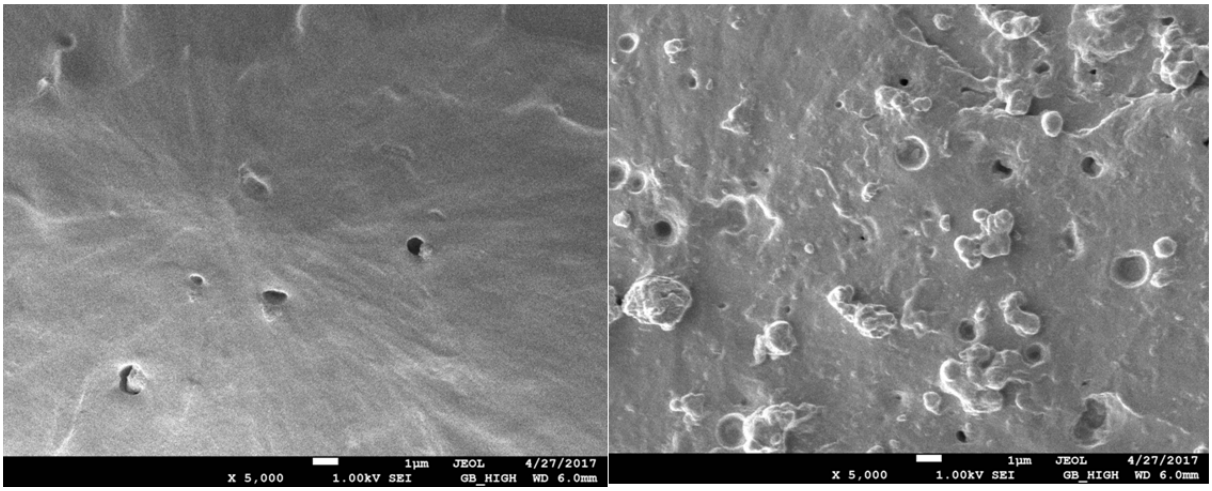

Figure 28 Secondary electrons SEM image of G100 (left) and G100R (right) samples with magnification ×5,000

Figure 30 shows SEM images of G70 and G70R samples. Although it is well mixed, G70 sample shows visible phase boundaries, confirming that PLA is not soluble in PHB in this amount. In case of G70R, with addition of Raschig bulk homogeneity is enhanced leading to smaller phases. However, there are cylindrical particles in the structure. They possessed a good adhesion to the matrix during freeze fracturing of the sample as the fracture passed through them. Existence of these structures may arise from orientation of the material during processing.

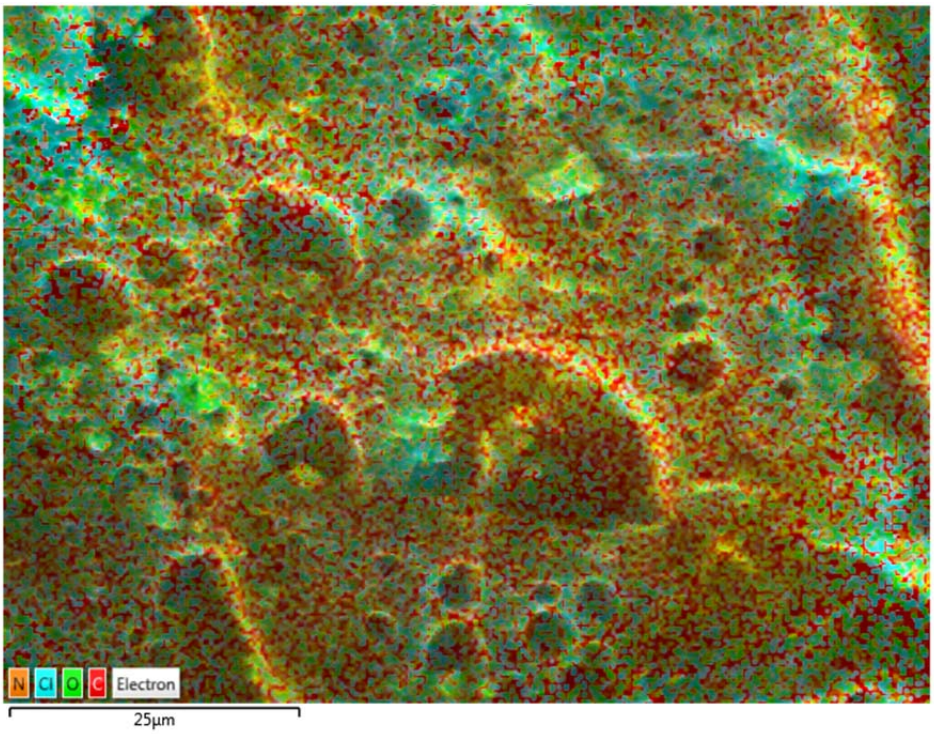

Figure 29 SEM-EDX image of G100R with magnification ×2,000

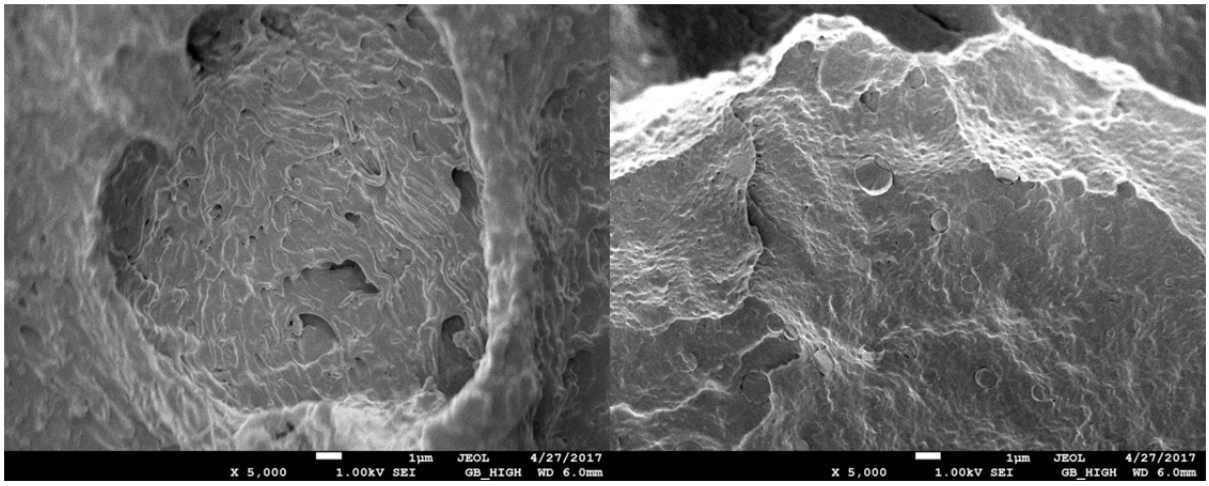

Figure 30 Secondary electrons SEM image of G70 (left) and G70R (right) samples with magnification ×5,000

In Figure 31, there are SEM images of G50 and G50R samples. G50 exhibits biphasic structure composed of continuous homogeneous phase and spherical particles with diameter around 1 µm. Seemingly, continuous phase consists of homogeneous solid solution of PHB and PLA and the second phase is made of the excess of one of them. Because discontinuous phase is formed by more viscous component during processing, it is assumed, that excluded spheres are made of PLA. Moreover, as used PLA is amorphous, it is expected to create smooth and rounded structures.

Sample G50R displayed similarly to G70R improved homogeneity together with the existence of cylindrical particles with good adhesion.

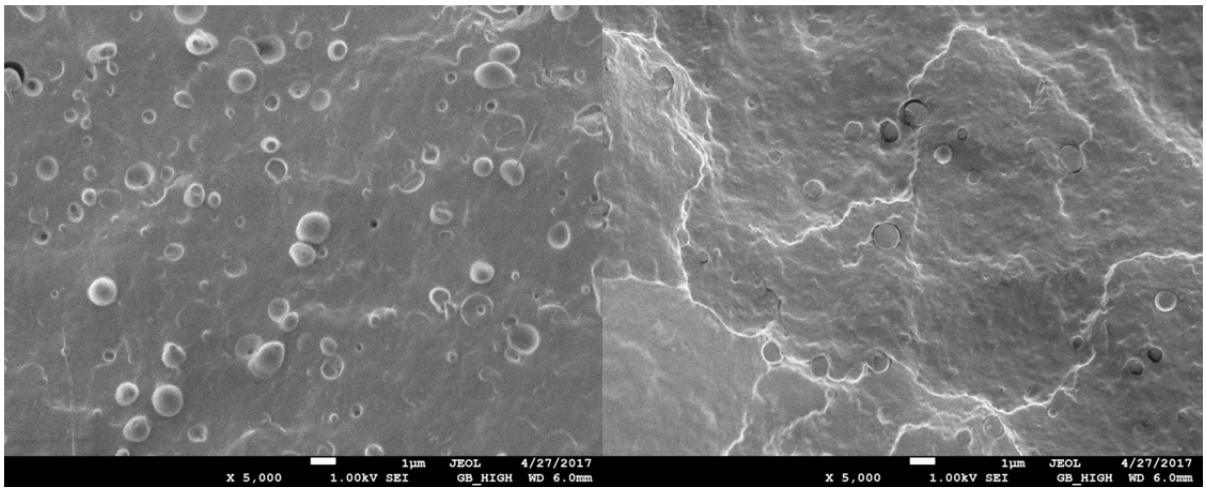

Figure 31 Secondary electrons SEM image of G50 (left) and G50R (right) samples with magnification ×5,000

Figure 32 depicts SEM images of G30 and G30R samples. In case of G30 sample, the majority of mixture is made of more viscous component, PLA. Therefore, it is difficult to incorporate PHB into it. As a result, an amount of PHB crystallites equal to the non-mixed part are formed.

Sample G30R shows similar morphology with improved interphase between continuous phase and PHB crystallites.

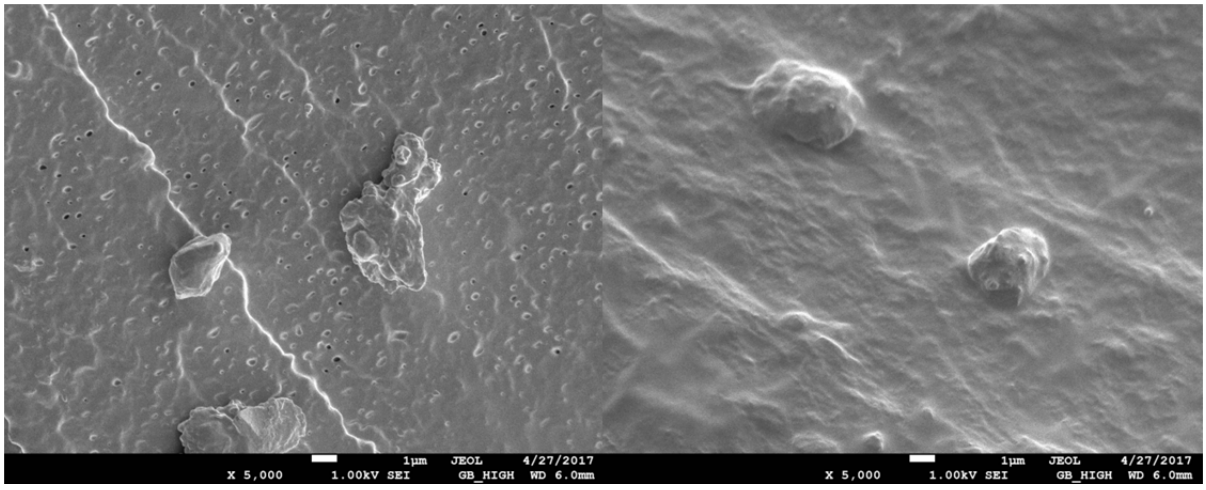

Figure 32 Secondary electrons SEM image of G30 (left) and G30R (right) samples with magnification ×5,000

SEM images of G0 and G0R samples can be seen in Figure 33. Image of G0 shows homogenous morphology with a domain containing numerous pores. These defects were caused during processing as PLA in the form of granules was dispensed into the machine at greater velocity than samples before and thus there was more gas inside. G0R sample confirmed phenomena observed in MDSC measurements, that weight composition of granules does not strictly follow PHB/(PHB+PLA) ratios. There was a small fraction of PHB in the form of rounded particles. In this amount, PHB is prevented from crystallization and therefore is not detectable by MDSC.

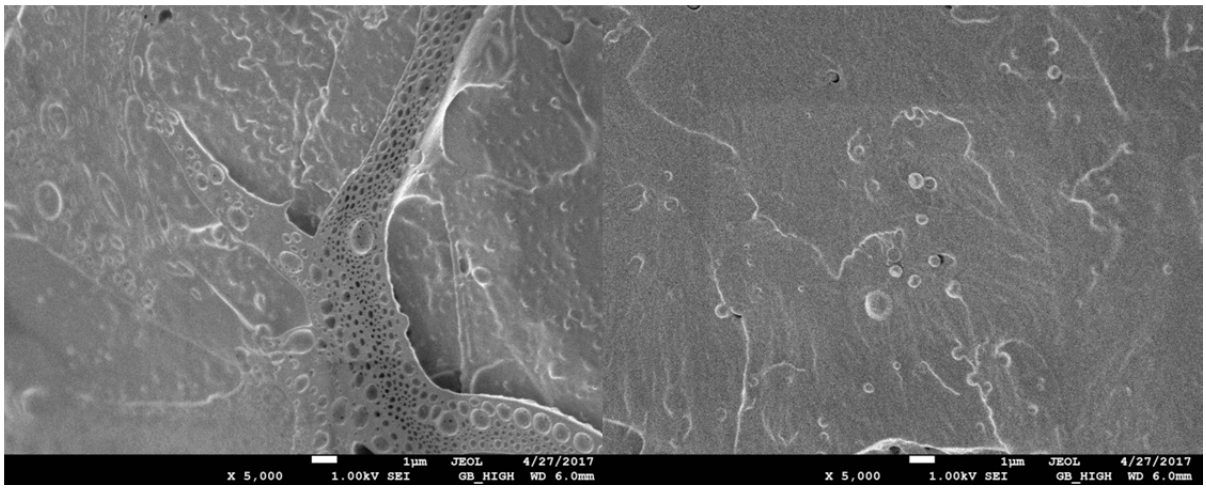

Figure 33 Secondary electrons SEM image of G0 (left) and G0R (right) samples with magnification ×5,000

3.7. Characterization of flat tapes

Flat tapes were produced from granules mixed with plasticizer for the purpose of testing mechanical and thermo-mechanical properties of studied polymer blends. This way, additional thermal processing is avoided and testing specimens are prepared directly from the tapes. Citrate plasticizer was used in order to enhance mechanical properties of blends because as described in chapter 1.1, PHB lacks superior mechanical properties.

Nevertheless, technical problem during processing made it impossible to dispense plasticizer into the extruder in required amount. TG analysis was performed in order to analyze its quantity in the samples.

3.7.1. Plasticizer observation by TGA

TG curves showing comparison between granules and flat tapes of corresponding PHB/(PHB+PLA) ratios for non-reactive and reactive series can be seen in Figure 34 and Figure 35, respectively.

Plasticized samples exhibited shift of degradation onset and peak temperatures to lower temperatures for both polymers in all samples. However, acetyltributylcitrate did not show any distinct degradation peak. It is assumed, that the amount of plasticizer in close proximity to the surface is evaporated, resulting in weight loss at lower temperatures than in the case of samples without plasticizers. As citrate is mixed in both polymers according to its distributing coefficient, its degradation is further on indistinguishable from the degradation of polymers. Therefore, it is impossible to determine its absolute quantity in the samples.

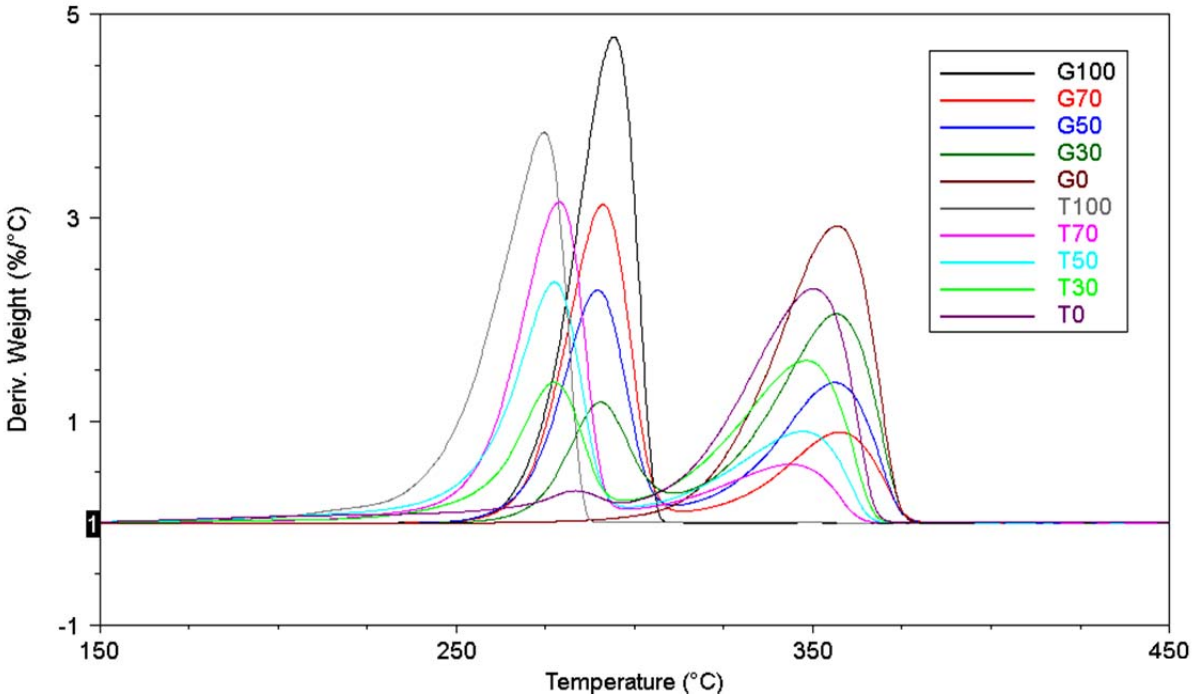

Figure 34 TGA curves of non-reactive series of granules and tapes

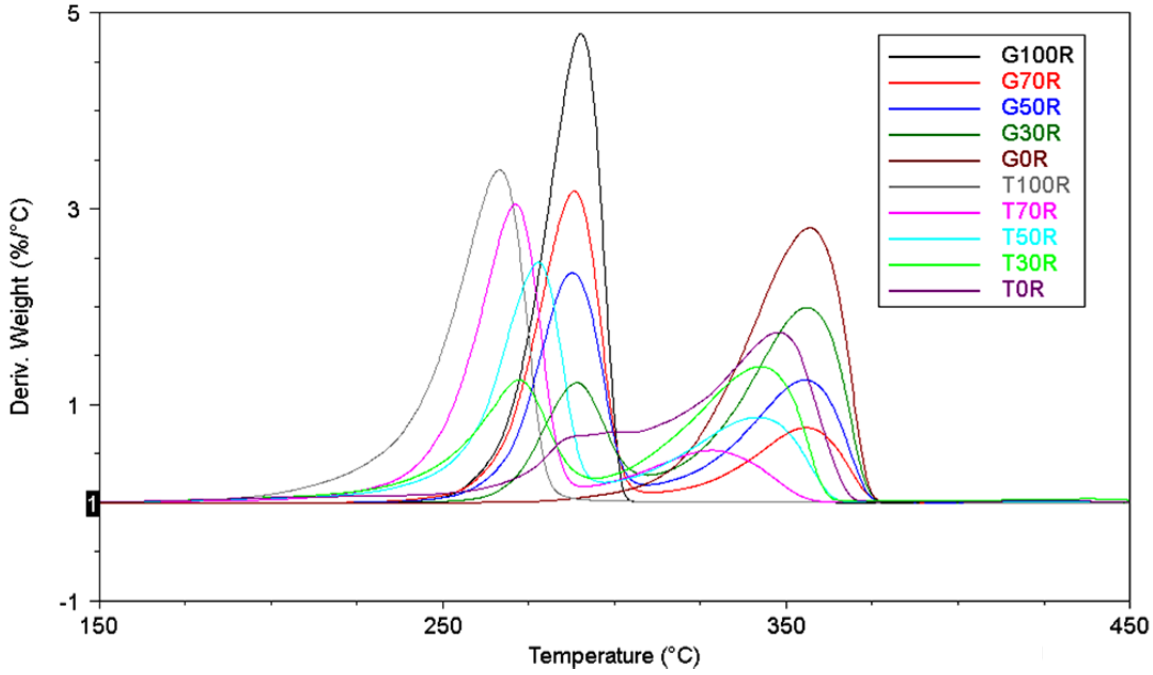

Figure 35 TGA curves of reactive series of granules and tapes

Due to the impossibility of accurate determination of plasticizer amount, two samples from previous experiments, marked 70 and 70R, with same composition as T70 and T70R were used for comparison. As can be seen from the resulting TG curves showed in Figure 36, beginning of the decomposition curves of prepared tapes and model samples is different. This indicates, that tested tape samples (T10–T0R) contain lower amount of citrate than intended.

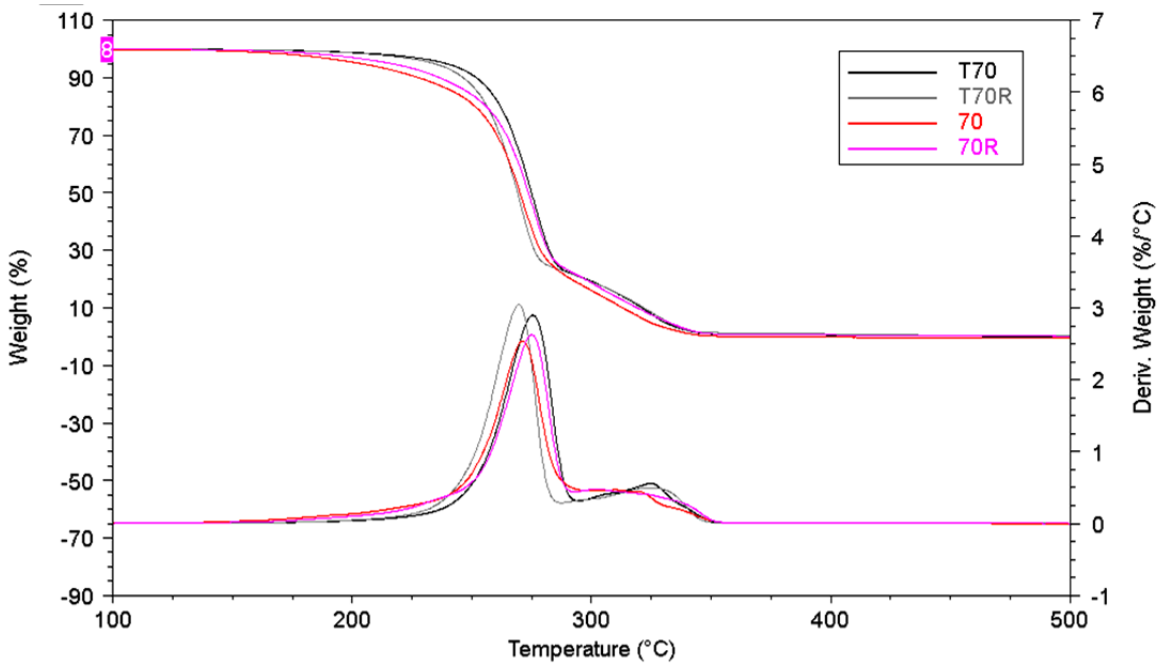

Figure 36 TGA of T70 and T70R samples with samples from previous experiments, 70 and 70R

3.7.2. Thermal analysis

Prepared tapes were subjected to thermal analysis via MDSD with results illustrated in Table 15. From the results of T0 and T0R samples, it is clear that mass composition of samples was further deviated. In these samples, existence of small fraction of PHB was proven by observing melting peak corresponding to PHB.

Table 15 Results of MDSC analysis of tapes

Sample name	PHB/(PLA+PHB) ratio	T_c (°C)	H_c (J/g)	T_g PHB (°C)	T_g PLA (°C)	T_m (°C)	H_m (J/g)
T100	100/100	116	77	0		168	97
T70	70/100	112	56	5	44	168	73
T50	50/100	104	39		51	164	51
T30	30/100	61	34	1	53	172	35
T0	0/100	*100*	*1*		45	*170*	*6*
T100R	100/100	91	65			171	89
T70R	70/100	114	54		38	167	66
T50R	50/100	109	50		43	164	53
T30R	30/100	100	21	−1	48	172	28
T0R	0/100				49	*169*	*3*

Nevertheless, T_g of PLA was noticeably reduced as a result of addition of plasticizer. Measurement sensitivity was not sufficient for PHB T_g detection for some samples. When T_g was detected, it was shifted to lower temperatures as well. In most of the samples, PHB exhibited decreased melting temperature. Both these changes can be attributed to plasticizing effect.

3.7.3. Mechanical and thermo-mechanical properties

Prepared samples were subjected to tensile testing and DMA in order to evaluate possible effect of Raschig addition on mechanical and thermo-mechanical properties of neat polymers and their blends.

3.7.3.1. Tensile testing

Graphs with measured values of E-modulus (approximate), yield strength and elongation at break can be seen in Figure 37, Figure 38 and Figure 39, respectively.

Young's modulus did not show any trend with changing the composition of blends. Its change with addition of Raschig is in between of error bars for all samples. Similarly in case of yield strength, there is no dependency on weight composition of polymers. Effect of Raschig was observed in case of T30R sample, where yield strength was decreased from (38.5 ± 0.4) MPa to (31.6 ± 1.2) MPa.

On the basis of previous experience with plasticized PHB/PLA blends, elongation at break values higher than 50 % were expected for studied samples. This expectation was only fulfilled for T50 and T50R blends and T0 and T0R (neat PLA and PLA with Raschig).

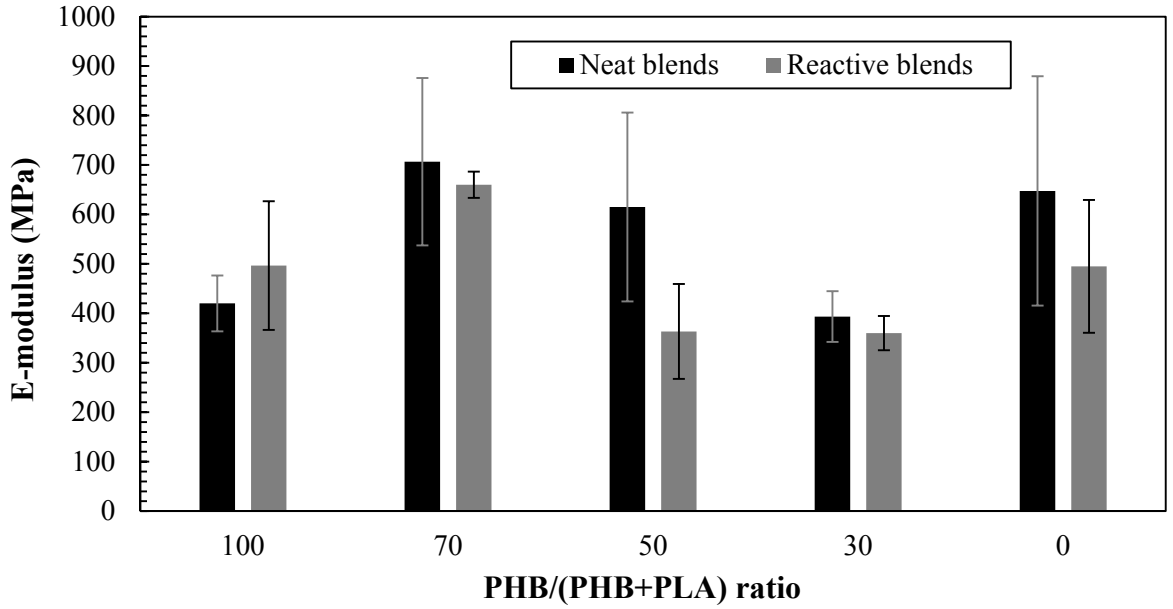

Figure 37 E-modulus measured by tensile testing of flat tapes

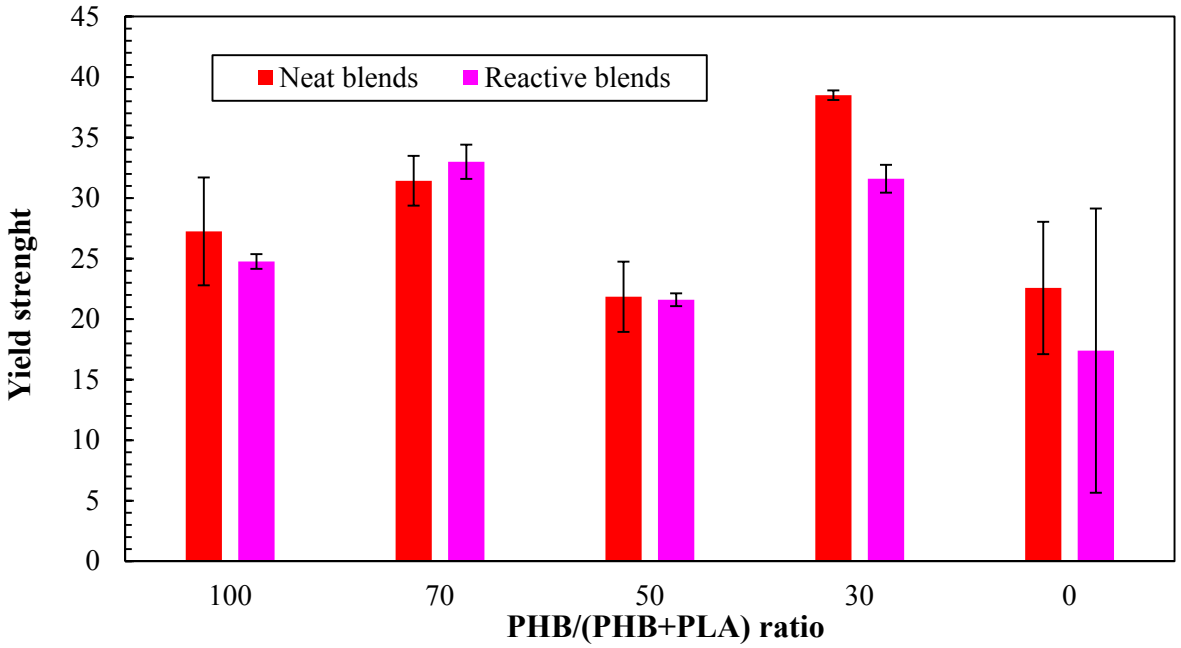

Figure 38 Yield strength measured by tensile testing of flat tapes

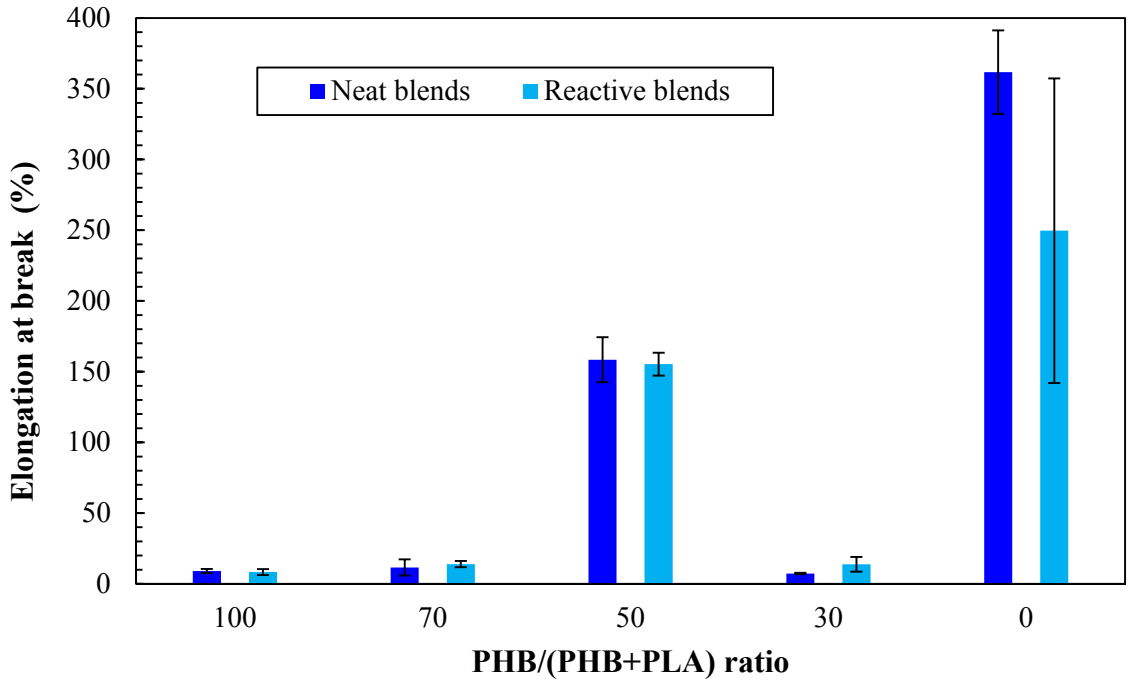

Figure 39 Elongation measured by tensile testing of flat tapes

These results correlated with the suspicion acquired after TG analysis, that samples do not contain sufficient amount of plasticizer to enhance their mechanical properties. Therefore, T70R, T70, 70 and 70R samples were pressed into foils with a thickness around 0.4 mm and shaped into 5A type dogbone specimens and tested for comparison. Results of this testing (Table 16) demonstrate that mechanical properties of prepared tapes do not correspond with the composition they should have. Yield strength of 70 and 70R samples is approximately two times lower and their elongation at break is more than ten times higher. Due to the technical problems, blends were not plasticized enough, which resulted in poor mechanical properties, which explains the abovementioned observations.

Table 16 Comparison between T70 and T70R and samples from previous experiments 70 and 70R

Sample name	PHB/(PLA+PHB) ratio	σ_y (MPa)	ε (%)
T70	70/100	66.8 ± 0.4	3.0 ± 0.1
T70R	70/100	57.3 ± 8.1	1.9 ± 0.4
70	70/100	29.4 ± 1.4	37.9 ± 8.0
70R	70/100	30.0 ± 1.6	40.5 ± 10.1

3.7.3.2. DMA measurement

DMA analysis was performed in order to study temperature dependent behaviour of dynamic modules of prepared plasticized samples. Measured range corresponds to the polymer rubbery plateau. Its appearance is related to the degree of crystallinity of a material. The modulus of crystalline material is typically higher than for high-molecular weight amorphous polymer. For fully amorphous polymers, the width of rubbery plateau as well as the properties in this region depends on molecular weight between entanglements.

Typical curve obtained from DMA measurement for samples T50 and T50R is shown in Figure 40, while the rest is enclosed in appendix 9-12. According to this, DMA T_g of these blends lies under 40 °C.

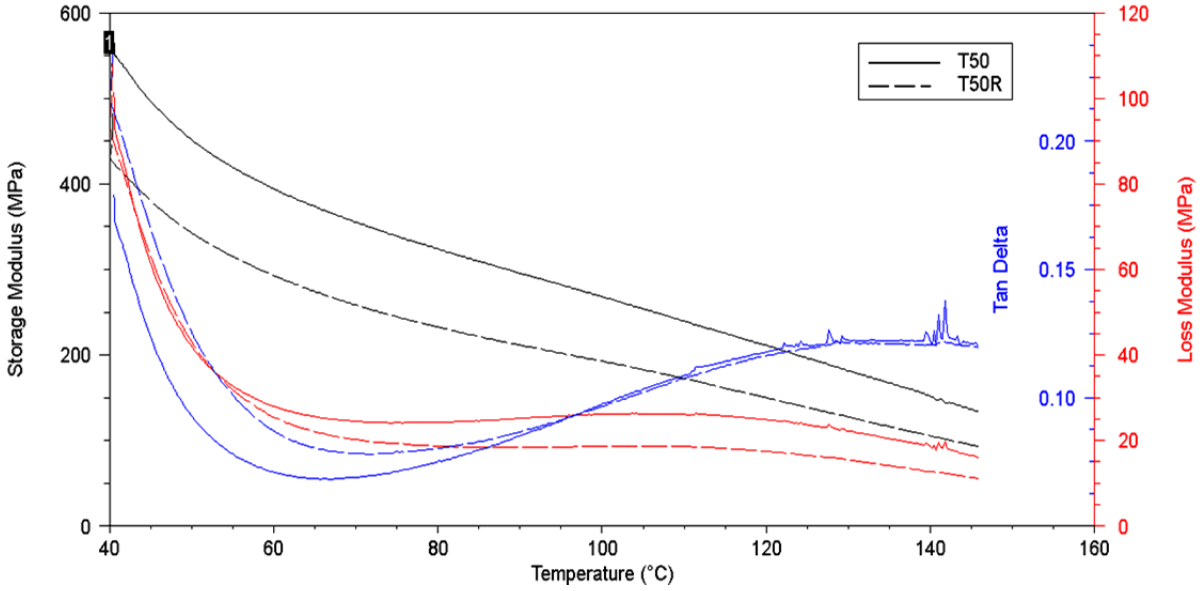

Figure 40 DMA analysis for samples T50 and T50R

Storage and loss modules as well as tan delta at 80 °C (in order to avoid influence of glass transition) for all samples were compared. Results are depicted in Figure 41 for G′, in Figure 42 for G″ and in Figure 43 for tan delta.

For both non-reactive and reactive series, the drop in storage and loss modules with increasing amount of PLA is observed. Opposite to this, tan delta is rising. This phenomenon correlates with increasing amount of amorphous fraction in rubbery state in blends making them softer. With addition of Raschig, storage modulus is shifted to lower values for all samples except T70R. Loss modulus was increased for T100R and T70R and decreased for

the rest of reactive samples. Tan delta dropped for T70R and T30R samples and otherwise rose.

However, no relations can be concluded from these measurements because of unknown amount of plasticizer in these samples, which could influence their thermo-mechanical behaviour.

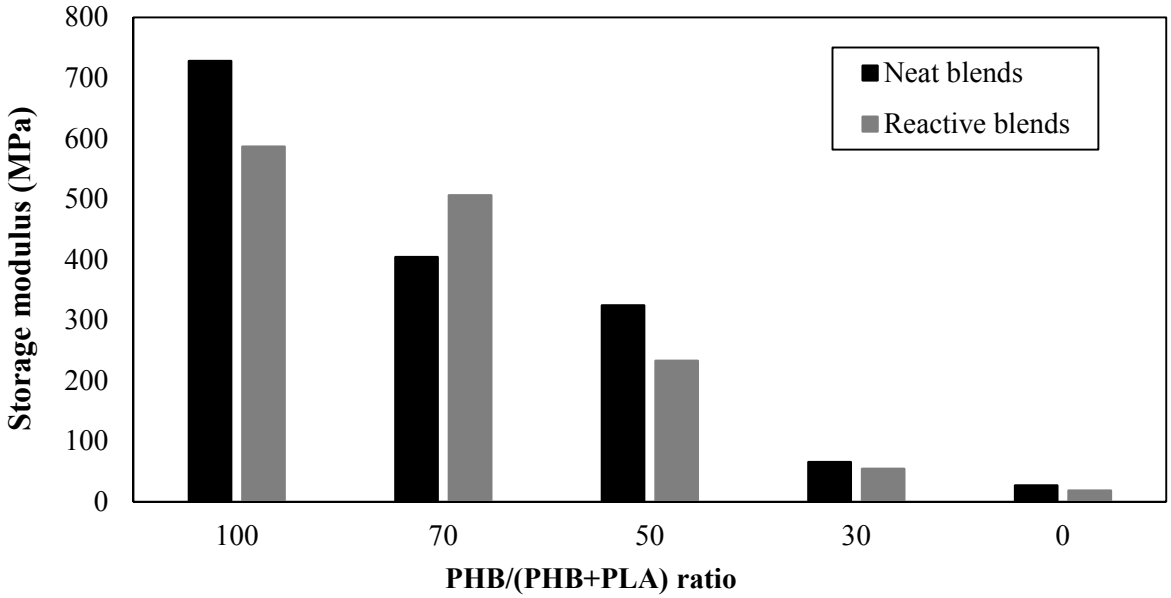

Figure 41 Values of storage modulus at 80 °C for tape samples as measured by DMA

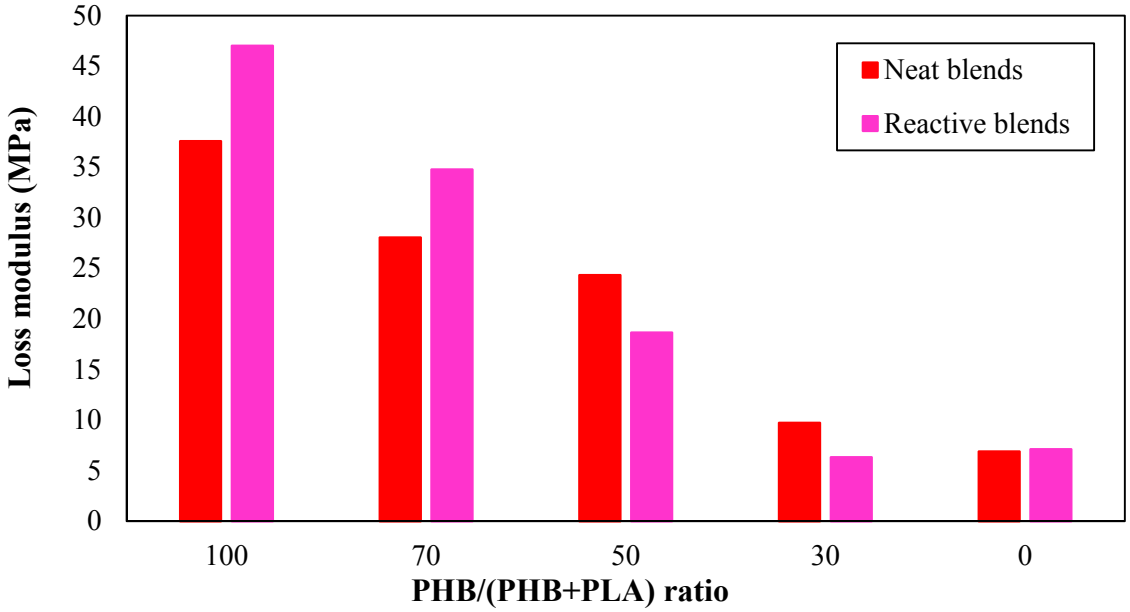

Figure 42 Values of loss modulus at 80 °C for tape samples as measured by DMA

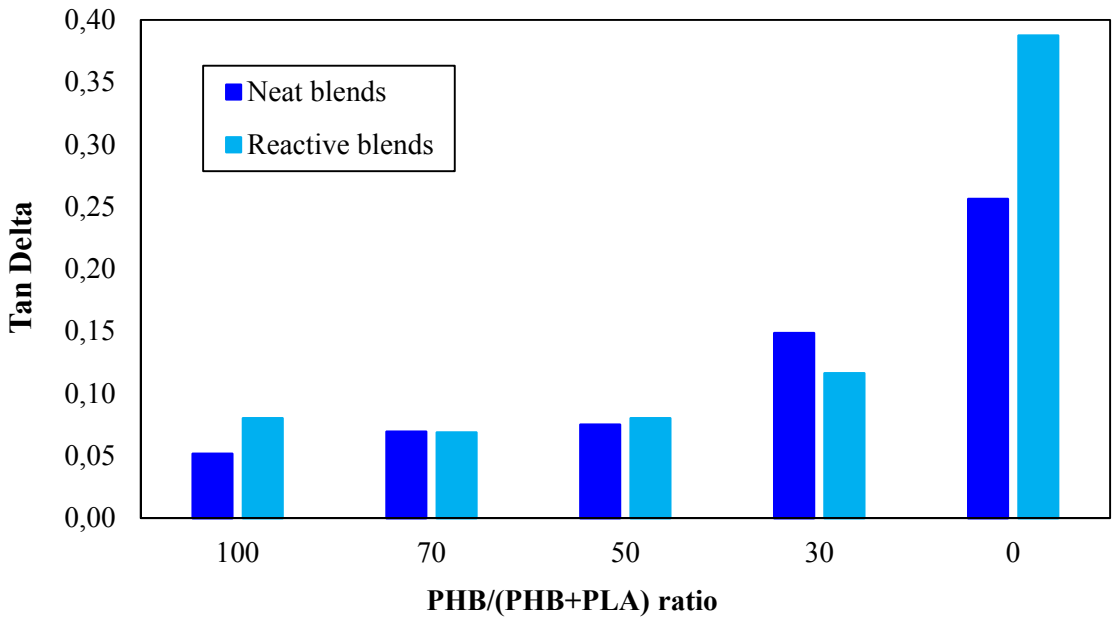

Figure 43 Values of tan delta at 80 °C for tape samples as measured by DMA

4. CONCLUSION

The aim of this thesis was to perform reactive compounding of biopolymer blends based on poly(3-hydroxy butyrate) and poly(lactic acid) with selected reagent and to study possible changes in their structure by means of thermal and rheological measurements.

Non-commercial PHB material from company Nafigate was used for studies, therefore the first part of experimental work deals with raw material characterization. Particularly, thermal stability as change in molecular weight and thermal properties with heat treatment was studied.

Reactive reagents described in literature for non-radical initiated reactions with PLA were selected, namely Joncryl, Raschig, and phosphites TPP and TNPP. DPDP, which is structurally similar, was added. Reactivity of these compounds was first investigated on neat PLA and PHB during processing in laboratory kneader instrumented with torque sensor. Reagents were added in amount of 2%wt. Torque related to melt viscosity was recorded for 8 minutes which corresponds to 5 minutes after feeding of reagent. In order to eliminate viscosity drop caused by thermal degradation of non-additivated polymer, obtained data were evaluated differentially. Among tested reagents, Raschig showed enhancement of melt viscosity during processing. The rest of the reagents is either non-reactive towards PHB, reaction rate or yield is insufficient. As a result, thermal degradation of material is dominant and viscosity drop is faster than in case of neat PHB. Therefore, these substances are not suitable for reactive compounding of PHB and its blends. On the contrary, PLA reacts willingly with all studied reagents as expected.

On the basis of these experiments, non-reactive and reactive, with addition of Raschig PHB/PLA, blends were prepared. Blends with 70/100, 50/100 and 30/100 PHB/(PHB+PLA) ratios were studied. Processing conditions were left unchanged.

So prepared samples of both polymers and their blends, as well as corresponding reactive samples, were characterized with rheology measurements, GPC and MDSC analysis. Rheology was used to study sample stability during simulated processing stresses (10 minutes time test, amplitude of deformation 300 %, frequency 0.833 Hz). Storage and loss modulus and complex viscosity as a function of time were evaluated together with subsequent structure recovery ability under amplitude of deformation 1 %. In case of non-reactive series of samples, there is inverse proportionality between total drop of G', G'' and $|\eta^*|$ and addition of PLA. Moreover, recovery ability is higher with increasing amount of PLA as it is less sensitive to thermal degradation and its viscosity decrease during time test is attributed to entanglement of molecules. Reactive samples followed this trend. In addition, these blends exhibited lower total decrease of G', G'' and $|\eta^*|$ and improved recovery ability comparing to corresponding non-reactive samples. This fact points out possible branching of reactive matrices structure. Further, G' and G'' dependency on angular frequency (frequency sweep) was measured and G' and G'' modulus crossover point was determined. The crossover frequency is indirectly proportional to the MW and the crossover modulus is indirectly proportional to the width of the MWD. Results indicated higher MW and broader MWD of reactive samples. This is contrary to results of GPC analysis, which confirmed broader MWD,

however, did not show MW change. These statements lead to conclusion, that Raschig causes structure changes, by forming of branched molecules, of studied polymers and their blends. Thus samples' MW was not changed and at the same time they displayed increase in G', G'' and $|\eta^*|$ of melt as observed by frequency sweep measurement. Structure changes were not reflected in thermal properties.

In order to gain samples suitable for mechanical tests, both series were prepared by twin-screw extrusion. Extruded granules were observed using SEM microscope. Dispersion homogeneity of Raschig in the matrix was first verified by EDX analysis. Reactive mixtures showed enhanced homogeneity with lower phase size compared to non-reactive matrices. Thermal measurements and SEM images of PLA samples revealed a shift in weight composition due to insufficient sample amount and long residence time of material in extruder.

It is known from literature that PHB/PLA blends without plasticizers are generally brittle with an elongation to break up to 10 %. Therefore, matrices plasticized with 15%wt. of acetyltributylcitrate were processed. However, due to technological problems with the liquid additive dispenser, required amount of plasticizer was not obtained in the samples. The fact was confirmed by TGA analysis. Therefore, mechanical properties of plasticized samples did not reach values known from previous experiments. To verify the method of measurement and above-mentioned assay, tensile test was performed on samples with a PHB/(PHB+PLA) ratio 70/100 and samples from previous experiments with the same ratio and sufficient plasticizer content. The results showed 13 and 21 times higher elongation at break for non-reactive and reactive sample, respectively, in case of softened comparative samples. In spite of this, DMA analysis was performed on prepared samples, which showed no trend, probably due to the inconsistent amount of plasticizer.

Information identified can be summarized into following fundamental points:

- Raschig, oligomeric polycarbodiimide, reacts with both polymers.
- Its reaction with PHB/PLA probably leads to branched structures.
- The rate of reaction is not sufficient to completely compensate decrease in viscosity due to processing degradation.
- For the same reason, its non-reacted quantity remains in matrix (with 2%wt. addition).
- Impact on mechanical and thermal properties has not been proved.

In conclusion, it can be stated, that Raschig behaves as a relatively effective stabilizer of rheological properties rather than as a reagent for the intentional modification of PHB/PLA blends' structure.

REFERENCES

[1] Biopolymers: Polyesters I Biological system and Biotechnological Production. Weinheim: Wiley-VCH, 2002, 460 s. ISBN 35-273-0224-7.

[2] KHANNA, Shilpi and Ashok K. SRIVASTAVA. Recent advances in microbial polyhydroxyalkanoates. *Process Biochemistry* [online]. 2005, vol. 40, issue 2, s. 607-619 [cit. 2014-10-24]. DOI: 10.1016/j.procbio.2004.01.053.

[3] ROY, Ipsita and P. M., Visakh P. M., VISAKH. Polyhydroxyalkanoate (PHA) based blends, composites and nanocomposites. Cambridge: Royal Society of Chemistry, 2015. RSC green chemistry series, 30. ISBN 18-497-3946-3.

[4] DI LORENZO, Maria Laura and Maria Cristina RIGHETTI. 2013. Effect of thermal history on the evolution of crystal and amorphous fractions of poly[(R)-3-hydroxybutyrate] upon storage at ambient temperature. *European Polymer Journal* [online]. 49(2).

[5] Thermal decomposition of biodegradable polyesters—I: Poly(β-hydroxybutyric acid). *Polymer Degradation and Stability* [online]. 52(1), 25-38.

[6] WANG, Liang, Wenfu ZHU, Xiaojuan WANG, Xianyu CHEN, Guo-Qiang CHEN and Kaitian XU. Processability modifications of poly(3-hydroxybutyrate) by plasticizing, blending, and stabilizing. Journal of Applied Polymer Science [online]. 2008-01-05, vol. 107, issue 1, s. 166-173 [cit. 2014-11-04]. DOI: 10.1002/app.27004.

[7] AURIEMMA, Maria, Amodio PISCITELLI et. al. Blending poly(3-hydroxybutyrate) with tannic acid: Influence of a polyphenolic natural additive on the rheological and thermal behavior. European Polymer Journal [online]. 2015, 63, 123-131 [cit. 2016-09-30]. DOI: 10.1016/j.eurpolymj.2014.12.021. ISSN 00143057.

[8] PERSICO, Paola, Veronica AMBROGI et. al. Enhancement of poly(3-hydroxybutyrate) thermal and processing stability using a bio-waste derived additive. International Journal of Biological Macromolecules [online]. 2012, 51(5), 1151-1158 [cit. 2016-09-30]. DOI: 10.1016/j.ijbiomac.2012.08.036. ISSN 01418130.

[9] HONG, Shinn-Gwo, Tsung-Kai GAU and Shih-Che HUANG. Enhancement of the crystallization and thermal stability of polyhydroxybutyrate by polymeric additives. Journal of Thermal Analysis and Calorimetry [online]. 2011, vol. 103, issue 3, s. 967-975 [cit. 2014-11-04]. DOI: 10.1007/s10973-010-1180-3.

[10] PUENTE, Jorge Arturo Soto, Antonella ESPOSITO, Frédéric CHIVRAC and Eric DARGENT. Effect of boron nitride as a nucleating agent on the crystallization of bacterial poly(3-hydroxybutyrate). Journal of Applied Polymer Science [online]. 2013-06-05, vol. 128, issue 5, s. 2586-2594 [cit. 2014-10-28]. DOI: 10.1002/app.38182.

[11] PAN, Pengju, Guorong SHAN, Yongzhong BAO and Zhixue WENG. Crystallization kinetics of bacterial poly(3-hydroxylbutyrate) copolyesters with cyanuric acid as a nucleating agent. Journal of Applied Polymer Science [online]. 2013, 129(3), 1374-1382 [cit. 2016-09-30]. DOI: 10.1002/app.38825. ISSN 00218995.

[12] EL-HADI, A, R SCHNABEL, E STRAUBE, G MÜLLER and S HENNING. Correlation between degree of crystallinity, morphology, glass temperature, mechanical properties and biodegradation of poly (3-hydroxyalkanoate) PHAs and their blends. Polymer

Testing [online]. 2002, vol. 21, issue 6, s. 665-674 [cit. 2014-11-04]. DOI: 10.1016/S0142-9418(01)00142-8.

[13] JACQUEL, Nicolas, Koichirou TAJIMA et. al. Nucleation mechanism of polyhydroxybutyrate and poly(hydroxybutyrate- co -hydroxyhexanoate) crystallized by orotic acid as a nucleating agent. Journal of Applied Polymer Science [online]. 2010,115(2), 709-715 [cit. 2016-09-30]. DOI: 10.1002/app.30873. ISSN 00218995.

[14] ERCEG, Matko, Tonka KOVAČIĆ and Ivka KLARIĆ. Thermal degradation of poly(3-hydroxybutyrate) plasticized with acetyl tributyl citrate. Polymer Degradation and Stability [online]. 2005, 90(2), 313-318 [cit. 2016-09-30]. DOI: 10.1016/j.polymdegradstab.2005.04.048. ISSN 01413910.

[15] WANG, Liang, Wenfu ZHU et. al. Processability modifications of poly(3-hydroxybutyrate) by plasticizing, blending, and stabilizing. Journal of Applied Polymer Science [online]. 2008,107(1), 166-173 [cit. 2016-09-30]. DOI: 10.1002/app.27004. ISSN 00218995.

[16] CHOI, Jae Shin a Won Ho PARK. Effect of biodegradable plasticizers on thermal and mechanical properties of poly(3-hydroxybutyrate). Polymer Testing [online]. 2004, 23(4), 455-460 [cit. 2016-09-30]. DOI: 10.1016/j.polymertesting.2003.09.005. ISSN 01429418.

[17] ARKIN, Ali Hakan a Baki HAZER. Chemical Modification of Chlorinated Microbial Polyesters. Biomacromolecules[online]. 2002, 3(6), 1327-1335 [cit. 2016-09-30]. DOI: 10.1021/bm020079v. ISSN 1525-7797.

[18] CHEN, Cheng, Shuwen PENG et. al. Synthesis and characterization of maleated poly(3-hydroxybutyrate). Journal of Applied Polymer Science [online]. 2003, 88(3), 659-668 [cit. 2016-09-30]. DOI: 10.1002/app.11771. ISSN 0021-8995.

[19] CASARANO, Romeu, Denise F. S. PETRI, Michael JAFFE a Luiz H. CATALANI. Block Copolymers Containing (R)-3-Hydroxybutyrate and Isosorbide Succinate or (S)-Lactic Acid Mers. Journal of Polymers and the Environment [online]. 2010, 18(1), 33-44 [cit. 2016-09-30]. DOI: 10.1007/s10924-009-0157-4. ISSN 1566-2543.

[20] IMPALLOMENI, Giuseppe, Giovanni Marco CARNEMOLLA et. al. Characterization of biodegradable poly(3-hydroxybutyrate-co-butyleneadipate) copolymers obtained from their homopolymers by microwave-assisted transesterification.Polymer [online]. 2013, 54(1), 65-74 [cit. 2016-09-30]. DOI: 10.1016/j.polymer.2012.11.030. ISSN 00323861.

[21] ZHAO, Qiang, Guoxiang CHENG et. al. Synthesis and characterization of biodegradable poly(3-hydroxybutyrate) and poly(ethylene glycol) multiblock copolymers: note II. Polymer [online]. 2005, 46(23), 10561-10567 [cit. 2016-09-30]. DOI: 10.1016/j.polymer.2005.08.014. ISSN 00323861.

[22] ZHIJIANG, Cai, Hou CHENGWEI a Yang GUANG. Crystallization behavior, thermal property and biodegradation of poly(3-hydroxybutyrate)/poly(ethylene glycol) grafting copolymer: note II. Polymer Degradation and Stability [online]. 2011,96(9), 1602-1609 [cit. 2016-09-30]. DOI: 10.1016/j.polymdegradstab.2011.06.001. ISSN 01413910.

[23] JIANG, Tao, Ping HU a Yang GUANG. Radiation-Induced Graft Polymerization of Isoprene onto Polyhydroxybutyrate: note II. Polymer Journal [online]. 2001, 33(9), 647- [cit. 2016-09-30]. DOI: 10.1295/polymj.33.647. ISSN 0032-3896

[24] HSIEH, Wen-Chuan a Yuki WADA. Effect of hydrophilic and hydrophobic monomers grafting on microbial poly(3-hydroxybutyrate): note II. Journal of the Taiwan Institute of Chemical Engineers [online]. 2009, 40(4), 413-417 [cit. 2016-09-30]. DOI: 10.1016/j.jtice.2008.10.005. ISSN 18761070.

[25] NGUYEN, Sophie a Robert H. MARCHESSAULT. Synthesis and Properties of Graft Copolymers Based on Poly(3-hydroxybutyrate) Macromonomers: note II. Macromolecular Bioscience [online]. 2004, 4(3), 262-268 [cit. 2016-09-30]. DOI: 10.1002/mabi.200300088. ISSN 1616-5187.

[26] VOGEL, Roland, Bernhard TÄNDLER, Dieter VOIGT, Dieter JEHNICHEN, Liane HÄUßLER a Lutz PEITZSCH. Melt Spinning of Bacterial Aliphatic Polyester Using Reactive Extrusion for Improvement of Crystallization: note II. Macromolecular Bioscience [online]. 2007, 7(6), 820-828 [cit. 2016-09-30]. DOI: 10.1002/mabi.200700041. ISSN 16165187.

[27] LEE, H. K., J. ISMAIL, H. W. KAMMER, M. A. BAKAR, Liane HÄUßLER a Lutz PEITZSCH. Melt reaction in blends of poly(3-hydroxybutyrate) (PHB) and epoxidized natural rubber (ENR-50): note II. Journal of Applied Polymer Science [online]. 2005, 95(1), 113-129 [cit. 2016-09-30]. DOI: 10.1002/app.20808. ISSN 0021-8995.

[28] KOLAHCHI, Ahmad Rezaei, Marianna KONTOPOULOU, H. W. KAMMER, M. A. BAKAR, Liane HÄUßLER a Lutz PEITZSCH. Chain extended poly(3-hydroxybutyrate) with improved rheological properties and thermal stability, through reactive modification in the melt state: note II. Polymer Degradation and Stability [online]. 2015, 121(1), 222-229 [cit. 2016-09-30]. DOI: 10.1016/j.polymdegradstab.2015.09.008. ISSN 01413910. Dostupné z: http://linkinghub.elsevier.com/retrieve/pii/S014139101530080X

[29] STEINBÜCHEL, A. a M. HOFRICHTER. Biopolymers. Chichester: Wiley-VCH, 2003. ISBN 35-273-0230-1.

[30] CASTRO-AGUIRRE, E., F. IÑIGUEZ-FRANCO, H. SAMSUDIN, X. FANG a R. AURAS. Poly(lactic acid)—Mass production, processing, industrial applications, and end of life. Advanced Drug Delivery Reviews [online]. 2016, [cit. 2016-10-14]. DOI: 10.1016/j.addr.2016.03.010. ISSN 0169409x.

[31] JACOBSEN, S. a H. G. FRITZ. Plasticizing polylactide – the effect of different plasticizers on the mechanical properties.Polymer Engineering [online]. 1999, 39(7), 1303-1310 [cit. 2016-10-14]. DOI: 10.1002/pen.11517. ISSN 0032-3888.

[32] LABRECQUE, L. V. Citrate esters as plasticizers for poly(lactic acid). Journal of Applied Polymer Science. 1997, 8(66), 1507–1513.

[33] MARTINO, V. P., A. JIMÉNEZ a R. A. RUSECKAITE. Processing and characterization of poly(lactic acid) films plasticized with commercial adipates. Journal of Applied Polymer Science [online]. 2009, 112(4), 2010-2018 [cit. 2016-10-14]. DOI: 10.1002/app.29784. ISSN 00218995.

[34] DARIE-NIŢĂ, Raluca N., Cornelia VASILE, Anamaria IRIMIA, Rodica LIPŞA a Maria RÂPĂ. Evaluation of some eco-friendly plasticizers for PLA films processing. Journal of Applied Polymer Science [online]. 2016, 133(13), n/a-n/a [cit. 2016-10-14]. DOI: 10.1002/app.43223. ISSN 00218995.

[35] KULINSKI, Z., E. PIORKOWSKA, K. GADZINOWSKA, M. STASIAK a Maria RÂPĂ. Plasticization of Poly(l -lactide) with Poly(propylene glycol). Biomacromolecules [online]. 2006, 7(7), 2128-2135 [cit. 2016-10-14]. DOI: 10.1021/bm060089m. ISSN 1525-7797.

[36] YU, Fengmei, Tao LIU, Xiuli ZHAO, Xuejiang YU, Ai LU a Jianhua WANG. Effects of talc on the mechanical and thermal properties of polylactide. Journal of Applied Polymer Science [online]. 2012, 125(S2), E99-E109 [cit. 2016-10-14]. DOI: 10.1002/app.36260. ISSN 00218995.

[37] HE, Dongran, Yaming WANG, Chunguang SHAO, Guoqiang ZHENG, Qian LI a Changyu SHEN. Effect of phthalimide as an efficient nucleating agent on the crystallization kinetics of poly(lactic acid). Polymer Testing [online]. 2013, 32(6), 1088-1093 [cit. 2016-10-14]. DOI: 10.1016/j.polymertesting.2013.06.005. ISSN 01429418.

[38] SUKSUT, B., C. DEEPRASERTKUL, Chunguang SHAO, Guoqiang ZHENG, Qian LI a Changyu SHEN. Effect of Nucleating Agents on Physical Properties of Poly(lactic acid) and Its Blend with Natural Rubber. Journal of Polymers and the Environment [online]. 2011, 19(1), 288-296 [cit. 2016-10-14]. DOI: 10.1007/s10924-010-0278-9. ISSN 1566-2543.

[39] PHUPHUAK, Yupin, Yong MIAO, Philippe ZINCK a Suwabun CHIRACHANCHAI. Balancing crystalline and amorphous domains in PLA through star-structured polylactides with dual plasticizer/nucleating agent functionality. Polymer[online]. 2013, 54(26), 7058-7070 [cit. 2016-10-14]. DOI: 10.1016/j.polymer.2013.10.006. ISSN 00323861.

[40] DETYOTHIN, Sukeewan, Susan E.M. SELKE, Ramani NARAYAN, Maria RUBINO a Rafael AURAS. Reactive functionalization of poly(lactic acid), PLA: Effects of the reactive modifier, initiator and processing conditions on the final grafted maleic anhydride content and molecular weight of PLA. Polymer Degradation and Stability [online]. 2013,98(12), 2697-2708 [cit. 2016-10-15]. DOI: 10.1016/j.polymdegradstab.2013.10.001. ISSN 01413910.

[41] CARLSON, Denise, Philippe DUBOIS, Li NIE, Ramani NARAYAN a Rafael AURAS. Free radical branching of polylactide by reactive extrusion: Effects of the reactive modifier, initiator and processing conditions on the final grafted maleic anhydride content and molecular weight of PLA. Polymer Engineering [online]. 1998, 38(2), 311-321 [cit. 2016-10-15]. DOI: 10.1002/pen.10192. ISSN 0032-3888.

[42] NERKAR, Manoj, Juliana A. RAMSAY, Bruce A. RAMSAY, Marianna KONTOPOULOU a Rafael AURAS. Dramatic Improvements in Strain Hardening and Crystallization Kinetics of PLA by Simple Reactive Modification in the Melt State: Effects of the reactive modifier, initiator and processing conditions on the final grafted maleic anhydride content and molecular weight of PLA. Macromolecular Materials and Engineering [online]. 2014, 299(12), 1419-1424 [cit. 2016-10-15]. DOI: 10.1002/mame.201400078. ISSN 14387492.

[43] YANG, Sen-lin, Zhi-Hua WU, Wei YANG, Ming-Bo YANG a Rafael AURAS. Thermal and mechanical properties of chemical crosslinked polylactide (PLA): Effects of

the reactive modifier, initiator and processing conditions on the final grafted maleic anhydride content and molecular weight of PLA. Polymer Testing [online]. 2008, 27(8), 957-963 [cit. 2016-10-15]. DOI: 10.1016/j.polymertesting.2008.08.009. ISSN 01429418.

[44] YOU, Jinxiu, Lijuan LOU, Wei YU, Chixing ZHOU a Rafael AURAS. The preparation and crystallization of long chain branching polylactide made by melt radicals reaction: Effects of the reactive modifier, initiator and processing conditions on the final grafted maleic anhydride content and molecular weight of PLA. Journal of Applied Polymer Science [online]. 2013, 129(4), 1959-1970 [cit. 2016-10-15]. DOI: 10.1002/app.38912. ISSN 00218995.

[45] JASZKIEWICZ, A., A. K. BLEDZKI, R. VAN DER MEER, P. FRANCISZCZAK a A. MELJON. How does a chain-extended polylactide behave?: a comprehensive analysis of the material, structural and mechanical properties. *Polymer Bulletin*[online]. 2014, **71**(7), 1675-1690 [cit. 2016-10-15]. DOI: 10.1007/s00289-014-1148-8. ISSN 0170-0839.

[46] NAJAFI, N., M.C. HEUZEY, P.J. CARREAU, Paula M. WOOD-ADAMS a A. MELJON. Control of thermal degradation of polylactide (PLA)-clay nanocomposites using chain extenders: note II. *Polymer Degradation and Stability* [online]. 2012,**97**(4), 554-565 [cit. 2016-10-15]. DOI: 10.1016/j.polymdegradstab.2012.01.016. ISSN 01413910.

[47] NAJAFI, N., M.C. HEUZEY, P.J. CARREAU, Paula M. WOOD-ADAMS a A. MELJON. Crystallization behavior and morphology of polylactide and PLA/clay nanocomposites in the presence of chain extenders: note II. *Polymer Engineering* [online]. 2013, **53**(5), 1053-1064 [cit. 2016-10-15]. DOI: 10.1002/pen.23355. ISSN 00323888.

[48] WANG, Yuanliang, Chunhua FU, Yongxiang LUO, Changshun RUAN, Yaoyao ZHANG a Ya FU. Melt synthesis and characterization of poly(L-lactic acid) chain linked by multifunctional epoxy compound: note II. *Journal of Wuhan University of Technology-Mater. Sci. Ed* [online]. 2010, **25**(5), 774-779 [cit. 2016-10-15]. DOI: 10.1007/s11595-010-0090-3. ISSN 1000-2413.

[49] PILLA, Srikanth, Seong G. KIM, George K. AUER, Shaoqin GONG, Chul B. PARK a Ya FU. Microcellular extrusion-foaming of polylactide with chain-extender: note II. *Polymer Engineering* [online]. 2009, **49**(8), 1653-1660 [cit. 2016-10-15]. DOI: 10.1002/pen.21385. ISSN 00323888.

[50] LIU, Jianye, Lijuan LOU, Wei YU, Ruogu LIAO, Runming LI a Chixing ZHOU. Long chain branching polylactide: Structures and properties. *Polymer* [online]. 2010, **51**(22), 5186-5197 [cit. 2016-10-15]. DOI: 10.1016/j.polymer.2010.09.002. ISSN 00323861.

[51] XIE, Ji-Xing and Rong-Jie YANG. 2012. Preparation and characterization of high-molecular-weight poly(l-lactic acid) by chain-extending reaction with phosphites. *Journal of Applied Polymer Science* [online]. **124**(5), 3963-3970.

[52] FURUKAWA, Tsuyoshi, Harumi SATO, Rumi MURAKAMI, et al. 2005. Structure, Dispersibility, and Crystallinity of Poly(hydroxybutyrate)/Poly(l -lactic acid) Blends Studied by FT-IR Microspectroscopy and Differential Scanning Calorimetry: The effect on thermal, mechanical, and biodegradation properties. Macromolecules [online]. 38(15), 6445-6454.

[53] ZHANG, Jianming, Harumi SATO, Tsuyoshi FURUKAWA, Hideto TSUJI, William NODA and Yukihiro OZAKI. 2006. Crystallization Behaviors of Poly(3-hydroxybutyrate) and Poly(l -lactic acid) in Their Immiscible and Miscible Blends: The effect on thermal, mechanical, and biodegradation properties. The Journal of Physical Chemistry B [online]. 110(48), 24463-24471.

[54] ZHANG, Min, Noreen L. THOMAS, Bor-Sen CHIOU, Syed IMAM, William ORTS and Emo CHIELLINI. 2011. Blending polylactic acid with polyhydroxybutyrate: The effect on thermal, mechanical, and biodegradation properties. Advances in Polymer Technology [online]. 30(2), 67-79.

[55] ABDELWAHAB, Mohamed A., Allison FLYNN, Bor-Sen CHIOU, Syed IMAM, William ORTS and Emo CHIELLINI. 2012. Polymer Degradation and Stability [online]. 97(9), 1822-1828.

[56] ARMENTANO, I., E. FORTUNATI, N. BURGOS, et al. 2015. Processing and characterization of plasticized PLA/PHB blends for biodegradable multiphase systems: The effect on thermal, mechanical, and biodegradation properties. Express Polymer Letters [online]. 9(7), 583-596.

[57] GUNARATNE, L.M. Wasantha K., R.A. SHANKS, Shifeng WANG, Mingqing CHEN, Xiaoxia CAI and Yong ZHANG. 2008. Miscibility, melting, and crystallization behavior of poly(hydroxybutyrate) and poly(D,L-lactic acid) blends: The effect on thermal, mechanical, and biodegradation properties. Polymer Engineering [online]. 48(9), 1683-1692.

[58] DONG, Weifu, Piming MA, Shifeng WANG, Mingqing CHEN, Xiaoxia CAI and Yong ZHANG. 2013. Effect of partial crosslinking on morphology and properties of the poly(β-hydroxybutyrate)/poly(d,l-lactic acid) blends: The effect on thermal, mechanical, and biodegradation properties. Polymer Degradation and Stability [online]. 98(9), 1549-1555.

[59] L. A. UTRACKI. 2000. *Polymer blends*. Shawbury, Shrewsbury: Rapra Technology.

[60] MANAS-ZLOCZOWER, Ica. c2009. *Mixing and compounding of polymers: theory and practice*. 2nd ed. Cincinnati: Hanser.

[61] BHATTACHARYA, A. 2004. Grafting: a versatile means to modify polymers Techniques, factors and applications. *Progress in Polymer Science* [online]. **29**(8), 767-814.

[62] BHATTACHARYA, Amit, James Wayne. RAWLINS and Paramita. RAY. c2009. *Polymer grafting and crosslinking*. Hoboken, N.J.: John Wiley.

[63] KE, Y., X.Y. ZHANG, S. RAMAKRISHNA, L.M. HE and G. WU. 2017. Reactive blends based on polyhydroxyalkanoates: Preparation and biomedical application. *Materials Science and Engineering: C* [online]. **70**.

[64] MOAD, G, X.Y. ZHANG, S. RAMAKRISHNA, L.M. HE and G. WU. 2017. The synthesis of polyolefin graft copolymers by reactive extrusion: Preparation and biomedical application. *Progress in Polymer Science* [online]. **24**(1), 81-142.

LIST OF ABBREVIATIONS

ATBC	acetyl tributyl citrate
CTBN	carboxyl-terminated butadiene acrylonitrile rubber
DCP	dicumyl peroxide
DMA	dynamic mechanical analysis
DPDP	isodecyl diphenyl phosphite
DSC	differential scanning calorimetry
EBSD	diffracted backscattered electrons
EDX	energy dispersive X-ray spectrometry
ETC	environmental test chamber
ENR	epoxidized natural rubber
FID	flame ionization detector
FS	frequency sweep
GC	gas chromatography
GMA	glycidyl methacrylate
GPC	gel permeation chromatography
HDT	heat distortion temperature
LCB	long chain branched
LDPE	low density poly(ethylene)
LVR	linear viscoelastic region
MDSC	modulated differential scanning calorimetry
MW	molecular weight
MWD	molecular weight distribution
OLA	lactic acid oligomer
PA	poly(amide)
PC	poly(carbonate)
PCDI	poly(carbodiimide)
PDI	polydispersity index
PDLA	*D*-poly(lactic acid)
PDLLA	*D,L*-poly(lactic acid)
PE	poly(ethylene)

PEG	poly(ethylene glycol)
PET	poly(ethylene terephthalate)
PETA	pentaerithritol triacrylate
PHA	poly(3-hydroxy alkanoate)
PHB	poly(3-hydroxy butyrate)
PLLA	*L*-poly(lactic acid)
PMDA	pyromellitic dianhydride
POM	poly(oxy methylene)
PP	poly(propylene)
PS	poly(styrene)
RID	refractive index detector
ROP	ring opening polymerization
RPM	revolution per minute
Scl-PHA	short chain length polyhydroxyalkanoates
SEC	size exclusion chromatography
SEM	scanning electron microscope
TAIC	triallyl isocyanurate
TAM	triallyl trimesate
TGA	thermogravimetric analysis
TGIC	triglycidyl isocyanurate
TNPP	tris(nonyl phenyl) phosphite
TPP	tri phenyl phosphite
TS	time sweep
WD	working distance

APPENDIXES

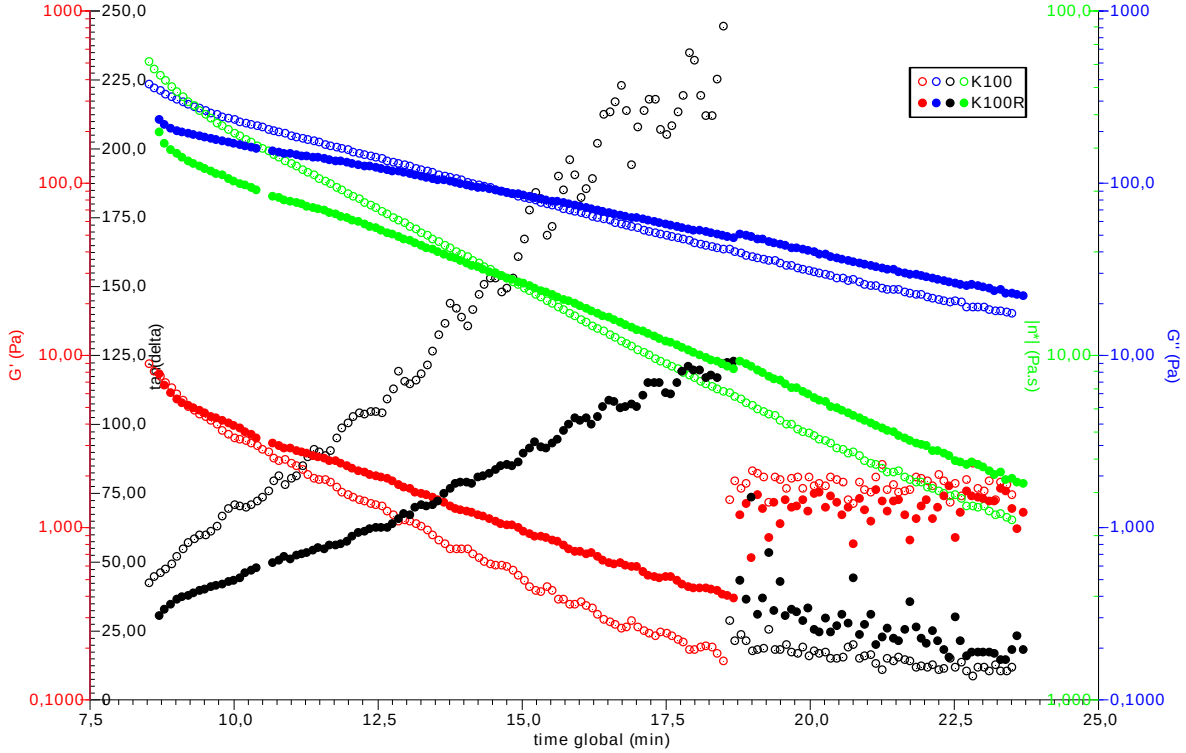

Appendix 1 Time sweep measurement for samples K100 and 100R

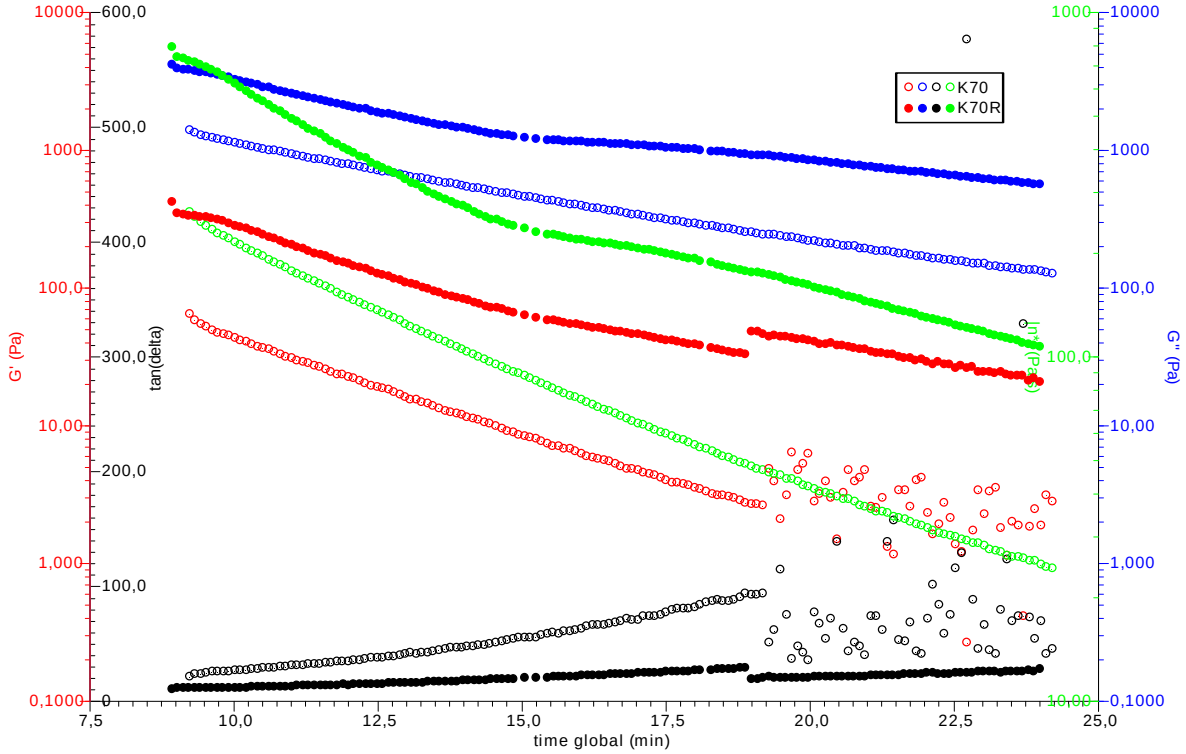

Appendix 2 Time sweep measurement for samples K70 and 70R

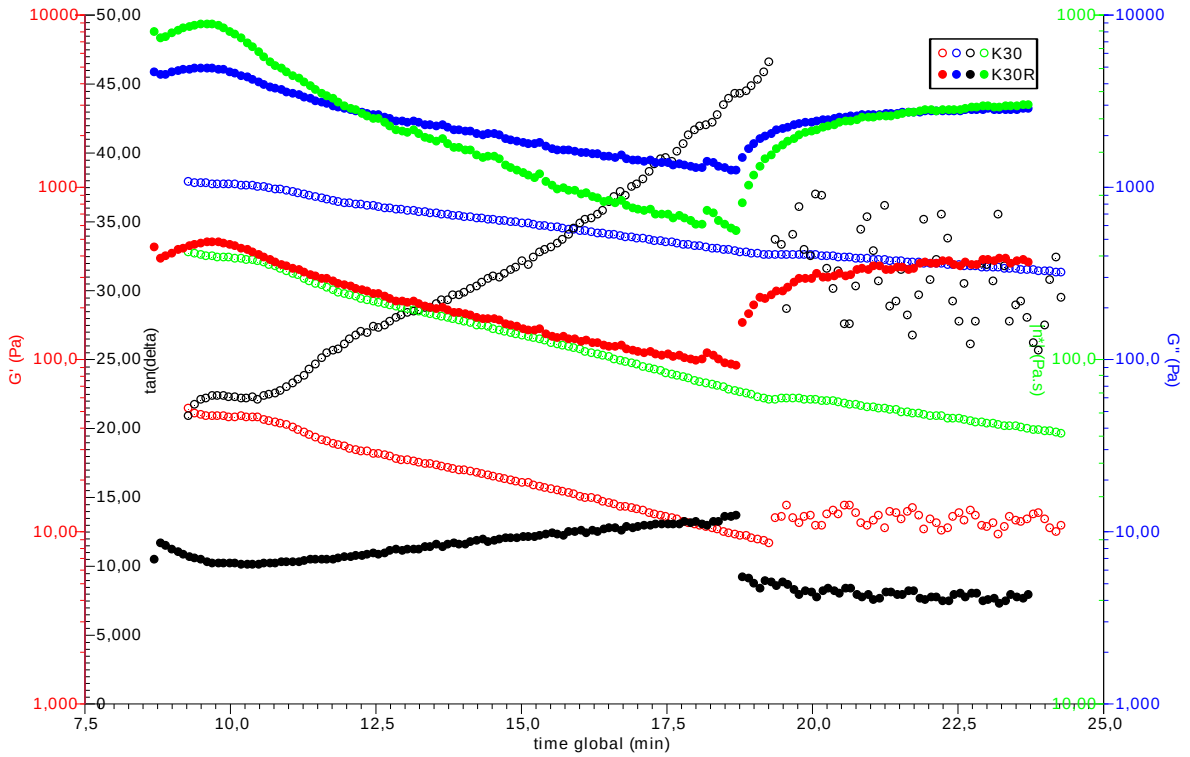

Appendix 3 Time sweep measurement for samples K30 and K30R

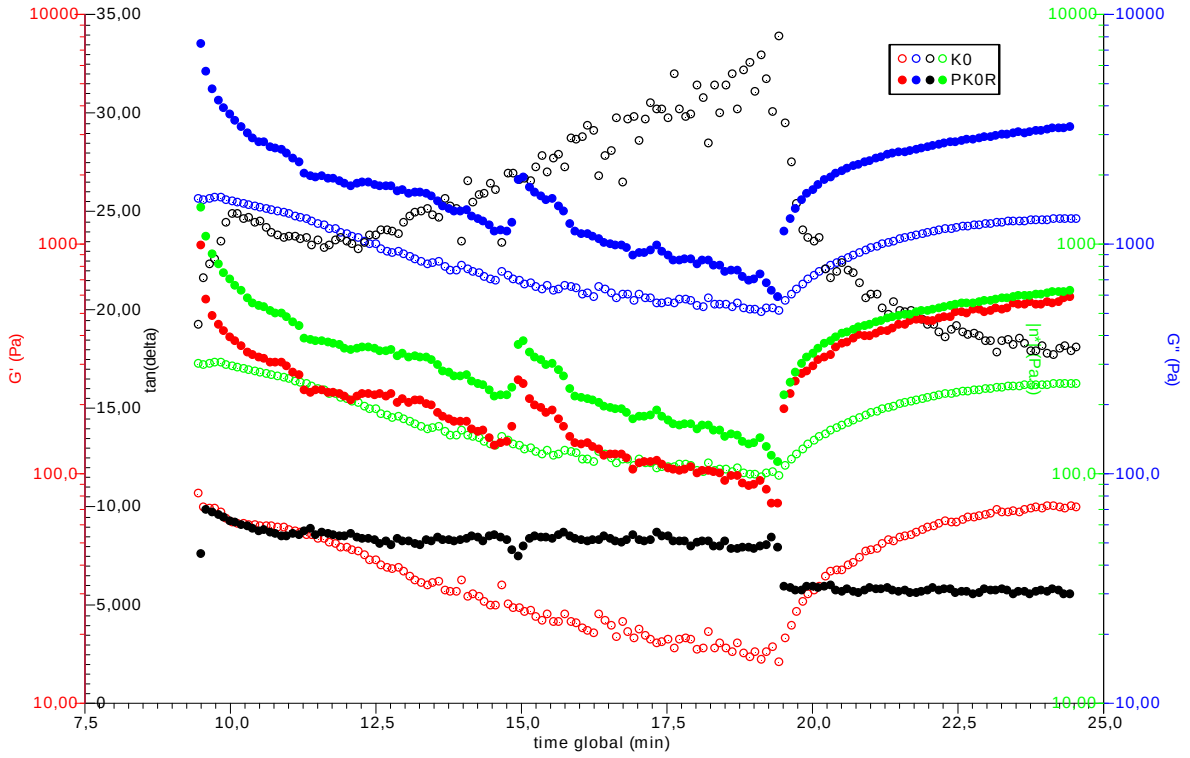

Appendix 4 Time sweep measurement for samples K0 and K0R

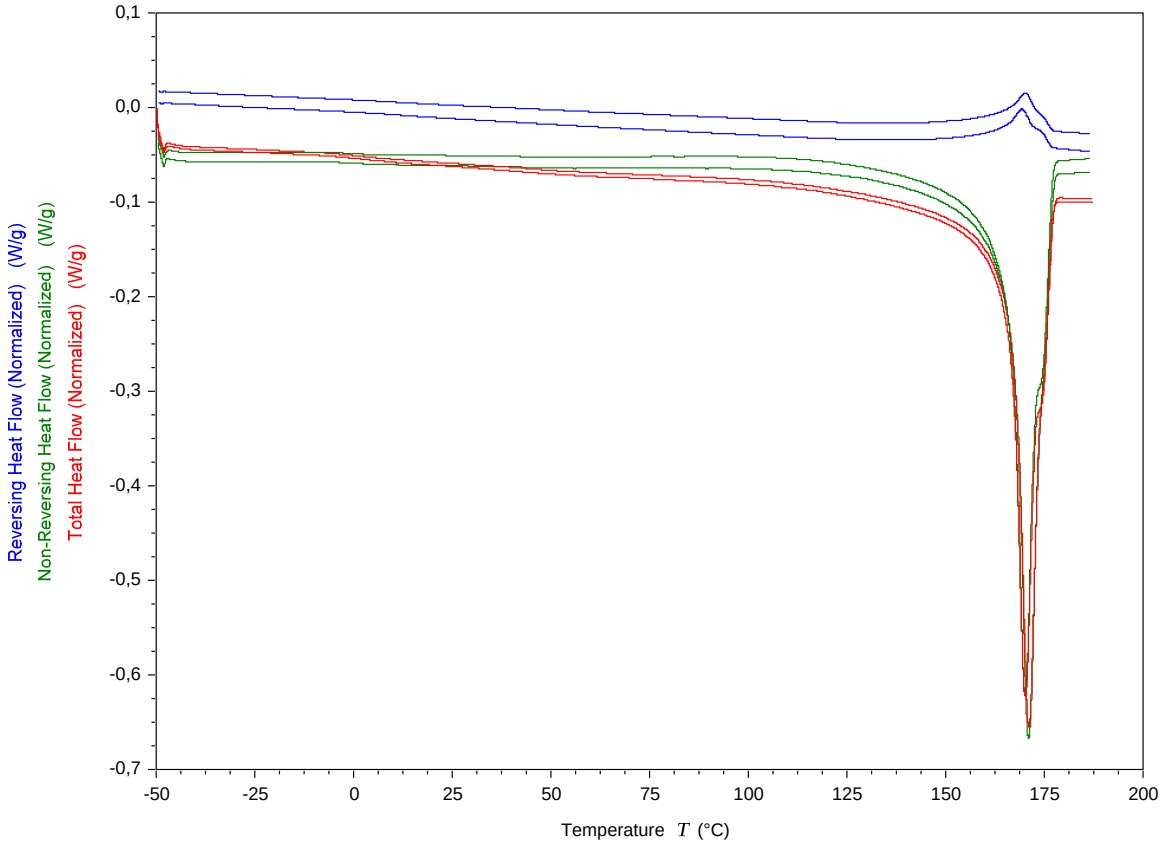

Appendix 5 MDSC curves for K100 and K100R samples

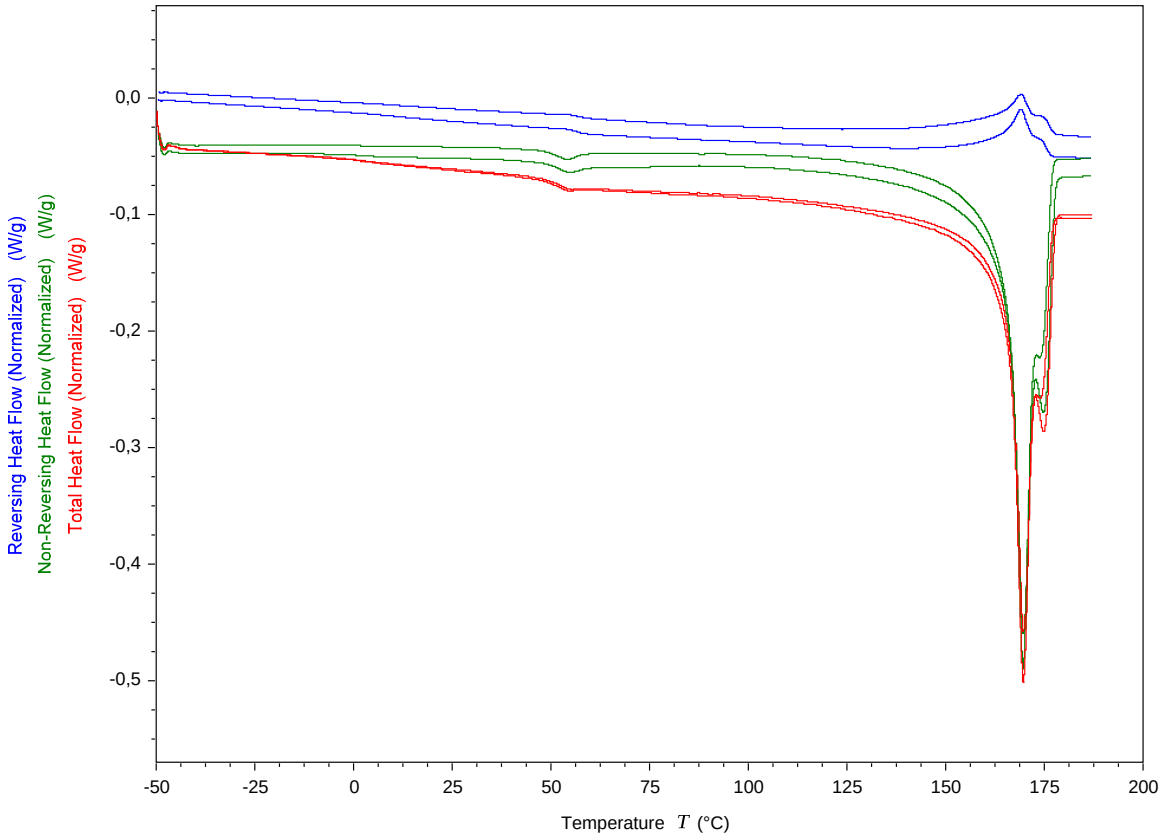

Appendix 6 MDSC curves for K70 and K70R samples

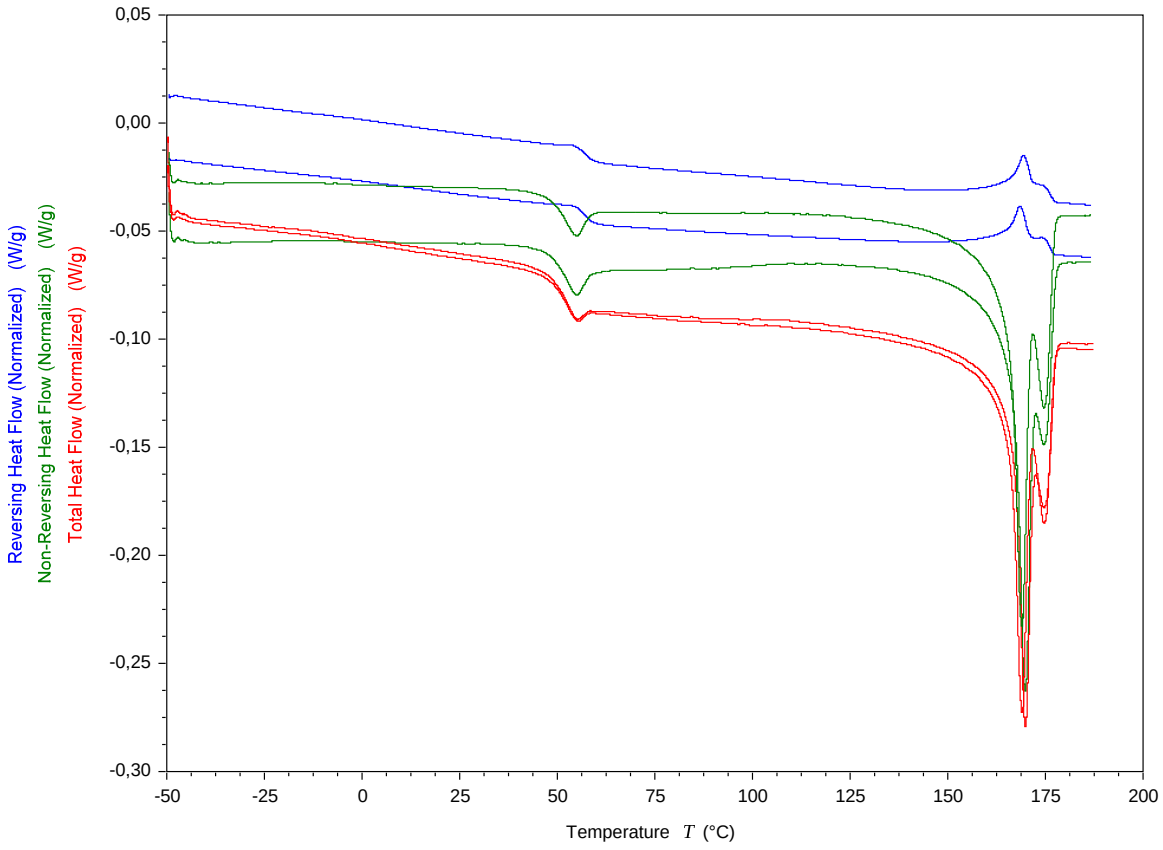

Appendix 7 MDSC curves for K30 and K30R samples

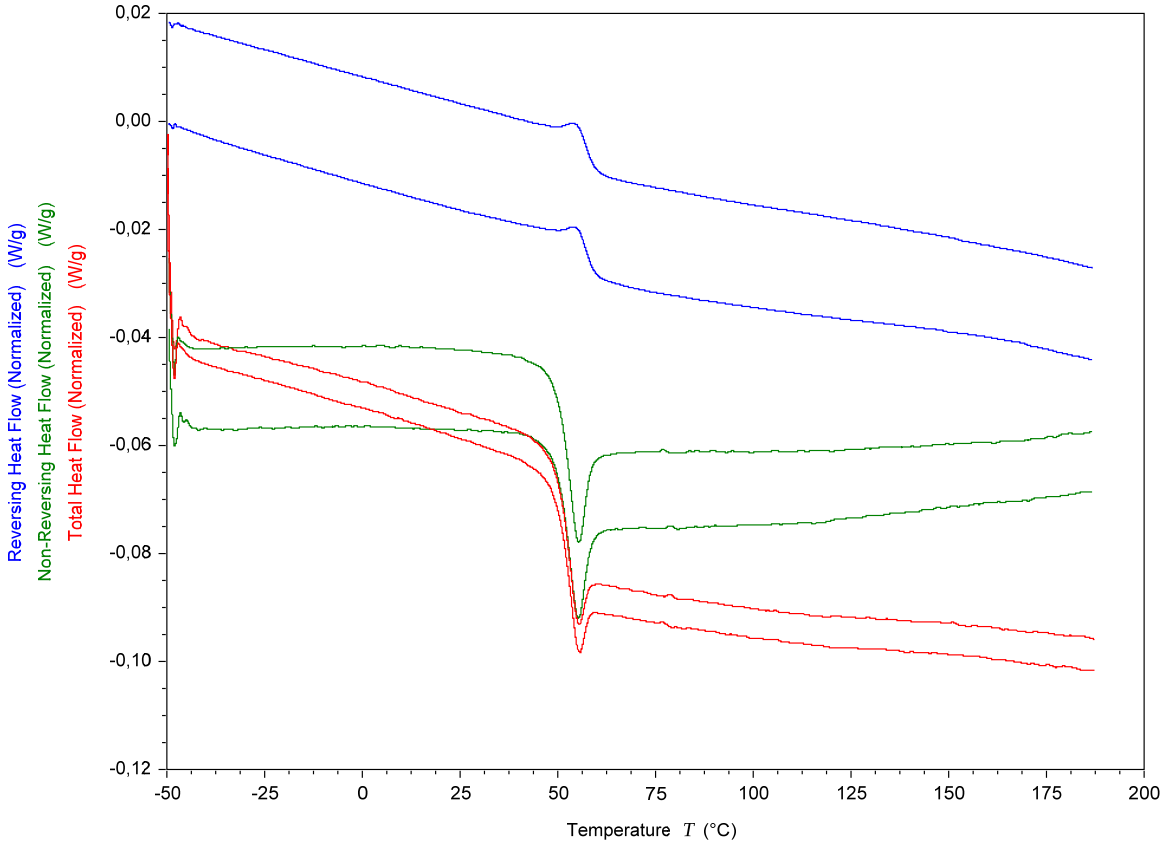

Appendix 8 MDSC curves for K0 and K0R samples

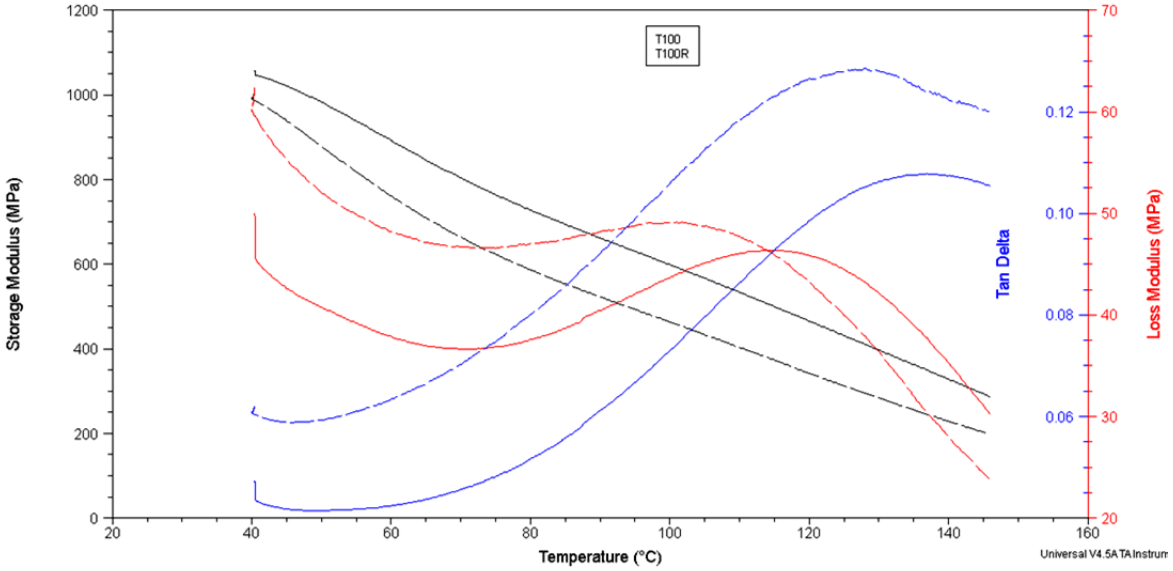

Appendix 9 DMA analysis for samples T100 and T100R

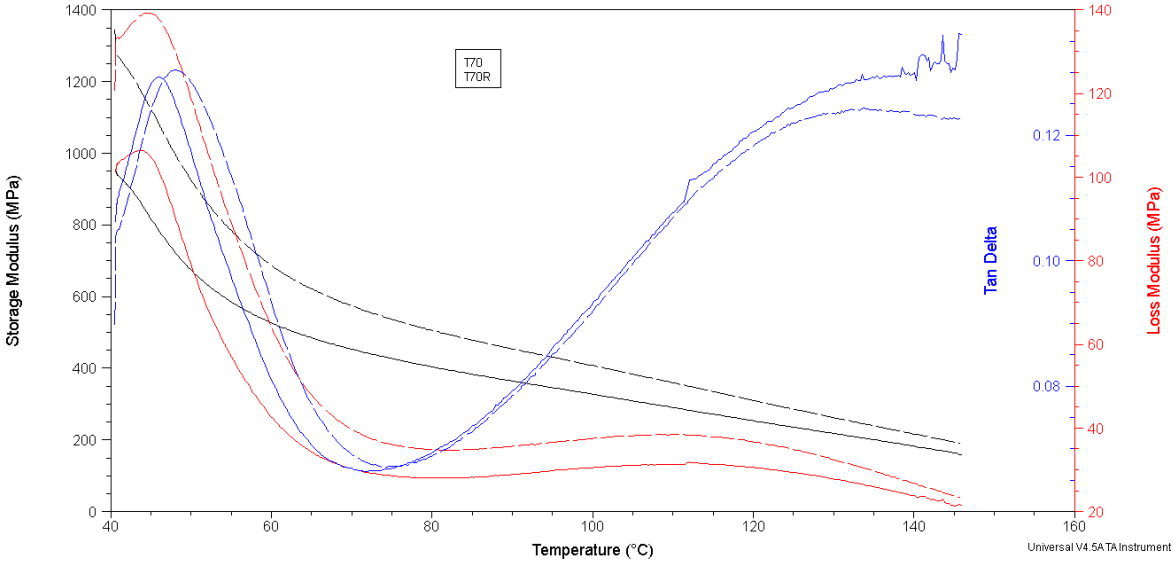

Appendix 10 DMA analysis for samples T70 and T70R

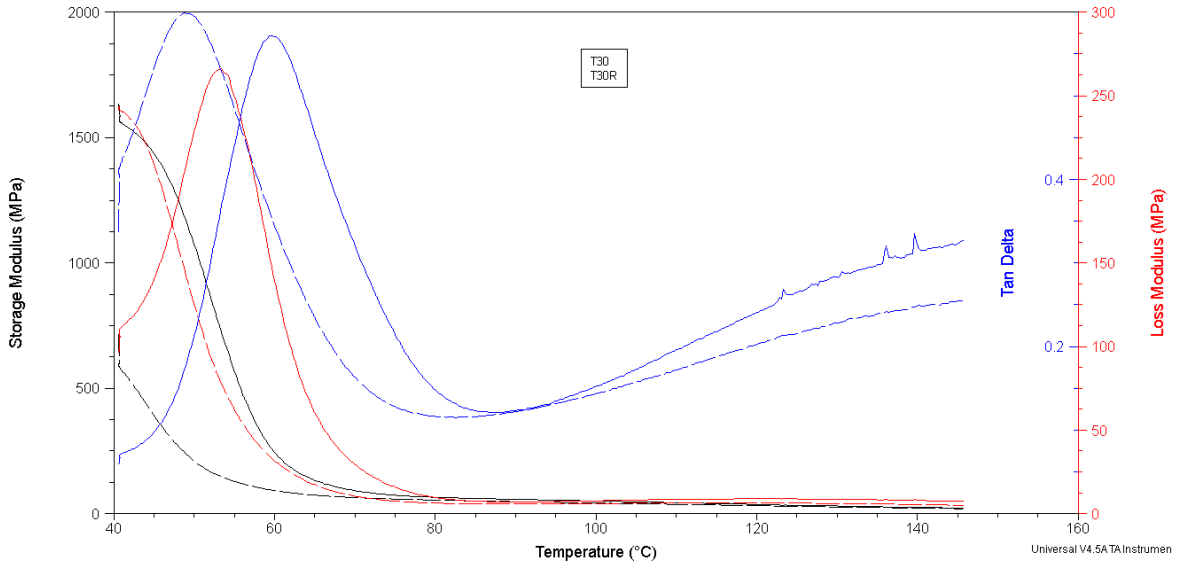

Appendix 11 DMA analysis for samples T30 and T30R

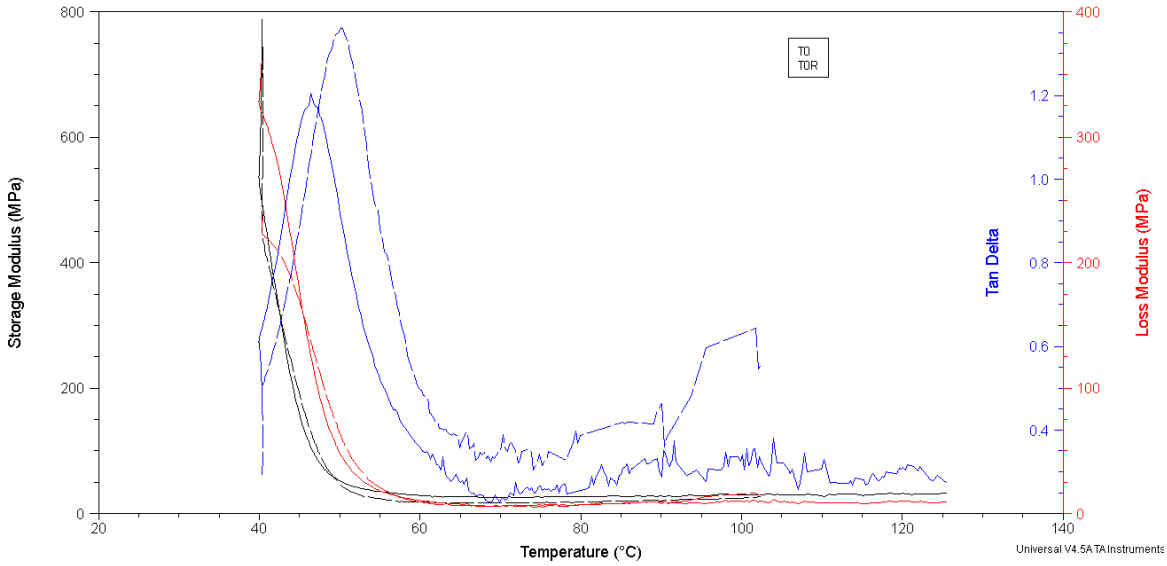

Appendix 12 DMA analysis for samples T30 and T30R